Description of Liquid-Liquid Equilibria including the Critical Region with the Crossover-NRTL Model

---

by

Aleidus van 't Hof

Graduation Thesis

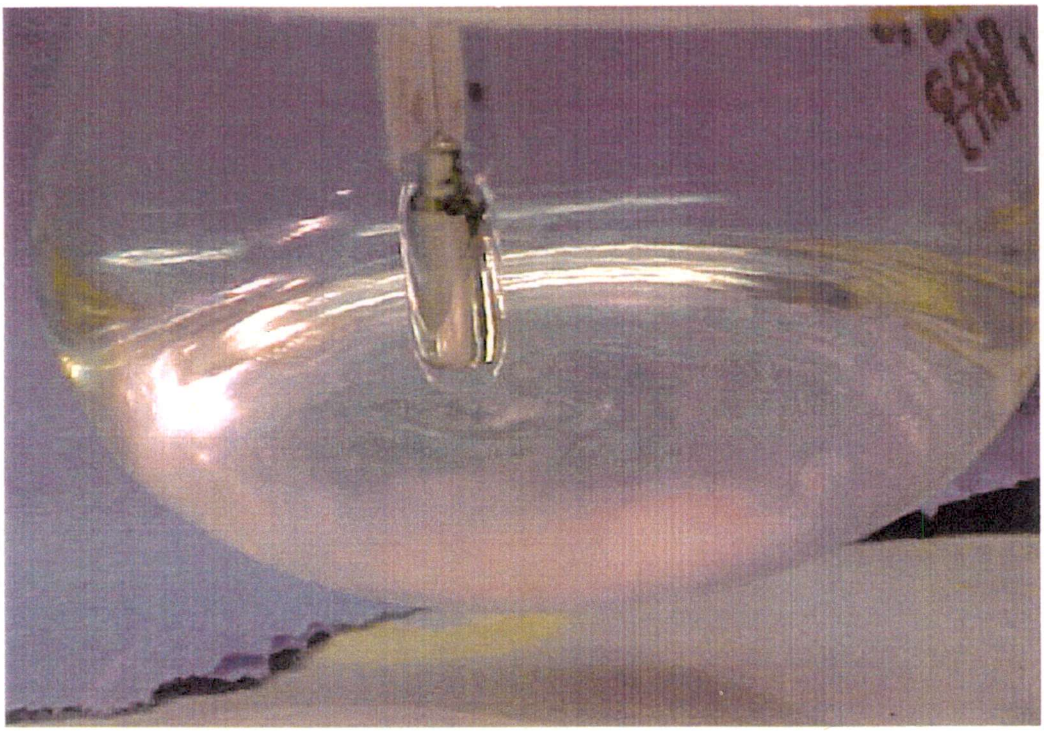

TU Delft
Technische Universiteit Delft

Faculteit der Scheikundige Technologie en der Materiaalkunde

Description of Liquid-Liquid Equilibria including the Critical Region with the Crossover-NRTL Model

by

Aleidus van 't Hof

Graduation Thesis

A thesis submitted in partial satisfaction of the requirements for the degree of Engineer in Chemical Engineering

at

Laboratory for Applied Thermodynamics and Phase Equilibria
Faculty of Applied Sciences
Delft University of Technology
The Netherlands

Delft, May 2000

Supervisors:

University of San Martín, Argentina
Prof. Dr. M. L. Japas

Delft University of Technology
Dr. Ir. C. J. Peters

Picture on the cover; critical opalescence

Some binary fluid mixtures show a critical temperature. Above T_c the fluids are miscible, but below T_c they separate into two phases of different composition. As a binary fluid is cooled towards T_c from above, the fully mixed phase is constantly fluctuating into phase-separated volumes and back again. As T_c is approached the length scale of the fluctuations grows and eventually reaches the scale of a fraction of a micron, *i.e.* of the same order as the wavelength of the light. If there is a difference in the refractive index of the different liquid phases, then light will be strongly scattered and the mixture of the phases appears cloudy. This phenomenon is called critical opalescence.

Preface

This thesis is the result of work done in the context of my Graduation Project leading to the Master's of Science of Chemical Engineering degree at Delft University of Technology. It represents the work I have performed from September 1999 to May 2000. I am very glad to have been able to contribute to the research efforts of the Department of Applied Thermodynamics and Phase Equilibria.

I would like to take this opportunity to thank the following people who have helped me substantially during the course of this project:

Prof. Dr. M. L. Japas from the university of San Martìn, Argentina, my supervisor, for all her ideas, help and advice in the broadest sense. I am very grateful for the discussions we had together and for her informal and pleasant way of helping. I also want to thank her for reviewing the concept of this report.

Dr. Ir. C. J. Peters, my principal thesis supervisor, for all his ideas and the discussions we had together. I also want to thank him for arranging this graduation project under supervision of Prof. Dr. M. L. Japas for me. I am aware of being in a privileged position with my 'own' supervisor from Argentina.

Prof. Dr. J. V. Sengers and Prof. Dr. M. A. Anisimov from the University of Maryland, USA. I want to thank Prof. Dr. M. A. Anisimov for the interesting discussions and his comments on my results. I also want to thank Prof. Dr. J. V. Sengers for his comments on my results and for taking part in my graduation committee.

Dr. Kh. Abdoulkadirova, post-doc at Delft University of Technology, for the discussions on crossover theory we had together, for supplying me with important scientific articles, and for taking part in my graduation committee.

Dr. T. A. Edison from the university of Texas, USA, and Dr. Ir. A. Van Pelt from Akzo Nobel Engineering, for supplying me with their crossover models.

I also want to thank the colleagues of the Department of Applied Thermodynamics and Phase Equilibria for the pleasant atmosphere and last but not least my family and in particular my girlfriend Gerine for always being interested in the 'incomprehensible' subject of this graduation report and for their mental support.

Aleidus van 't Hof, Delft, May 2000

Summary

A system near its critical point exhibits long-range fluctuations in the order parameter associated with the critical-point phase transition. In the case of binary liquids these critical fluctuations, *i.e.* concentration fluctuations, lead to an enhancement in properties like the susceptibility and the heat capacity in a very large range of temperatures and concentrations. The size of the long-range fluctuations near the critical point is very large compared to the molecular size. This makes that the behaviour of a system near and at the critical point is not determined by the type of molecule but by its collective, critical behaviour.

Asymptotically close to the critical point, the thermodynamic properties satisfy scaling laws with universal critical exponents and universal scaling functions. The range of validity of the asymptotic scaling laws is extremely small. On the other hand, critical effects on the thermodynamic properties of fluids are observed in practice in a large range of temperatures and concentrations around the critical point. Farther away form the critical point correction-to-scaling terms should be taken into account. However, even scaling laws with a large number of correction-to-scaling terms do not make contact with the classical region. On the other hand, there are many closed-form equations of state, which provide a reasonable description of the thermodynamic behaviour far away from the critical point, but fail close to it. Hence, it becomes important to develop a thermodynamic description for the global thermodynamic critical behaviour, which not only satisfies the asymptotic critical scaling laws and leading corrections-to-scaling terms, but also incorporates the crossover to regular thermodynamic behaviour far away from the critical point. A theoretical procedure to account for the effects of the long-range fluctuations is provided by the renormalisation group theory of critical phenomena.

In this work a crossover model, based on the renormalisation group theory of critical phenomena, is applied to the Non-Random Two-Liquid equation in order to be able to describe liquid-liquid equilibria both in the classical and the critical regions. The Crossover-NRTL model is based on the work of T. A. Edison *et al.* Edison's model contains some fundamental errors. The errors were found by comparing Edison's Crossover-NRTL model with a simplified 2T-Landau model (without kernel term and implicit dependence of the crossover variable *Y* on the order parameter *M*) and with a normal 2T-Landau model (with kernel term and implicit dependence of *Y* on *M*).

The capability of the Landau models to give estimates for the crossover parameters and NRTL parameters, needed for data regression with the Crossover-NRTL model, has been investigated. The simplified 2T-Landau expansion gives rather good estimates for the crossover parameters. The normal 2T-Landau expansion can also give rough estimates for the NRTL parameters $\tilde{b}$ and $\tilde{d}$, but they are not particularly good.

The optimisation routines for the optimisation of the crossover parameters and the NRTL parameters have been written in Matlab®. The optimisation routines are much more flexible than the common optimisation routines because they require neither calculation of the crossover variable *Y* in an inner loop nor the calculation of the propagated error.

The corrected Crossover-NRTL model is used to describe the phase boundaries of 7 different binary liquids. The model is able to describe rather asymmetric coexistence curves. The transformed Gibbs energy of mixing has the universal scaling behaviour near the consolute critical point and has a smooth crossover to classical behaviour far away from the critical point. The model is able to predict the divergence in the supercritical heat capacity C_{px}. A caloric background function, which is analytic in temperature, must be added to the regular part of the Gibbs energy of mixing to account for a background contribution to the heat capacity. In the present work, the C_{px}-values in the subcritical region could not be represented adequately. The calculations of the thermal response function in the 2-phase region, usually split into a frozen phase-equilibrium response and material relaxation to the new equilibrium state, need to be improved.

A short survey of the significance of the obtained NRTL parameters and crossover parameters is given. The relation between the NRTL interaction energies and the local mole fractions is very clear. The crossover parameter $\bar{u}$ decreases with an increasing range of intermolecular interactions. This increasing range of intermolecular interactions enlarges the range of validity of the classical theory, which is expressed in a larger Ginzburg number. For the analysed systems, the exponent β_{eff} equals the Ising exponent asymptotically close to the critical point, farther away from the critical point it increases towards the mean field value but, before reaching that limit, it drops steeply. The results for $\bar{u}$ and the effective exponent β_{eff} point out that all considered binary liquids in this work can be considered as 'simple'.

The results of the Crossover-NRTL model seem to be very promising. However, there are very little data sets with both accurate data in the critical region and an extended range in temperature. The validity of the Crossover-NRTL model should be tested with data sets with more extended ranges in temperature than the ones that are used in this work.
The calculation of C_{px} was only a prediction from the NRTL parameters and crossover parameters that were calculated from data regression of the Crossover-NRTL model to the phase-boundary. A better value for Λ and $\bar{u}$, and maybe a better representation of the coexistence curve can be obtained by optimising the NRTL parameters and crossover parameters to both heat-capacity data and phase-boundary data simultaneously.

Table of contents

Appendices

1 Introduction

1.1 General overview on liquid-liquid equilibria in the critical region

A system near its critical point exhibits enhanced values of susceptibilities. The inverse of these susceptibilities, related to the curvature of the thermodynamic potential, determines the ability of the system to react to external perturbations or to internal non-equilibrium configurations.
As a liquid-liquid system approaches its critical point, the restoring force that drives a microscopic system into the equilibrium state vanishes. Configurations different from the equilibrium configuration become long-lived, and the systems displays patches where local values of concentration differ from the equilibrium values. As the critical point is approached, the average value of this difference, the concentration fluctuation, increases. Also the average size of the patches, or *correlation length*, diverges close to the critical point, reaching values of several thousand Ångstroms very close to the critical point, while at the critical point they become infinite and a second phase forms. The correlation length near the critical point is very large compared to the molecular size. Therefore, different system types involving distinctly different materials share a common universal critical behaviour near the critical point. The behaviour of a system is not determined by the type of molecule but by its collective, critical behaviour.
Asymptotically close to the critical point, the thermodynamic properties satisfy scaling laws with universal critical exponents and universal scaling functions, *i.e.* sufficiently close to the critical point the properties vary as a simple power of the temperature difference or concentration difference from the critical point, apart from a regular classical part. The power laws are incorporated by the fundamental postulate that, close to the critical point, the Helmholtz energy density assumes a scaled expression. The universal exponents depend on the thermodynamic property, on the path of approach of the critical point, and on the universality class. Binary fluid mixtures belong tot the universality class of 3-dimensional Ising-like systems. Liquid-gas systems, uniaxial ferromagnetism, polymer-solvent solutions, and protein solutions all belong to this universality class.

The exponents of the power laws can be calculated for classical models. However, the classical models do not reproduce the universal exponents of the universality class of 3-dimensional Ising-like systems because they do not account for the long-range fluctuations near the critical point. The classical equations remain analytic at the critical point and fail to describe the singular behaviour of some thermodynamic properties.

The range of validity of the asymptotic power laws is extremely small. On the other hand, critical effects on the thermodynamic properties of fluids are observed in practice in a large range of temperatures and concentrations around the critical point. Farther away form the critical point correction-to-scaling terms must be taken into account. These corrections to the asymptotic scaling laws are often referred to as Wegner corrections. The agreement with experimental data deteriorates very rapidly as soon as the asymptotic scaling laws with Wegner corrections are extrapolated outside their limited range of validity. Hence, it becomes important to develop a thermodynamic

description for the global thermodynamic critical behaviour, which not only satisfies the asymptotic critical scaling laws and leading Wegner corrections, but also incorporates the crossover to regular thermodynamic behaviour far away from the critical point.
A theoretical procedure to account for the effects of the long-range fluctuations is provided by the renormalisation group theory of critical phenomena. Based on the renormalisation group theory, different crossover models have been developed. The crossover models incorporate the correct asymptotic behaviour near the critical point as well as the classical behaviour far away from the critical point.

1.2 Objectives of this graduation project

The NRTL equation is a well-known excess Gibbs energy model in engineering applications. Alike all classical equations, the NRTL model neglects long-range fluctuations near the critical point. Therefore, it cannot describe the critical region, does reproduce the wrong critical exponents and fails to describe the singular behaviour of some thermodynamic properties.
In this work, the crossover model of Chen *et al.* [1], is applied to the Non-Random Two Liquid equation in order to be able to describe liquid-liquid equilibria in the global critical region. The Crossover-NRTL model, is based on the work of T. A. Edison *et al.* [2]. Edison's model contains some fundamental errors. The main goal of this graduation project is to correct these errors and to check the limiting behaviour of the calculated phase boundaries.
Furthermore, Edison described only one liquid-liquid phase boundary. Another objective is the application of the Crossover-NRTL model to different liquid-liquid mixtures with more asymmetric coexistence curves.
Finally, the capability of the 2T-Landau model to give festimates for the NRTL parameters and crossover parameters that are needed in the optimisation of the Crossover-NRTL model to phase-boundary data can be investigated.

1.3 Structure of the report

The structure of this graduation report is the following. The basic theory of the critical point and crossover theory will be dealt with in chapter 2. Chapter 2 gives an indication of what is, in general, wrong in the classical equations and how the behaviour near the critical point can be corrected. Part of the theory of liquid-liquid equilibria and the Non-Random Two Liquid model is given in chapter 3. Chapter 4 contains the results of the modelling of liquid-liquid equilibria with the Non-Random Two Liquid model and the discussion of these results. Chapter 5 describes the different programs and subroutines, which are needed to optimise the different parameters of the crossover-NRTL equation to phase-boundary data. This chapter is followed by conclusions and recommendations.

2 Basic theory of critical phenomena and crossover theory

2.1 The critical point

Critical phenomena are second order phase transitions in which the quantities describing the macroscopic state of the system vary continuously but present an angular point corresponding to the divergence of the derivatives. The second order phase transition is illustrated in Figure 2.1.

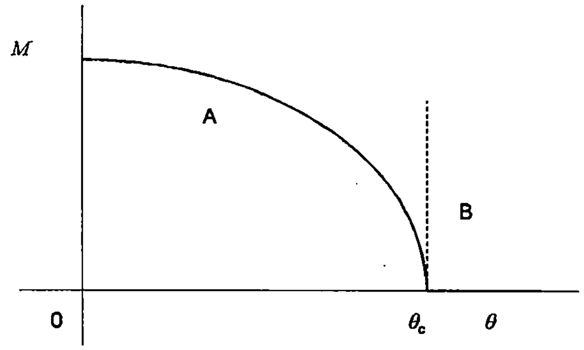

Figure 2.1: Second order (critical) phase transition

The variable θ controls the phase transition. For the gas-liquid critical point its critical value, θ_c, corresponds to the critical temperature. The *control or order parameter M* is a parameter that vanishes in the fluid phase B ($T>T_c$), and is non-zero in zone A ($T<T_c$). The order parameter, M, is continuous at $T=T_c$, however, its derivative diverges, as can be seen in Figure 2.1 [3]. The concept of order parameter was introduced when critical behaviour was studied in magnetic systems [4]. The spontaneous magnetisation of a magnetic material at zero magnetic field H diminishes with temperature and disappears at the Curie point. Below the Curie point, an ordered state exists in which the atomic spins are at least partially arranged. Above the Curie point no such order exists. Therefore, spontaneous magnetisation is called the *order parameter*. In uniaxial ferromagnets and in the Ising model, spins can only assume the 'values' up and down and are therefore represented as scalars. The behaviour of a fluid in its weak direction is reminiscent of that of uniaxial ferromagnets. Below the critical point, there are two states of different density corresponding to the states of aligned spins pointing up or down. Above the critical point the density difference has disappeared. Therefore, a scalar order parameter is ascribed to the critical behaviour of fluids. In one-component fluids this order parameter is often assumed to be the density difference between the actual and the critical density. The choice is dictated principally by the observed symmetry of the property with respect to the critical density.

According to the phase rule of Gibbs, a one-component fluid has two degrees of freedom. When two phases coexist, only one degree of freedom is left. Therefore, the condition of coexistence defines a curve in the space of the two independent field variables. In the two coexisting phases all field variables are equal. Extensive properties or densities are generally not the same in the coexisting phases. The gas-liquid critical point is an endpoint on the coexisting curve at which not only all fields but also all densities are the same. The result is that at the critical point the two coexisting phases can not be distinguished anymore [5].

2.2 Divergences and power laws

In experiments, the properties K_T, α_p, and C_p (equation 2.1) show a strong divergence in a broad temperature and density region around the critical point.

$$K_T = -\frac{1}{V}\left(\frac{\partial V}{\partial p}\right)_T \qquad \alpha_p = \frac{1}{V}\left(\frac{\partial V}{\partial T}\right)_p = K_T\left(\frac{\partial p}{\partial T}\right)_V$$
$$C_p = C_V + T\left(\frac{\partial p}{\partial T}\right)_V\left(\frac{\partial V}{\partial T}\right)_p = C_V + TVK_T\left(\frac{\partial p}{\partial T}\right)_V^2 \qquad (2.1)$$

where	$K_T =$	isothermal compressibility	[Pa^{-1}]
	$V =$	volume	[m^3]
	$p =$	pressure	[Pa]
	$T =$	temperature	[K]
	$\alpha_p =$	isobaric expansivity	[K^{-1}]
	$C_p =$	isobaric heat capacity	[J/(mole·K)]
	$C_v =$	isochoric heat capacity	[J/(mole·K)]

Experiments also show that the isochoric heat capacity C_V diverges at the critical point, however the divergence is less pronounced than that of C_p.

It is assumed that the thermodynamic properties near and at the critical point can be described by power laws. To define a power law five parameters or variables are needed:

- The property in question Q, measured with respect to its critical value Q_c, if it does not diverge;
- An independent variable r_1, measured with respect to its critical value r_{1c};
- The path of approach, in the form of other independent variables r_2 held constant;
- A non-negative critical exponent ε;
- A critical amplitude E.

In the case of a diverging property the property is made dimensionless by an appropriate combination of critical parameters. If the property is expressed in reduced units the critical amplitude becomes a dimensionless number. The power laws for non-diverging and diverging properties are of the following form [6]:

$$\left|\frac{Q-Q_c}{Q_c}\right| = E\left|\frac{r_1 - r_{1c}}{r_{1c}}\right|^{+\varepsilon} \qquad \left|\tilde{Q}\right| = E\left|\frac{r_1 - r_{1c}}{r_{1c}}\right|^{-\varepsilon} \quad \text{at } r_2 = \text{constant} \qquad (2.2)$$

It is clear that only dimensionless groups can be scaled in a physically realistic way. The variables are often reduced in the following way [7]:

$$\tilde{\rho}=\frac{\rho}{\rho_c} \qquad \tilde{T}=-\frac{T_c}{T} \qquad \tilde{\mu}=\frac{\rho_c T_c}{p_c}\frac{\mu}{T} \qquad \tilde{A}=\frac{A T_c}{p_c V T} \qquad \tilde{p}=\frac{p}{T}\frac{T_c}{p_c}$$

$$\tilde{C}_V=\frac{C_V T_c}{V P_c} \qquad \Delta\tilde{T}=\tilde{T}+1 \qquad \Delta\tilde{\rho}=\tilde{\rho}-1 \qquad \Delta\tilde{\mu}=\tilde{\mu}-\tilde{\mu}_0(\tilde{T}) \qquad \tilde{\chi}=\frac{\chi p_c T}{\rho_c^{\,2} T_c} \tag{2.3}$$

where A = Helmholtz energy [J/mole]
μ = chemical potential [J/mole]
$\tilde{\mu}_0(\tilde{T})$ = analytic background function of $\Delta\tilde{T}$ subject to the condition that at the critical point, $\Delta\tilde{\mu}=0$ [J/mole]
χ = symmetrized isothermal compressibility [mol^2/(J·m^3)]
ρ_c = molar critical density [mol/m^3]
p_c = critical pressure [Pa]
T_c = critical temperature [K]

The exponents of the power laws depend on the thermodynamic property, the path along which the critical point is approached, and the way the distance from the critical point is measured [5]. A number of power laws with accompanying critical amplitudes, critical exponents, and paths of approach are given in Table 2.1.

Table 2.1: Power laws and paths of approach

Property	Power law	Path of approach	Exp.
Chemical potential	$\Delta\tilde{\mu}=D_0\,(\Delta\tilde{\rho})\,\lvert\Delta\tilde{\rho}\rvert^{\delta-1}$	Critical isotherm ($T=T_c$)	δ
Symm. isothermal compressibility	$\tilde{\chi}=\Gamma_0\,\lvert\Delta\tilde{T}\rvert^{\gamma}$	Critical isochore ($T\geq T_c$, $\rho=\rho_c$)	γ
Symm. isothermal compressibility	$\tilde{\chi}=\Gamma_0'\,\lvert\Delta\tilde{T}\rvert^{\gamma'}$	Coexistence curve ($T\leq T_c$, $\rho=\rho_{coex}$)	γ'
Isochoric heat capacity	$\tilde{C}_V=(A_0^{+}/\alpha)\,\lvert\Delta\tilde{T}\rvert^{-\alpha}$	Critical isochore ($T\geq T_c$, $\rho=\rho_c$)	α
Isochoric heat capacity	$\tilde{C}_V=(A_{0\,I}^{-}/\alpha')\,\lvert\Delta\tilde{T}\rvert^{-\alpha'}$	Coexistence curve ($T\leq T_c$, $\rho=\rho_{coex}$)	α'
Isochoric heat capacity	$\tilde{C}_V=(A_{0\,II}^{-}/\alpha'')\,\lvert\Delta\tilde{T}\rvert^{-\alpha''}$	Critical isochore ($T\leq T_c$, $\rho=\rho_c$)	α''
Density	$\Delta\tilde{\rho}_{coex}=\pm B_0\,\lvert\Delta\tilde{T}\rvert^{\beta}$	Coexistence curve ($T\leq T_c$, $\rho=\rho_{coex}$)	β
	$d^2\tilde{p}_{coex}/d\tilde{T}^2\propto\lvert\Delta\tilde{T}\rvert^{-\theta p}$	Coexistence curve ($T\leq T_c$)	θ_p
	$d^2\tilde{\mu}_{coex}/d\tilde{T}^2\propto\lvert\Delta\tilde{T}\rvert^{-\theta\mu}$	Coexistence curve ($T\leq T_c$)	θ_μ
Pressure	$\Delta\tilde{p}=D_0\,(\Delta\tilde{\rho})\,\lvert\Delta\tilde{\rho}\rvert^{\delta-1}$	Critical isotherm ($T=T_c$)	δ

2.3 Exponent equalities and exponent inequalities

The critical exponents introduced in Table 2.1 are not all independent of each other. The laws of thermodynamics impose several inequalities between combinations of the thermodynamic exponents [8,9,10]. The exponent inequality of Griffiths and Rushbrooke reads [8,11]:

$$\alpha''+\beta(\delta+1)\geq 2 \tag{2.4}$$

The exponent inequality of Liberman is given by [12]:

$$\beta(\delta-1)\leq\gamma' \tag{2.5}$$

The exponent inequality of Rushbrooke and Fisher is the result of the combination of the exponent inequalities of Griffiths and Liberman [13,14,15]:

$$\alpha''+2\beta+\gamma'\geq 2 \tag{2.6}$$

Another exponent inequality, related to the heat capacities in the one-phase region and in the two-phase region is:

$$\alpha'\leq\alpha'' \tag{2.7}$$

The different paths and exponents in the $\Delta\tilde{p}$ - $\Delta\tilde{T}$ -plane are given in Figure 2.2.

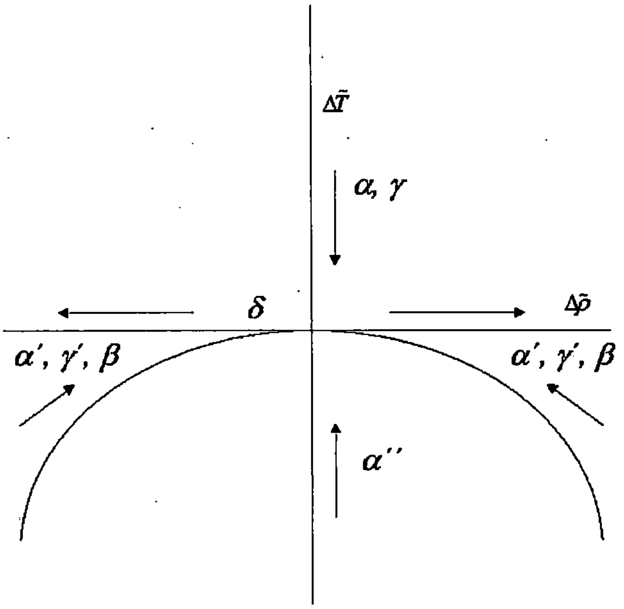

Figure 2.2: Paths and exponents

The exponents of the following derivatives,

$$\left.\frac{\mathrm{d}^2 p}{\mathrm{d}\,T^2}\right|_{\mathrm{coex}} \sim |\Delta T^*|^{-\theta_p} \qquad \left.\frac{\mathrm{d}^2 \mu}{\mathrm{d}\,T^2}\right|_{\mathrm{coex}} \sim |\Delta T^*|^{-\theta_\mu} \tag{2.8}$$

are constrained by [9,16]:

$$\theta_p\leq\alpha''+\beta \qquad \theta_\mu\leq\alpha''+\beta \tag{2.9}$$

The scaling hypothesis for thermodynamic properties, to be introduced in this chapter, leads to the following exponent equalities [5]:

$$\begin{aligned} &\alpha = \alpha' = \alpha'' = \theta_p \qquad && \gamma = \gamma' \\ &2 - \alpha = \beta(\delta + 1) && \gamma = \beta(\delta - 1) \end{aligned} \tag{2.10}$$

Relation (2.10) contains 8 exponents and 6 exponent equalities. Therefore, it is clear that only two thermodynamic exponents can be chosen independently.

2.4 Classical theory

Characteristics of classical or *mean-field* equations are an analytic dependence of the Helmholtz energy density or the pressure on volume and temperature while the conditions for the critical point are given by relation (2.11).

$$\left(\frac{\partial p}{\partial V}\right)_T = 0 \qquad \left(\frac{\partial^2 p}{\partial V^2}\right)_T = 0 \qquad -\left(\frac{\partial^3 p}{\partial V^3}\right)_T \geq 0 \tag{2.11}$$

It is possible to explore the characteristic pattern of the critical anomalies of the classical equations by studying a Taylor series expansion of the equation of state near the critical point [5]. If the power laws also hold for the classical equations of state, the critical exponents and amplitudes can be determined by comparison of the scaling laws with the Taylor series expansion. The expansion procedure is often called the *Landau theory* [17], but in fact it is the work of Van der Waals and Van Laar. The Taylor series expansion in the vicinity of the critical point is given by:

$$\tilde{X}(\Delta\tilde{\rho}, \Delta\tilde{T}) = \sum_{m=0}^{\infty}\sum_{n=0}^{\infty} \frac{1}{m!}\frac{1}{n!} X_{mn} (\Delta\tilde{\rho})^m (\Delta\tilde{T})^n$$

$$\text{where } \tilde{X} = \tilde{A},\ \tilde{p},\ \tilde{\mu} \ \text{ and } \ X_{mn} = \frac{\partial^{m+n}\tilde{X}}{\partial\tilde{\rho}^m \partial\tilde{T}^n} \tag{2.12}$$

The reduced variables are given by equation (2.3). The amplitudes X_{mn} in equation (2.12) do completely specify the thermodynamic behaviour of the system.
Using the Taylor series expansions mentioned above, expressions for several thermodynamic properties can be given. Comparison of the classical expansions and the power laws in Table 2.1 results in values for the critical amplitudes and critical exponents. The behaviour of the Van der Waals equation of state in the limit $(\Delta\tilde{T} \to 0,\ \Delta\tilde{\rho} \to 0)$ can be written in terms of power laws with the following critical amplitudes [5]:

$$D_0 = \frac{p_{30}}{3!} = \frac{9}{2} \qquad \Gamma_0 = {p_{11}}^{-1} = \frac{1}{3} \qquad \Gamma_0' = \frac{{p_{11}}^{-1}}{2} = \frac{1}{6} \qquad B_0 = \sqrt{\frac{3!\mu_{11}}{\mu_{30}}} = 2 \tag{2.13}$$

The following critical exponents are generally valid in the classical theory:

$$\delta = 3 \qquad \gamma = \gamma' = 1 \qquad \alpha = \alpha' = \alpha'' = 0 \qquad \beta = \frac{1}{2} \qquad \theta_p = \theta_\mu = 0 \tag{2.14}$$

The exponent α = 0 means that $\tilde{C}_V$ does not show an anomalous increase in approaching the critical point from within the one-phase region. The classical exponent β = 1/2 indicates that the top of the coexistence curve is quadratic. In the classical theory, the critical exponents obey the exponent inequalities (2.4), (2.5), and (2.6) as equalities:

$$\alpha''+\beta(1+\delta)=2 \qquad \alpha''+2\beta+\gamma'=2 \qquad \beta(\delta-1)=\gamma' \tag{2.15}$$

2.5 Incorrect description of the critical region with classical models

Unfortunately, the classical equations do not predict correctly the asymptotic shape of the coexistence curve and the critical isotherm of real fluids since classical critical exponents differ from the experimental ones [5,6,18]. The classical critical isotherm has a cubic shape with horizontal inflection point since the exponent δ equals 3 for all equations of state that can be expanded at the critical point and have two derivatives zero. The exponent β = 1/2. The exponent α = 0 means that the heat capacity C_V remains finite at the critical point and shows a jump on crossing the phase boundary at the critical density. The exponent γ for the isothermal compressibility K_T equals 1. The correlation length in the classical theory of Ornstein and Zernike diverges with an exponent $\nu = 1/2$, so that the correlation length ξ^2 diverges as the compressibility [19].

For real fluids the coexistence curve is flatter than parabolic with a roughly cubic shape with critical exponent β = 0.326. The heat capacity C_V shows a weak divergence with an exponent α = 0.11. The value of the exponent γ for the isothermal compressibility K_T equals 1.24. The critical isotherm is flatter than predicted by the classical theory with an exponent δ = 4.8. The exponent for the correlation length, ν = 0.63, is slightly larger than in the classical case [6].

The classical or mean-field approximation for the attractive interaction between molecules is rigorous in the limit of weak long-range intermolecular forces. In real fluids, however, the attractive forces are usually not long-ranged. This is the reason why the mean-field theories fail to represent the observed thermodynamic behaviour near the critical point [5].

The shortcomings of a classical equation of state that obeys statistical mechanics can be investigated by an analysis of the partition function. The thermodynamic properties of a system can be calculated from its partition function. The partition function is given by:

$$Z_N = \exp\left(-\frac{A}{k_B T}\right) = \frac{1}{N!\Lambda^{3N}}\int\ldots\int \exp\left(-\frac{U_N}{RT}\right) \mathrm{d}r_1\ldots\mathrm{d}r_N \tag{2.16}$$

where	Z_N =	Grand canonical partition function	[-]
	N =	number of molecules	[-]
	A =	Helmholtz energy of a system consisting of N molecules in a volume V with potential energy U_N	[J]
	k_B =	Boltzman constant	[J/K]
	Λ =	thermal or De Broglie wavelength	[m]

The potential energy, U_N, is separated into the potential energy of an unperturbed (reference) system, $U_N^{(0)}$, and the potential energy of a perturbation, $U_N^{(1)}$:

$$U_\mathrm{N} = U_\mathrm{N}{}^{(0)} + U_\mathrm{N}{}^{(1)} \qquad (2.17)$$

where $U_N^{(0)}$ = potential energy of the reference system with N molecules [J]
$U_N^{(1)}$ = potential energy of the perturbation for a system N molecules [J]

Now, the partition function is given by:

$$Z_\mathrm{N} = Z_\mathrm{N}{}^{(0)} \left\langle \exp\left(-\frac{U_\mathrm{N}{}^{(1)}}{k_\mathrm{B}T} \right) \right\rangle_0 \qquad (2.18)$$

$$Z_\mathrm{N}{}^{(0)} = \frac{1}{N!\Lambda^{3N}} \int \ldots \int \exp\left(-\frac{U_\mathrm{N}{}^{(0)}}{k_\mathrm{B}T} \right) \mathrm{d}r_1 \ldots \mathrm{d}r_N$$

The average $<>_0$ is taken over the reference system. Now, the Helmholtz energy can be written in the following way:

$$-\frac{A}{k_\mathrm{B}T} = \ln(Z_\mathrm{N}{}^{(0)}) + \ln \left\langle \exp\left(\frac{-U_\mathrm{N}{}^{(1)}}{k_\mathrm{B}T} \right) \right\rangle_0 = -\frac{A^{(0)}}{k_\mathrm{B}T} - \frac{A^{(1)}}{k_\mathrm{B}T} \qquad (2.19)$$

where $A^{(0)}$ = Helmholtz energy of the reference system [J]
$A^{(1)}$ = Helmholtz energy of the perturbation [J]

It is assumed that $Z_N^{(0)}$ is known and that $U_N^{(1)}$ is small enough to expand the exponential in equation (2.18) in terms of $U_N^{(1)}/(k_BT)$:

$$\left\langle \exp\left(\frac{-U_\mathrm{N}{}^{(1)}}{k_\mathrm{B}T} \right) \right\rangle_0 = 1 - \frac{\left\langle U_\mathrm{N}{}^{(1)} \right\rangle_0}{k_\mathrm{B}T} + \frac{1}{2!(k_\mathrm{B}T)^2} \left\langle \left(U_\mathrm{N}{}^{(1)} \right)^2 \right\rangle_0 + \ldots \qquad (2.20)$$

Expansion of the natural logarithm in relation (2.19) results in:

$$\begin{aligned}
&\ln\left(1 - \frac{\left\langle U_\mathrm{N}{}^{(1)} \right\rangle_0}{k_\mathrm{B}T} + \frac{1}{2!(k_\mathrm{B}T)^2} \left\langle (U_\mathrm{N}{}^{(1)})^2 \right\rangle_0 \right) = -\frac{\left\langle U_\mathrm{N}{}^{(1)} \right\rangle_0}{k_\mathrm{B}T} + \frac{1}{2!(k_\mathrm{B}T)^2} \left\langle (U_\mathrm{N}{}^{(1)})^2 \right\rangle_0 \\
&-\frac{1}{2}\left[\frac{1}{(k_\mathrm{B}T)^2} \left\langle (U_\mathrm{N}{}^{(1)}) \right\rangle_0^2 + \frac{1}{4(k_\mathrm{B}T)^4} \left\langle (U_\mathrm{N}{}^{(1)})^2 \right\rangle_0^2 - \frac{1}{(k_\mathrm{B}T)^3} \left\langle (U_\mathrm{N}{}^{(1)}) \right\rangle_0 \left\langle (U_\mathrm{N}{}^{(1)})^2 \right\rangle_0 \right] + \cdots \qquad (2.21) \\
&= -\frac{\left\langle U_\mathrm{N}{}^{(1)} \right\rangle_0}{k_\mathrm{B}T} + \frac{1}{2!(k_\mathrm{B}T)^2} \underbrace{\left[\left\langle (U_\mathrm{N}{}^{(1)})^2 \right\rangle_0 - \left\langle (U_\mathrm{N}{}^{(1)}) \right\rangle_0^2 \right]}_{\textit{fluctuation}} + O\left(\frac{1}{(k_\mathrm{B}T)^3} \right)
\end{aligned}$$

In the mean-field theory, higher-order terms like $<(U_N^{(1)})^2>_0$ are neglected. However, this second-order term is positive and important close to the critical point. By neglecting contributions from the second-order term, the mean-field theory fails to account for fluctuations. Therefore, the mean-field Helmholtz energy gives only a lower bound on the true Helmholtz energy.

2.6 Weak and strong directions and divergences

Griffiths and Wheeler designed a theory that leads to a classification of the types of divergences to be expected in certain thermodynamic derivatives. The simplest form of the theory describes a one-component fluid in terms of field variables with p and T as the independent and μ as the dependent variable. The pressure, chemical potential, and temperature are equal in both coexisting phases. The slopes $(\partial p/\partial T)_\mu = s$ and $(\partial p/\partial \mu)_T = \rho$ vary discontinuously when the coexistence line is crossed. Therefore, this coexistence line is a fault in the thermodynamic surface with different slopes on both sides. The difference between the slopes decreases at higher temperatures and vanishes at the critical point. The tangent to this coexistence line at the critical point is called the *special* or *weak direction* [5,13]. The exponents α and γ are defined on this path. This direction refers to variables that are distinct in the coexisting phases. Griffiths and Wheeler called such variables *densities* and examples are volume, density, enthalpy, and entropy.

According to Griffiths and Wheeler, the special direction is the only direction that characterises the nature of the phase transition at the critical point [20]. Therefore, the singular character of the thermodynamic functions will depend on the way in which the critical point is approached. Approaching the critical point in a direction that is asymptotically parallel to the special direction or approaching the critical point in a direction that crosses the special direction changes the singular behaviour. Any path that intersects the special or weak direction in the p-T-plane is called *strong*. All strong directions have the same singular behaviour. Examples are the critical isotherm and the critical isobar. The strong direction refers to variables that are equal in the coexisting phases, *i.e.* fields. The following derivatives show divergences with the same critical exponent:

$$-\left(\frac{\partial^2 \mu}{\partial T^2}\right)_p = \frac{C_p}{T} \qquad -\left(\frac{\partial^2 \mu}{\partial p^2}\right)_T = VK_T \tag{2.22}$$

If the role of p and T in the second order derivatives of $\mu(p,T)$ is changed, the singular behaviour does not change, while the co-ordinate axes of p and T both cross the special direction [16]. In the ρ-T-plane, the strong and the weak direction are reversed. Curves of constant volume, enthalpy, and entropy intersect the coexistence curve at the critical point, while the isotherm, isobar, iso-chemical potential curve, and gravity curve are tangent to the coexistence curve.

The values of the critical exponents depend on the dependent and independent variables chosen and on the path of approach to the critical point, *i.e.* along a weak or a strong direction. The dependence of the exponent value on the path of approach is called *exponent renormalisation*. If, for example, the path of approach is the critical isobar instead of the critical isochore, the critical exponent of the compressibility is renormalised from γ to $\gamma/(\beta\delta)$. Likewise, the exponent α is renormalised from α to $\alpha/(\beta\delta)$. See for exponent renormalisations of the isothermal compressibility and the isochoric heat capacity Table 2.2 [6]:

Table 2.2: Path dependence of divergences

					Exponent value	
Property	Divergence	Path of approach		Exponent	Classical	Non-classical
$K_T(\Delta\tilde{T})$	strong	Crit. Isochore	weak	γ	1	1.239
$K_T(\Delta\tilde{T})$	strong	Crit. Isobar	strong	$\gamma/(\beta\delta)$	2/3	0.792
$K_T(\Delta\tilde{p})$	strong	Crit. Isotherm	strong	$\gamma/(\beta\delta)$	2/3	0.792
$K_T(\Delta\tilde{\rho})$	strong	Crit. Isotherm	strong	γ/β	2	3.8
$C_V(\Delta\tilde{T})$	weak	Crit. Isochore	weak	α	0	0.110
$C_V(\Delta\tilde{T})$	weak	Crit. Isobar	strong	$\alpha/(\beta\delta)$	0	0.070
$C_V(\Delta\tilde{p})$	weak	Crit. Isotherm	strong	$\alpha/(\beta\delta)$	0	0.070
$C_V(\Delta\tilde{\rho})$	weak	Crit. Isotherm	strong	α/β	0	0.337

The second derivatives,

$$-\left(\frac{\partial^2\mu}{\partial T^2}\right)_p = \left(\frac{\partial S}{\partial T}\right)_p = \frac{C_p}{T} \qquad -\left(\frac{\partial^2\mu}{\partial p^2}\right)_T = -\left(\frac{\partial V}{\partial p}\right)_T = VK_T$$

$$\left(\frac{\partial^2\mu}{\partial p\partial T}\right) = \left(\frac{\partial V}{\partial T}\right)_p = V\alpha_p \tag{2.23}$$

where V= molar volume [m^3/mole]
S= molar entropy [J/(mole·K)]

diverge strongly at the critical point. These derivatives are called *susceptibilities*. A susceptibility is a response of a density to a change in the conjugate field, with other fields held constant [19]. It is concluded that second derivatives of the dependent field variable with respect to the independent fields, which are first derivatives of densities with respect to fields, *in directions that are oblique to the coexistence surface (strong field)* are strongly divergent.

Griffiths and Wheeler state that second derivatives of the dependent field variable with respect to the independent ones or first derivatives of a density to a field variable, taken *along the coexisting curve,* which is the weak direction, are in fact derivatives in which a density is kept constant. These derivatives diverge weakly at the critical point [5]. For example the adiabatic compressibility $K_s=-1/V(\partial V/\partial p)_S$ and the isochoric heat capacity $C_V=T(\partial S/\partial T)_V$ diverge weakly. These derivatives remain finite in the classical theory.

Derivatives of densities with respect to densities at constant field or derivatives of fields with respect to fields at constant density are generally well behaved and finite at the critical point. For example $(\partial S/\partial V)_T=(\partial p/\partial T)_V$. The latter derivative is the slope of the vapour pressure curve, which is known to have a finite limiting value at the critical point [19].

Griffiths and Wheeler also gave a description of the critical phenomena in fluid mixtures by investigating the geometry of the critical region in the space of the field variables. The critical behaviour of a binary- or multi-component mixture is a generalisation of the one-component fluid critical behaviour. This is a requirement of the critical-point universality because it states that the critical behaviour of a *n*-component fluid must be in the same universality class as that of one-component fluids and the Ising model [21].

For a binary mixture, the 2-dimensional coexistence surface terminates in a 1-dimensional critical line. In the one-component fluid, the critical point could be approached along the special direction determined by the coexistence curve, or along the strong direction, which is at an angle with the special direction. In multi-component mixtures three directions exist; the one intersecting the coexistence surface, the one parallel to the coexistence surface but not parallel to the critical line, and the one asymptotically parallel to the critical line or critical surface. In binary fluids critical lines are smooth curves in field space and therefore derivatives taken in this direction are expected to be non-divergent. For this direction, a new type of exponent renormalisation occurs. This type of renormalisation is called *Fisher-renormalisation.* On such a path, where two densities are kept constant, the exponents γ, δ, and β are renormalised by a factor $1/(1-\alpha)$ [6]. An example of such derivatives is the adiabatic compressibility at constant composition:

$$\left(\frac{\partial^2 \mu_2}{\partial p^2}\right)_{Sx} = \left(\frac{\partial V}{\partial p}\right)_{Sx} = -VK_{Sx} \tag{2.24}$$

where K_{sx} = adiabatic compressibility at constant composition [Pa^{-1}]

These derivatives diverge weakly for one-component fluids and in general remain finite for mixtures. Derivatives of densities with respect to densities at two constant fields remain, in analogy with one-component fluids, finite. An example is the partial molar volume:

$$\left(\frac{\partial V}{\partial x}\right)_{pT} = -\left(\frac{\partial V}{\partial p}\right)_{Tx} \Big/ \left(\frac{\partial x}{\partial p}\right)_{VT} = VK_{Tx} \Big/ \left(\frac{\partial x}{\partial p}\right)_{VT} \tag{2.25}$$

where K_{Tx} = isothermal compressibility at constant composition [Pa^{-1}]

In analogy with the one-component fluid, a derivative of a density with respect to a field with one field and one density constant is taken along a path asymptotically parallel to the coexistence curve and diverges weakly with an exponent α:

$$\begin{aligned} &\left(\frac{\partial^2 \mu_2}{\partial p^2}\right)_{Tx} = \left(\frac{\partial V}{\partial p}\right)_{Tx} = -VK_{Tx} \qquad &&-\left(\frac{\partial^2 \mu_2}{\partial T^2}\right)_{px} = \left(\frac{\partial S}{\partial T}\right)_{px} = C_{px}/T \\ &\left(\frac{\partial^2 p}{\partial \mu_1^2}\right)_{T\rho_2} = \left(\frac{\partial \rho_1}{\partial \mu_1}\right)_{T\rho_2} &&\left(\frac{\partial^2 p}{\partial \mu_2 \partial T}\right)_{\rho_1} = \left(\frac{\partial \rho_2}{\partial T}\right)_{\rho_1} \end{aligned} \tag{2.26}$$

where C_{px} = isobaric heat capacity at constant composition [J/(mole·K)]

These derivatives remain finite in the classical case. In general properties that diverge strongly in one-component fluids only diverge weakly in binary mixtures of constant composition or constant molar density of one of the components.

In analogy with the one-component case, a derivative of a density with respect to a field with two fields constant intersects the coexistence surface and is taken in a strong direction. The potential $\mu_2(\Delta=\mu_2-\mu_1,p,T)$ leads to the strongly diverging second order derivatives:

$$\left(\frac{\partial^2 \mu_2}{\partial \Delta^2}\right)_{pT} = \left(\frac{\partial x}{\partial \Delta}\right)_{pT} \qquad \left(\frac{\partial^2 \mu_2}{\partial p^2}\right)_{\Delta T} = -VK_{T\Delta} \qquad -\left(\frac{\partial^2 \mu_2}{\partial T^2}\right)_{p\Delta} = \left(\frac{\partial S}{\partial T}\right)_{p\Delta} = \frac{C_{p\Delta}}{T} \tag{2.27}$$

where $K_{T\Delta}$ = isothermal compressibility at constant chemical potential difference [Pa^{-1}]
$C_{p\Delta}$ = isobaric heat capacity at constant chemical potential difference [J/(mole·K)]

These derivatives diverge with an exponent γ along the weak path and with a renormalized exponent $\gamma/(\beta\delta)$ along a strong path. There are exceptions to the general rules mentioned in this paragraph, for example when the critical surface or the coexistence surface has a special direction with respect to the co-ordinate axes.

The theory of the gas-liquid critical point can be changed to also describe the critical phenomena near the critical point of a binary liquid by using the fundamental differential relation at constant pressure ($\Delta=\mu_1-\mu_2$):

$$d\mu_2 = -SdT - xd\Delta \tag{2.28}$$

where x = mole fraction [-]

On comparing this relation with the differential relation $-dp=-sdT-\rho d\mu$ for a one-component fluid, it can be concluded that the behaviour of the fundamental equation $\mu_2(T,\Delta)$ for binary liquids at constant p near the critical mixing point is analogous to that of $p(T,\mu)$ near the critical point of a one-component fluid. The concentration or mole fraction x is now the order parameter, analogous to the magnetisation of a ferromagnet near the Curie point and the density of a fluid near the gas-liquid critical point [5]. Some thermodynamic properties showing analogous behaviour in vapour-liquid systems and liquid-liquid systems are listed in Table 2.3:

Table 2.3: Analogy between gas-liquid critical points and consolute points		
	'One-component'	'Binary liquid at constant p'
Fundamental Equation	$p(T,\mu)$	$\mu_2(T,\Delta)$
Order parameter	$\rho=(\partial p/\partial\mu)_T$	$x=-(\partial\mu_2/\partial\Delta)_{Tp}$
Coexistence curve	$\rho(T)$	$x(T)$
Equation of state	$\mu(\rho,T)$	$\Delta(x,T)$
Susceptibility (strongly divergent)	$\chi_T=(\partial^2 p/\partial\mu^2)_T$	$\chi_T=-(\partial^2\mu_2/\partial\Delta^2)_{Tp}$
Specific heat (weakly divergent)	$C_V/V=T(\partial^2 p/\partial T^2)_\rho$	$C_{px}=-T(\partial^2\mu_2/\partial T^2)_{xp}$

Now, the critical exponents α, β, γ and δ respectively refer to the power-law behaviour of $C_{px}(T)$, the composition difference between the coexisting phases as a function of temperature, the osmotic susceptibility as a function of temperature and the critical isotherm of μ_2 as a function of concentration. A comprehensive review of critical exponent values for binary fluids has been given by Scott [22]. The close agreements between the experimentally found values of β and γ for binary liquids and the ones calculated by the renormalisation group theory do support the hypothesis of universality for critical behaviour of binary liquids.

2.7 Postulate for the homogeneity of the Helmholtz energy density

In the former paragraphs it has been shown that there is experimental evidence for the existence of power laws. Whether there is also theoretical evidence or not will be investigated in this paragraph.

The critical or singular part of the Helmholtz energy density is assumed to be a generalised homogeneous function of $\Delta\tilde{T}$ and $\Delta\tilde{\rho}$. In a homogeneous function, one variable can be eliminated by a proper scaling. This postulate of homogeneity is based on the known properties of the lattice gas. However, since the lattice gas is a highly artificial model of a fluid, the assumption of homogeneity and the choice of variables for real fluids remain empirical postulates. If it is assumed that the chemical potential is antisymmetric with respect to the critical point, that the critical exponent θ_μ equals zero, and that the critical exponents satisfy the exponent equalities, the Helmholtz energy density can be written in the following way [5]:

$$\tilde{A} = \tilde{A}_0(\Delta\tilde{T}) + \tilde{\rho}\tilde{\mu}_0(\Delta\tilde{T}) + \Delta\tilde{A}_{\text{sing}}(\Delta\tilde{T},\Delta\tilde{\rho}) \tag{2.29}$$

where $\tilde{A}_0(\Delta\tilde{T})$ = mechanical background, analytic in temperature [-]
$\tilde{\mu}_0(\Delta\tilde{T})$ = caloric background, analytic in temperature [-]
$\Delta\tilde{A}_{\text{sing}}$ = singular part of the dimensionless Helmholtz energy density [-]

$\Delta\tilde{A}_{\text{sing}}$ is a symmetric function of $\Delta\tilde{\rho}$, which follows from $(\partial\Delta\tilde{A}_{\text{sing}}/\partial\Delta\tilde{\rho})_T = \Delta\tilde{\mu}$. All critical anomalies are accommodated in the term $\Delta\tilde{A}_{\text{sing}}$. The postulate of homogeneity results in [13]:

$$\Delta\tilde{A}_{\text{sing}}(\lambda^{a_T}\Delta\tilde{T},\lambda^{a_\rho}\Delta\tilde{\rho}) = \lambda\Delta\tilde{A}_{\text{sing}}(\Delta\tilde{T},\Delta\tilde{\rho}) \tag{2.30}$$

where a_ρ = exponent in homogeneity relation [-]
a_T = exponent in homogeneity relation [-]
λ = scaling parameter in homogeneity relation [-]

The exponents a_T and a_ρ can be expressed in the known exponents [13]:

$$a_\rho = \frac{1}{(\delta+1)} = \frac{\beta}{2\text{-}\alpha} \qquad a_T = \frac{1}{\beta(\delta+1)} = \frac{1}{2\text{-}\alpha} \tag{2.31}$$

A scaling law with the new scaling variable x can be made:

$$\frac{\Delta\tilde{A}_{\text{sing}}}{|\Delta\tilde{\rho}|^{\delta+1}} = \Delta\tilde{A}_{\text{sing}}(x,1) \quad \text{with} \quad x = \frac{\Delta\tilde{T}}{|\Delta\tilde{\rho}|^{1/\beta}} \tag{2.32}$$

The coexistence curve can be described by defining:

$$x_0 = B_0^{-1/\beta} \qquad \text{or} \qquad B_0 = x_0^{-\beta} \qquad \text{with} \quad -x_0 = x \tag{2.33}$$

Equations (2.29) and (2.32) can be rewritten as:

$$\tilde{A} = \tilde{A}_0(\tilde{T}) + \tilde{\rho}\tilde{\mu}_0(\tilde{T}) + |\Delta\tilde{\rho}|^{\delta+1}\, Da\left(\frac{x}{x_0}\right) \quad \text{with} \quad Da\left(\frac{x}{x_0}\right) = \Delta\tilde{A}_{\text{sing}}(x,1) \qquad (2.34)$$

where $a(x/x_0)$ = scaling function [-]

In the same way:

$$\tilde{\mu} = \tilde{\mu}_0(\tilde{T}) + \Delta\tilde{\rho}\,|\Delta\tilde{\rho}|^{\delta-1}\, Dh\left(\frac{x}{x_0}\right) \quad \text{with} \quad Dh\left(\frac{x}{x_0}\right) = \Delta\tilde{\mu}(x,1) \qquad (2.35)$$

where $h(x/x_0)$ = scaling function [-]

Universality predicts that, for example, plots of $\Delta\tilde{\mu}/\Delta\tilde{\rho}|\Delta\tilde{\rho}|^{\delta-1}$ versus x/x_0 must coincide for different fluids with proper choice of D and x_0. [6,23].
The homogeneity property of $\Delta\tilde{A}_{\text{sing}}$ means that the derivatives of $\Delta\tilde{A}_{\text{sing}}$ to $\Delta\tilde{\rho}$ or $\Delta\tilde{T}$ also are generalised homogeneous functions of $\Delta\tilde{\rho}$ and $\Delta\tilde{T}$. Differentiation and redefining λ results in scaled expressions for different thermodynamic properties.

The anomalous contributions along every curve of constant x vary as a power law. The curves of constant x in the $\Delta\tilde{T}$-$\Delta\tilde{\rho}$-plane are indicated schematically in Figure 2.3. The curve with $x = -x_0$ is the coexistence curve, the curve with $x=\infty$ is the critical isochore and the curve with $x=0$ is the critical isotherm.

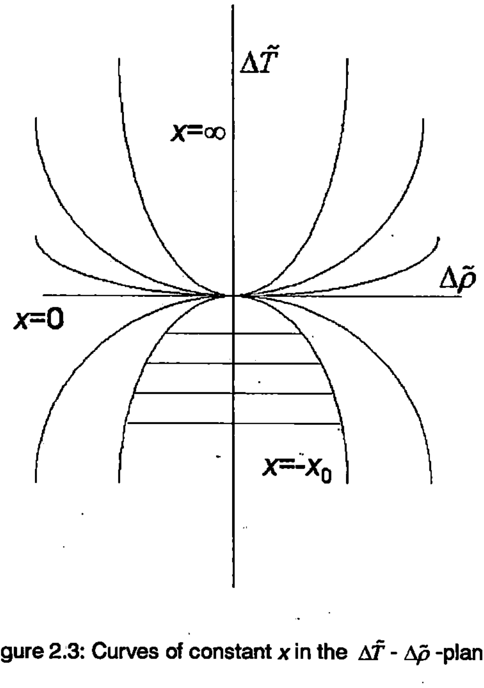

Figure 2.3: Curves of constant x in the $\Delta\tilde{T}$ - $\Delta\tilde{\rho}$ -plane

2.8 Universality of critical behaviour

The key idea in the development of scaled expressions for the critical behaviour of fluids and fluid mixtures is that of critical-point universality. To characterise the behaviour of the thermodynamic properties of systems near a critical point, systems are grouped into universality classes that are defined in terms of the dimension of the system, the dimension of the order parameter, and the range of intermolecular interactions. Systems within a universality class have the same universal critical exponents and scaling functions. Fluids are expected to belong to the universality class of 3-dimensional Ising-like systems (3-dimensional systems with a 1-dimensional order parameter and with short-range forces) for which the universal quantities have been calculated with considerable accuracy. Many detailed theoretical predictions have become available for the Ising-like universality class, the major part by the RG-Theory of critical phenomena applied to spin systems. Recent theoretical critical exponents for the universality class of Ising-like systems are [21]:

$$\begin{aligned} &\alpha = 0.110 \pm 0.003 \quad \beta = 0.326 \pm 0.002 \\ &\gamma = 1.239 \pm 0.002 \quad \delta = 4.80 \pm 0.02 \end{aligned} \tag{2.36}$$

Within the accuracy of the measurements the critical exponents satisfy the following exponent equalities:

$$\begin{aligned} &\alpha = \alpha' = \alpha'' = \theta_p \qquad \alpha + 2\beta + \gamma = 2 \\ &\gamma = \gamma' \qquad\qquad\qquad \alpha + \beta(\delta + 1) = 2 \end{aligned} \tag{2.37}$$

The hypothesis of universality also implies universality of the amplitude ratios of the power laws in Table (2.1), Γ_0^+/Γ_0^-, $\Gamma_0^+ D_0 B_0^{\delta-1}$, A_0^+/A_0^-, $A_0^+\Gamma_0^+/B_0^2$, and $\Gamma_0^+ D_0\, B_0^{\delta-1}$, so that only two amplitudes are independent of each other. Examples of universal ratios of amplitudes are [7]:

$$\frac{\Gamma_0^+}{\Gamma_0^-} = 4.95 \pm 0.15 \quad \frac{A_0^+}{A_0^-} = 0.52 \pm 0.01 \quad \frac{A_0^+ \Gamma_0^+}{B_0^2} = 0.058 \pm 0.001 \quad \frac{\Gamma_0^+ D_0}{B_0^{\delta-1}} = 1.67 \tag{2.38}$$

The scaling laws are only valid in a very small range around the critical point and it can be concluded that corrections to asymptotic scaling should be present in the entire temperature range. These corrections may vary from fluid to fluid. The thermodynamic scaling law for the pressure is given by [5]:

$$\tilde{p} = |u_t|^{2-\alpha} f\left(\frac{u_h}{|u_t|^{\beta\delta}}\right) + \sum_i \sum_j p_{ij} (\Delta\tilde{T})^i (\tilde{\mu} - \tilde{\mu}_c)^j \tag{2.39}$$

where u_t = scaling field, analytic functions of $\tilde{\mu}$ and $\tilde{T}$ [-]

u_h = scaling field, analytic functions of $\tilde{\mu}$ and $\tilde{T}$ [-]

Suppose that the scaling fields u_h and u_t are properly defined and that the hypothesis of scaling is made. As stated above, this hypothesis will only be valid in a limited range around the critical point. Away from the critical point, corrections to scaling have to be made. The RG-theory also provides estimates of the sizes and forms of the correction terms beyond the asymptotic range. Instead of retaining only the scaling fields u_h and u_t in (2.39), also irrelevant scaling fields must be retained, resulting in a so-called Wegner expansion [24,25]:

$$\tilde{p}_{\mathrm{sing}}(u_h,u_t,u_1,u_2,\ldots)=|u_t|^{2-\alpha} f\left(\frac{u_h}{|u_t|^{\beta\delta}},u_1|u_t|^{\Delta_1},u_2|u_t|^{\Delta_2},\ldots\right) \tag{2.40}$$

where $u_{1,2}$ = irrelevant scaling field [-]

$\tilde{p}_{\mathrm{sing}}$ = singular part of the reduced pressure [-]

Unlike the relevant scaling fields, the irrelevant scaling fields do not approach zero at the critical point and scale with the so-called gap exponents. These exponents are expected to be universal. Estimates for the 3-dimensional Ising model are Δ_1=0.50 and Δ_2=1.5 [26]. The irrelevant scaling fields do not contribute to the critical anomalies but they only lead to corrections to the asymptotic scaling laws. Universality of the correction-to-scaling functions also implies some ratios of correction-to-scaling amplitudes to be universal. Values for the amplitude ratios of the first correction-to-scaling terms are [7]:

$$\frac{A_1}{\Gamma_1}=0.72 \qquad \frac{B_1}{\Gamma_1}=0.87 \qquad \frac{A_1^-}{B_1}=0.83 \tag{2.41}$$

2.9 Crossover theory

2.9.1 The need for a crossover model

To be able to describe the whole thermodynamic surface one is forced to supplement the singular limit in the asymptotic critical region with a classical global Van der Waals-like equation outside the critical region. However, this causes discontinuities in the thermodynamic properties in the intermediate region. A theory, which describes the crossover between these two limits, is needed. Many crossover models have been developed. Most of them are based on the renormalisation group (RG) theory of critical phenomena. In the RG-Theory, the co-operative effect of fluctuations with all wavelengths down to a minimum cutoff wavelength of the order of the range of the molecular interaction is taken into account [27,28]. To obtain the critical behaviour, the effects due to the cutoff are neglected because the correlation length near the critical point is much longer than the range of molecular interaction. By linearisation of the RG-equations the Wegner expansions are obtained. However, to solve the crossover problem the non-linear RG-equations have to be solved. They must be solved to effectively sum the Wegner series expansion, including the cutoff effects, to ensure that the theory reduces to the proper molecular theory at distances far away from the critical point where the correlation length becomes of the same order as the range of molecular interactions [5].

How close to the critical point should one expect the asymptotic scaling laws to be applicable? How close can one approach the critical point neglecting the effects of critical fluctuations and continue to use classical theories for the thermodynamic properties? Answers to these questions can be formulated using a classical approach. A rough estimate for the range where fluctuations can be neglected is given by the Ginzburg criterion. To deduce this criterion a first order estimate of the fluctuations, based on the classical theory, is made.

To account for critical fluctuations, a local order parameter $\phi(\vec{r})$, which is a function of position and whose average value in the volume V corresponds to the reduced density difference $\Delta\tilde{\rho}$, is introduced:

$$<\phi(\vec{r})>=\frac{1}{V}\int\phi(\vec{r})\mathrm{d}\vec{r}=\Delta\tilde{\rho} \qquad (2.42)$$

where $\phi(\vec{r})$ = position-dependent order parameter [-]

The local Helmholtz energy density, $a(\phi(\vec{r}))$, and the local ordering field, $h(\phi(\vec{r}))\equiv\partial a/\partial\phi(\vec{r})$, are related to the corresponding macroscopic quantities by:

$$<a(\phi(\vec{r}))>=\Delta\tilde{A} \qquad <h(\phi(\vec{r}))>=\Delta\tilde{\mu} \qquad (2.43)$$

where $a(\phi(\vec{r}))$ = position-dependent Helmholtz energy density [-]
$h(\phi(\vec{r}))$ = position-dependent ordering field

In the classical theory, the fluctuations are neglected and the variables equal their average values. The local Helmholtz energy density and the ordering field can be written in the form of a Landau expansion [30]:

$$a(\phi(\vec{r}))=\frac{1}{2}a_0\Delta\tilde{T}\phi^2(\vec{r})+\frac{1}{4!}u_0\phi^4(\vec{r})+..... \qquad h(\phi(\vec{r}))=a_0\Delta\tilde{T}\phi(\vec{r})+\frac{1}{3!}u_0\phi^3(\vec{r})+..... \qquad (2.44)$$

where a_0, u_0 = Landau amplitudes [-]

The inverse compressibility at the critical isochore, ($\rho=\rho_c$, $\Delta\tilde{T}\geq 0$), will asymptotically vary as:

$$\tilde{\chi}^{-1}(\rho_c,\Delta\tilde{T}\geq 0)=\left(\frac{\partial h}{\partial\phi}\right)_{\Delta\tilde{T}}=a_0\Delta\tilde{T} \qquad (2.45)$$

The finite jump of the isochoric heat capacity at the critical isochore upon crossing the critical temperature is given by [5]:

$$\lim_{T\to T_c}\left[\tilde{C}_V(\rho_c,T\leq T_c)-\tilde{C}_V(\rho_c,T\geq T_c)\right]=\frac{3a_0^{\ 2}}{u_0} \qquad (2.46)$$

If the fluctuations are not neglected, the order parameter becomes a function of the position $\vec{r}$. In the classical theory this dependence is given by the square gradient $(\nabla\phi)^2$. Equation (2.44) for the local free Helmholtz energy density to lowest order becomes:

$$a(\phi(\vec{r})) = \frac{1}{2}a_0\Delta\tilde{T}\phi^2(\vec{r}) + \frac{1}{4!}u_0\phi^4(\vec{r}) + \frac{1}{2}c_0(\nabla\phi)^2..... \qquad (2.47)$$

where c_0 = system-dependent coefficient related to the square of a so-called short-range correlation length [-]

The Ornstein-Zernike theory yields for the correlation function of the order parameter ϕ between positions $\vec{r}_1$ and $\vec{r}_2$:

$$\langle\phi(\vec{r}_1)\phi(\vec{r}_2)\rangle - \langle\phi\rangle^2 = \frac{v_0}{4\pi c_0}\frac{e^{-r/\xi}}{r} \qquad (2.48)$$

where v_0 = volume per molecule [Å^3]
ξ = correlation length [Å]

The correlation length in equation (2.48) is related to the susceptibility by:

$$\xi^2 = c_0\tilde{\chi} = c_0 / a_0\left|\Delta\tilde{T}\right|^{-1} \qquad (2.49)$$

Now, the fluctuation contribution to the susceptibility and the heat capacity along the critical isochore can be determined [31]:

$$\begin{aligned} \tilde{\chi}^{-1}(\rho_c,\Delta\tilde{T}\geq 0) &= a_0\Delta\tilde{T}\left[1-\frac{u_0v_0}{8\pi a_0^{2}\bar{\xi}_0^{3}}\left|\Delta\tilde{T}\right|^{-1/2}\right] \\ \Delta\tilde{C}_V(\rho_c,\Delta\tilde{T}\geq 0) &= \frac{v_0}{16\pi\bar{\xi}_0^{3}}\left|\Delta\tilde{T}\right|^{-1/2} \end{aligned} \qquad (2.50)$$

where $\bar{\xi}_0$ = mean-field correlation-length amplitude [Å]
$\Delta\tilde{C}_V$ = jump in the reduced heat capacity [-]

Comparison of the classical heat capacity and susceptibility with the same properties when fluctuations have not been neglected results in a criterion for the range of validity of the classical theory. Such a criterion is to require that the fluctuation contribution to the heat capacity (2.50) be small compared to the classical jump of the heat capacity (2.46) or that the fluctuation contribution to the compressibility be small (2.45, 2.50) [31]:

$$\Delta\tilde{T} >> \frac{u_0^{2}}{(48\pi)^2 a_0^{4}}\left(\frac{v_0}{\bar{\xi}_0^{3}}\right)^2 \qquad \Delta\tilde{T} >> \frac{u_0^{2}}{64\pi^2 a_0^{4}}\left(\frac{v_0}{\bar{\xi}_0^{3}}\right)^2 \qquad (2.51)$$

From these equation it follows that the effects of fluctuations can be neglected when:

$$\Delta\tilde{T} >> N_G \qquad N_G = \frac{{u_o}^2}{64\pi^2 {a_o}^4}\left(\frac{v_o}{\bar{\xi}_0^{\,3}}\right)^2 \tag{2.52}$$

where N_G = Ginzburg number [-]

Here, the Ginzburg number is related to the susceptibility in the one-phase region. Since the susceptibility is closely related to the correlation length (2.49), it can serve as a measure of the distance from the critical point in the one-phase region [1,32]. The Ginzburg number can be estimated by the Van der Waals parameters a_0 and u_0 and by the assumption that $v_0 = 4\pi\bar{\xi}_0^{\,3}/3$. These values result in $Gi \approx 0.01$. Thus, as a rough approximation, classical equations of state for fluids will be applicable as long as $\Delta\tilde{T} >> 0.01$.

2.9.2 Asymptotic crossover by renormalisation-group matching

A crossover approach based on the work of Nicoll, Albright and Chen, is given here [1,33-39]. The Landau theory asserts that along the path $\phi=0$, the thermodynamic potential, $a(\Delta\tilde{T},\phi)$, can be expanded as a power series in the order parameter ϕ. The Landau expansion is given here in physical variables:

$$\tilde{A}(\Delta\tilde{T},\Delta\tilde{\rho}) = \tilde{A}(\Delta\tilde{T},0) + \left.\frac{\partial\tilde{A}}{\partial\Delta\tilde{\rho}}\right|_{\Delta\tilde{\rho}=0}\Delta\tilde{\rho} + \frac{1}{2!}\left.\frac{\partial^2\tilde{A}}{\partial\Delta\tilde{\rho}^2}\right|_{\Delta\tilde{\rho}=0}\Delta\tilde{\rho}^2 + \frac{1}{3!}\left.\frac{\partial^3\tilde{A}}{\partial\Delta\tilde{\rho}^3}\right|_{\Delta\tilde{\rho}=0}\Delta\tilde{\rho}^3 + \ldots \tag{2.53}$$

The derivatives in equation (2.53) may in turn be expanded into powers of $\Delta\tilde{T}$:

$$\begin{aligned}
&\tilde{A}(\Delta\tilde{T},\Delta\tilde{\rho}) = \\
&\left(\tilde{A}_{00} + \tilde{A}_{10}\Delta\tilde{T} + \frac{1}{2!}\tilde{A}_{20}\Delta\tilde{T}^2 + \ldots\right) + \\
&\left(\tilde{A}_{01} + \tilde{A}_{11}\Delta\tilde{T} + \frac{1}{2!}\tilde{A}_{21}\Delta\tilde{T}^2 + \ldots\right)\Delta\tilde{\rho} + \\
&\left(\tilde{A}_{02} + \tilde{A}_{12}\Delta\tilde{T} + \frac{1}{2!}\tilde{A}_{22}\Delta\tilde{T}^2 + \ldots\right)\Delta\tilde{\rho}^2 + \ldots
\end{aligned} \tag{2.54}$$

In principle, this series expansion contains an infinite number of terms. In order to get a practical thermodynamic potential, the series expansion is terminated after a certain number of terms. The conditions for incipient immiscibility at the critical point requires the derivatives $\tilde{A}_{02}$ and $\tilde{A}_{03}$ to be zero. Mechanical stability requires $\tilde{A}_{04}$ to be positive. Decomposing the thermodynamic potential into a background or regular part and a critical or singular part can further reduce the number of terms. The terms that are zero order in $\Delta\tilde{\rho}$ are referred to as the mechanical background and the terms that are linear in $\Delta\tilde{\rho}$ are referred to as the caloric background.

The property κ^2 is a measure of the distance from the critical point. In the classical theory this property can be calculated by differentiating the Helmholtz energy density two times to the reduced density difference $\Delta\tilde{\rho}$. It is clear that both the mechanical and the caloric background do not contribute to κ^2 and therefore, do not play a role in the critical behaviour of fluids. The decomposition of the Helmholtz energy density in physical variables is again given by:

$$\tilde{A} = \tilde{A}_0(\Delta\tilde{T}) + \Delta\tilde{\rho}\tilde{\mu}_0(\Delta\tilde{T}) + \Delta\tilde{A}_{\text{sing}}(\Delta\tilde{T},\Delta\tilde{\rho}) \qquad (2.55)$$

The term $\Delta\tilde{A}_{\text{sing}}(\Delta\tilde{T},\Delta\tilde{\rho})$ in equation (2.53) represents the remaining, higher-order, terms in equation (2.52). In the classical theory, $\Delta\tilde{T}$ along the coexistence curve varies to lowest order as $\Delta\tilde{\rho}^2$:

$$\Delta\tilde{T} = -\frac{1}{6}\Delta\tilde{\rho}^2 \frac{\tilde{A}_{04} + \frac{1}{4!}\tilde{A}_{05}\Delta\tilde{\rho}}{\tilde{A}_{12} + \frac{1}{2!}\tilde{A}_{13}\Delta\tilde{\rho}} \approx -\frac{1}{6}\left(\frac{\tilde{A}_{04}}{\tilde{A}_{12}}\right)\Delta\tilde{\rho}^2 \qquad (2.56)$$

Therefore, terms like $\Delta\tilde{T}\Delta\tilde{\rho}^2$ are expected to have the same magnitude as $\Delta\tilde{\rho}^4$. Bearing this in mind, all terms of higher order than four are ignored. The resulting expansion is called the *Two-Term Landau Expansion* for the critical or singular part of the Helmholtz energy density:

$$\Delta\tilde{A}_{\text{sing}}(\Delta\tilde{T},\Delta\tilde{\rho}) = \frac{1}{2!}\tilde{A}_{12}\Delta\tilde{T}\Delta\tilde{\rho}^2 + \frac{1}{4!}\tilde{A}_{04}\Delta\tilde{\rho}^4 \qquad (2.57)$$

Note that equation (2.57) is still a classical expansion! $\Delta\tilde{A}_{\text{sing}}$ will become a singular function after the effects of critical fluctuations are taken into account. The classical Landau expansion for the critical part of the Helmholtz energy density (2.57) is written in the following form [1,38]:

$$\Delta\tilde{A}_{\text{sing}} = \frac{1}{2}tM^2 + \frac{u^*\bar{u}\Lambda}{4!}M^4 + \ldots\ldots \qquad t = c_t\Delta\tilde{T} \qquad M = c_\rho\Delta\tilde{\rho} \qquad (2.58)$$

where c_t, c_ρ = system-dependent rescaling amplitudes [-]
Λ = dimensionless cutoff wave number [-]
$\bar{u}$ = rescaled coupling constant [-]
u^* = fixed-point coupling constant for 3-dimensional Ising-like systems [-]
M = order parameter [-]
t = temperature-like variable [-]

Note that a_0 and u_0 in equation (2.44) equal $\tilde{A}_{12}$ and $\tilde{A}_{04}$ in equation (2.57) respectively. The order parameter ϕ in equation (2.44) is called M in equation (2.58). The coefficient a_0 in equation (2.44) has been absorbed in $c_t c_\rho^2$. $\bar{u}=u/u^*$ is the ratio of the actual coupling constant of the system over u^*. u^* is the so-called *fixed-point coupling constant for 3-dimensional Ising-like systems.* Its value is 0.472 [40]. Λ is a dimensionless cutoff wave number, which is related to the maximum cutoff wavenumber, Λ_0, of the critical fluctuations.

The expansion of the classical isothermal compressibility is proportional to κ_{cl}^2. It is given by [31,39]:

$$\tilde{\chi}_{\mathrm{cl}}^{-1} \propto \kappa_{\mathrm{cl}}^{2} = \left(\frac{\partial \Delta \tilde{A}_{\mathrm{sing}}}{\partial M^2} \right)_t = t + \frac{1}{2} u^* \bar{u} \Lambda M^2 \propto \xi^{-2} \tag{2.59}$$

Because of the long-range fluctuations, the Helmholtz energy density satisfies a RG-equation that shows how the Helmholtz energy density changes with a change in length scale. To obtain a complete crossover expression from the non-linear renormalisation equations one considers the solution for a special value of the length scale that is called the *match-point value* [33,35,41]. The non-classical, renormalised Helmholtz energy density $\Delta\tilde{A}_{\mathrm{R}}$ is related to the singular part of the classical Helmholtz free-energy density, $\Delta\tilde{A}_{\mathrm{sing}}$, by the following transformations and the addition of a kernel factor [39]:

$$t \to t\mathcal{T}\mathcal{U}^{-1/2} \qquad M \to M\mathcal{D}^{1/2}\mathcal{U}^{1/4} \qquad -\frac{1}{2}t^2\mathcal{K} \tag{2.60}$$

The classical expansion (2.58) is transformed by the renormalization-group matching procedure to:

$$\Delta\tilde{A}_{\mathrm{R}} = \frac{1}{2} t M^2 \mathcal{T}\mathcal{D} + \frac{u^* \bar{u} \Lambda}{4!} M^4 \mathcal{D}^2 \mathcal{U} - \frac{1}{2} t^2 \mathcal{K} \ldots\ldots \tag{2.61}$$

where $\Delta\tilde{A}_{\mathrm{R}}$ = renormalised singular part of the Helmholtz energy density [-]

And equation (2.59) is transformed into:

$$\kappa^2 = \left(\frac{\partial \Delta\tilde{A}_{\mathrm{R}}(t\mathcal{T}, M\mathcal{D}^{1/2})}{\partial (M\mathcal{D}^{1/2})^2} \right)_t = t\mathcal{T} + \frac{1}{2} u^* \bar{u} \Lambda M^2 \mathcal{D}\mathcal{U} \tag{2.62}$$

The rescaling *functions* $\mathcal{T}$, $\mathcal{U}$, $\mathcal{D}$, and $\mathcal{K}$ can be calculated from the RG-coefficients but it is easier to represent them by closed-form approximates [42]. There are several closed-form approximates varying in complexity and accuracy. The approximates of crossover model II, as developed by Chen *et al.* [1,42], and the crossover equation in terms of the parametric variable *Y* are given by:

$$\mathcal{T} = Y^{(2\nu-1)/\Delta} \qquad \mathcal{D} = Y^{(\gamma-2\nu)/\Delta} \qquad \mathcal{U} = Y^{\nu/\Delta} \qquad \mathcal{K} = \frac{\nu}{\alpha \bar{u} \Lambda}\left(Y^{-\alpha/\Delta} - 1\right)$$
$$1 - (1 - \bar{u})Y = \bar{u}\frac{\Lambda}{\kappa} Y^{\nu/\Delta} \tag{2.63}$$

where $\mathcal{T}, \mathcal{U}, \mathcal{D}, \mathcal{K}$ = rescaling functions [-]
Y = crossover variable [-]

The asymptotic critical limit and the classical limit are given by:

$$\lim_{\Lambda/\kappa\to\infty} Y = \left(\frac{\kappa}{\bar{u}\Lambda}\right)^{\Delta/\nu} \qquad \lim_{\Lambda/\kappa\to 1} Y = 1 \tag{2.64}$$

In the asymptotic critical limit the asymptotic scaling laws, including the correction-to-scaling contributions, are recovered and in the classical limit the classical Landau equation (2.58) is recovered [31,39].

2.9.3 Non-asymptotic crossover behaviour

The crossover from asymptotic singular critical behaviour to asymptotic classical critical behaviour has been considered. However, the crossover from singular behaviour near the critical point to the actual non-asymptotic classical behaviour far away from the critical point is needed. Chen *et al.* introduced a solution to the non-asymptotic crossover problem by introducing a number of additional effects [1].
The correlation length, ξ, in the Landau theory refers to the correlation length associated with the critical fluctuations only. As a result, the classical limit is not reached when $\Lambda/\kappa\to 1$ (2.64) but when $\Lambda/\kappa\to 0$. This effect can be incorporated by replacing Λ/κ in equation (2.63) by $(1+\Lambda^2/\kappa^2)^{1/\omega_c}$ [33]. Instead of (2.63), the crossover equation becomes [39]:

$$1-(1-\bar{u})Y = \bar{u}(1+\Lambda^2/\kappa^2)^{1/\omega_c} Y^{\nu/\Delta} \tag{2.65}$$

where ω_c =	crossover exponent	[-]

After this modification, the parameter Λ is the actual microscopic cutoff wavenumber Λ_0. The classical theory will not be valid unless one moves far away from the critical point. However, far away from the critical point an asymptotic two-term expansion (2.61) will no longer be adequate. Chen *et al.* extend the classical Landau expansion (2.57) to a six-term classical Landau expansion [1]:

$$\Delta\tilde{A}_{\mathrm{sing}} = \frac{1}{2}tM^2 + \frac{u^*\bar{u}\Lambda}{4!}M^4 + \frac{1}{5!}\tilde{A}_{05}M^5 + \frac{1}{6!}\tilde{A}_{06}M^6 + \frac{1}{4!}\tilde{A}_{14}tM^4 + \frac{1}{2!2!}\tilde{A}_{22}t^2M^2 + \dots \tag{2.66}$$

The renormalisation transformation can be generalised to include the higher-order terms in the Landau expansion. M^5 is to be replaced by [31]:

$$M^5 \to M^5\mathcal{D}^{5/2}\mathcal{V}\mathcal{U} \qquad \mathcal{V} = Y^{(2\Delta_a-\nu)/2\Delta} \tag{2.67}$$

where Δ_a =	crossover exponent	[-]
$\mathcal{V}$ =	rescaling function	[-]

The exponent Δ_a equals 1.323 and is an additional critical exponent associated with the leading term asymmetric in the order parameter [34,43-45]. The renormalised Helmholtz energy density becomes [1]:

$$\Delta\tilde{A}_{\mathrm{R}} = \frac{1}{2} t M^{2} \mathcal{T}\mathcal{D} + \frac{u^{*}\bar{u}\Lambda}{4!} M^{4} \mathcal{D}^{2} \mathcal{U} + \frac{1}{5!} \tilde{A}_{05} M^{5} \mathcal{D}^{5/2} \mathcal{V}\mathcal{U} + \frac{1}{6!} \tilde{A}_{06} M^{6} \mathcal{D}^{3} \mathcal{U}^{3/2} + \frac{1}{4!} \tilde{A}_{14} t M^{4} \mathcal{T}\mathcal{D}^{2} \mathcal{U}^{1/2} + \frac{1}{2!2!} \tilde{A}_{22} t^{2} M^{2} \mathcal{T}^{2} \mathcal{D}\mathcal{U}^{-1/2} - \frac{1}{2} t^{2} \mathcal{K} \ldots.. \tag{2.68}$$

While the 3-dimensional Ising model and a magnetic system near the critical point are symmetric in the magnetisation *M*, a fluid is not symmetric in the reduced density. Thus, equation (2.68) is valid for a hypothetical symmetric fluid. The term proportional to *M* ^{5} and the exponent Δ_a partially account for this lack of symmetry. The lack of symmetry can be accounted for by the following mixing of the relevant scaling fields [1,34,38,46]:

$$\begin{gathered} \Delta\tilde{A}(t,M) = \Delta\tilde{A}_{\mathrm{R,symm}}(t,M) - c\left(\frac{\partial\Delta\tilde{A}_{\mathrm{R,symm}}}{\partial M}\right)_{t}\left(\frac{\partial\Delta\tilde{A}_{\mathrm{R,symm}}}{\partial t}\right)_{M} \\ t = c_{t}\Delta\tilde{T} + c\left(\frac{\partial\Delta\tilde{A}_{\mathrm{R,symm}}}{\partial M}\right)_{t} \qquad M = c_{\rho}(\Delta\tilde{\rho} - d_{1}\Delta\tilde{T}) + c\left(\frac{\partial\Delta\tilde{A}_{\mathrm{R,symm}}}{\partial t}\right)_{M} \end{gathered} \tag{2.69}$$

where c, d_1 = system-dependent coefficients [-]

$\Delta\tilde{A}_{\mathrm{R}}$ = renormalised singular part of the Helmholtz energy density for a symmetric system [-]

2.10 Global crossover behaviour

Even the non-asymptotic crossover model of Chen *et al.* fails to make connection with the behaviour of fluids very far away from the critical point. One would like to have a simple closed-form equation, which would describe the behaviour of a fluid accurately over the entire thermodynamic surface. There are many classical closed-form equations of state which, depending on their quality, provide a reasonable description of thermodynamic properties far away from the critical point but fail close to it. Attempts have been made to correct some of these closed-form equations of state for the effects of critical fluctuations. Such corrected equations should provide both the universal critical behaviour near the critical point and the non-critical regular behaviour far away from the critical point. Kostrowicka Wyczalkowska *et al.* applied the crossover theory to the Van der Waals equation of state, Van Pelt *et al.* applied the crossover theory to the Carnahan-Starling-DeSantis equation of state, and Edison *et al.* applied it to the NRTL excess Gibbs model [2,47,48].

3 Liquid-Liquid Equilibria

3.1 Calculation of liquid-liquid equilibria

Insight in liquid-liquid phase equilibria is best obtained by an analysis of the Gibbs energy, *G*. The Gibbs energy of an ideal mixture, G^{id}, is given by:

$$G^{\mathrm{id}} = \sum_{i}^{N} x_i G_i + RT\sum_{i}^{N} x_i \ln(x_i) \qquad (3.1)$$

where G^{id} = Gibbs energy of an ideal mixture [J/mole]
G_i = Gibbs energy of pure *i* [J/mole]
x_i = mole fraction of component *i* [$\mathrm{mole_i/mole_{tot}}$]
N = number of components [-]
R = universal gas constant [J/(mole·K)]

Many liquid mixtures do not show ideal mixing behaviour and are partial miscible or immiscible at normal temperatures. According to the second law of thermodynamics, the total Gibbs energy of a closed system at constant temperature and pressure is at its minimum at equilibrium. Therefore, the total Gibbs energy of liquid phases that are in equilibrium must be lower than the Gibbs energy of a homogeneous liquid mixture. Deviations from ideal mixing behaviour can be accounted for by a correction factor like the activity coefficient γ_i:

$$G = \sum_{i}^{N} x_i G_i + RT\sum_{i}^{N} x_i \ln(x_i) + RT\sum_{i}^{N} x_i \ln(\gamma_i) \qquad (3.2)$$

The third part of equation (3.2), which accounts for the non-ideality, is called the excess Gibbs energy, G^E, of the mixture. The second and the third term form the Gibbs energy of mixing, ΔG. Liquid-liquid phase equilibria can be calculated by equality of the activities, $a_i = x_i\gamma_i$ or chemical potentials, μ_i, of both coexisting phases:

$$(x_i\gamma_i)' = (x_i\gamma_i)'' \qquad \mu_i' = \mu_i'' \qquad (3.3)$$

where γ_i = activity coefficient of component *i* in phase ' [-]
μ_i = chemical potential of component *i* in phase ' [J/mole]

In order to calculate the activity or the chemical potential, one needs a model to describe the excess Gibbs energy. One such a model is the Non-Random Two Liquid model.

3.2 The Non-Random Two Liquid (NRTL) theory

Excess functions have commonly been expressed by algebraic expansions of mole fractions with arbitrary temperature-dependent coefficients, which are obtained by fitting experimental data. In order to represent the experimental data, as many terms and parameters as necessary are introduced.

Wilson showed that the excess Gibbs energy could be conveniently expressed by an algebraic expression of local composition [49]. Local composition models take into account the non-randomness in liquid mixtures. The local compositions are different from the overall compositions. They account for the short-range order and the non-random molecular orientations that are the result of differences in molecular size and differences in molecular forces between molecules of different components. Wilson suggested the following relation between local mole fraction x_{11} of molecules 1 and local mole fraction x_{21} of molecules 2, which are in the immediate neighbourhood of molecules 1:

$$\frac{x_{21}}{x_{11}}=\frac{x_2}{x_1}\cdot\frac{\exp(-g_{21}/RT)}{\exp(-g_{11}/RT)} \qquad \frac{x_{12}}{x_{22}}=\frac{x_1}{x_2}\cdot\frac{\exp(-g_{12}/RT)}{\exp(-g_{22}/RT)} \tag{3.4}$$

where			
	g_{ij} =	interaction energy between an *i-j* pair of molecules	[J/mole]
	g_{ii} =	interaction energy between an *i-i* pair of molecules	[J/mole]
	x_{ij} =	local mole fraction of molecule *i* in the immediate neighbourhood of molecule *j*	[-]

The NRTL theory, as proposed by Renon and Prausnitz, is a modification of the relation given by Wilson. Renon and Prausnitz introduced a non-randomness factor α_{12} in the relation of Wilson [50]:

$$\frac{x_{21}}{x_{11}}=\frac{x_2}{x_1}\cdot\frac{\exp(-\alpha_{12}g_{21}/RT)}{\exp(-\alpha_{12}g_{11}/RT)} \qquad \frac{x_{12}}{x_{22}}=\frac{x_1}{x_2}\cdot\frac{\exp(-\alpha_{12}g_{12}/RT)}{\exp(-\alpha_{12}g_{22}/RT)} \tag{3.5}$$

where α_{12}= non-randomness parameter [-]

The local mole fractions are related by:

$$x_{21}+x_{11}=1 \qquad x_{12}+x_{22}=1 \tag{3.6}$$

According to equation (3.5) and (3.6), the local mole fractions are given by:

$$x_{21}=\frac{x_2\exp\left(-\alpha_{12}(g_{21}-g_{11})/RT\right)}{x_1+x_2\exp\left(-\alpha_{12}(g_{21}-g_{11})/RT\right)} \qquad x_{12}=\frac{x_1\exp\left(-\alpha_{12}(g_{12}-g_{22})/RT\right)}{x_2+x_1\exp\left(-\alpha_{12}(g_{12}-g_{22})/RT\right)} \tag{3.7}$$

To obtain an expression for the excess Gibbs energy, Scott's two-liquid theory of binary mixtures is used [51]. Scott assumes that there are two kinds of cells in a binary mixture: one with molecule 1 at the centre and one with molecule 2 at the centre. See Figure (3.1).

The residual Gibbs energy of a cell containing molecule 1 at its centre is given by:

$$g^{(1)}=x_{11}g_{11}+x_{21}g_{21} \tag{3.8}$$

where $g^{(i)}$= residual Gibbs energy of a cell containing molecule *i* at its centre

The residual Gibbs energy for a cell containing pure liquid 1 with molecule 1 at its centre is:

$$g_{pure}^{(1)} = g_{11} \tag{3.9}$$

where $g_{pure}^{(i)}$ = Gibbs energy of a cell containing pure i

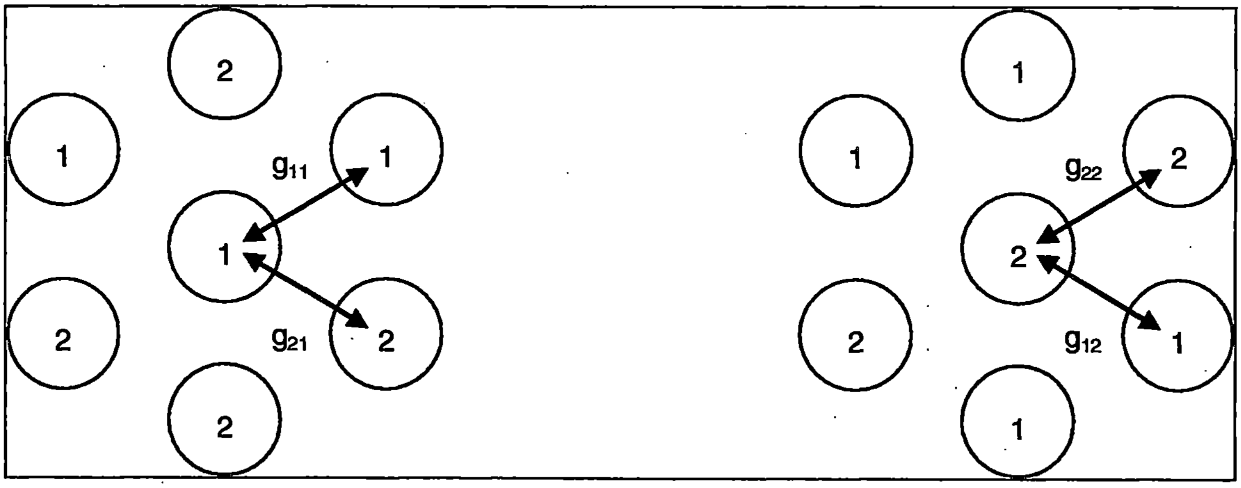

Figure 3.1: Left picture, molecule 1 at centre of cell and right picture, molecule 2 at centre of cell. The interaction energies between particles are also indicated in this picture.

The molar excess Gibbs energy for a binary solution is the sum of two changes in the residual Gibbs energy. First that of transferring x_1 molecules from a cell of pure liquid 1 into a cell 1 of the solution, and second, that of transferring x_2 molecules of pure liquid 2 into a cell of the solution. Therefore, the molar excess Gibbs free energy can be written as:

$$G^E = x_1(g^{(1)} - g_{pure}^{(1)}) + x_2(g^{(2)} - g_{pure}^{(2)}) = x_1 x_{21}(g_{21} - g_{11}) + x_2 x_{12}(g_{12} - g_{22}) \tag{3.10}$$

The NRTL equation follows from equation (3.7) and (3.10):

$$\frac{G^E}{RT} = x_1 x_2 \left\{ \frac{\frac{(g_{21} - g_{11})}{RT} \exp\left(\frac{-\alpha_{12}(g_{21} - g_{11})}{RT}\right)}{x_1 + x_2 \exp\left(\frac{-\alpha_{12}(g_{21} - g_{11})}{RT}\right)} + \frac{\frac{(g_{12} - g_{22})}{RT} \exp\left(\frac{-\alpha_{12}(g_{12} - g_{22})}{RT}\right)}{x_2 + x_1 \exp\left(\frac{-\alpha_{12}(g_{12} - g_{22})}{RT}\right)} \right\} \tag{3.11}$$

The non-randomness factor α_{12} is the analogue of the inverse of the co-ordination number, *1/z*, in the theory of Guggenheim [52]. However, α_{12} is not based on a lattice model and is assumed to be an empirical constant, independent of temperature. The co-ordination number in the theory of Guggenheim is of the order 6-12, and α_{12} can be expected to be a positive constant of the order of 0.1-0.3. According to the theory of Guggenheim, it is clear that the physical significance of α_{12} is obscure for values of α_{12} smaller than 0.1 and larger than 0.3. However, values exceeding 0.3 are found for associated mixtures for which Guggenheim's theory is not applicable [50].

Compared to the Wilson equation, the NRTL equation has an advantage in that it, with a suitable selection of the parameter α_{12}, can describe partial miscibility.
The NRTL equation shows several complications. The major complication is the great and scarcely predictable flexibility of this equation, which even permits description of two two-phase regions for a binary system so that, up to six pairs of compositions of coexisting phases may be obtained [53]. Either one or two pairs are thermodynamically stable. After optimisation of the NRTL parameters by data regression, the dependence of the Gibbs energy of mixing, $\Delta G/(RT)$, on the mole fraction, x_i, should be checked. An example is given in Figure (3.2). The solutions *a-c*, *a-d*, *e-c*, and *e-b* are unstable because they do not minimise the total Gibbs energy of mixing. The only stable solution is *a-e*.

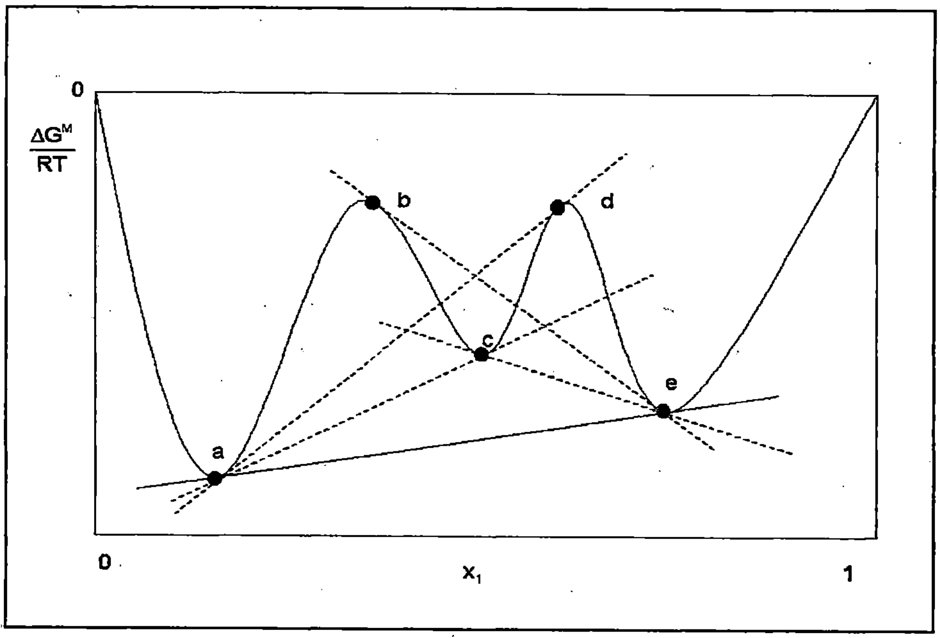

Figure 3.2: Stable and unstable solutions for the Gibbs energy of mixing

In principle, the NRTL equation contains three parameters. In the initial stages of the application of this equation, attempts were made to employ the values of α_{12} recommended by the authors, which was gradually found unsuitable. At present, all three parameters are often optimised. An ideal system can be realised by zero values of τ_{12} and τ_{21} at every value of α_{12}. It is clear that in slightly non-ideal systems, algorithms determining all three parameters will not work [53].
The value of $\alpha_{12} = -1$ recommended in the literature cannot be considered universal, as it is suitable only for some systems [54]. Just as the NRTL equation with $\alpha_{12} > 0.426$ cannot describe partial miscible systems, so the equation with $\alpha_{12} = -1$ cannot describe systems with $x_c = \notin (0.16; 0.84)$. Renon and Prausnitz recommend $\alpha_{12}=0.2$ for mixtures of saturated hydrocarbons with polar non-associated liquids and $\alpha_{12}=0.4$ for mixtures of saturated hydrocarbons and the homolog perfluorocarbons [50]. For $\alpha_{12} = 0.2$, the critical point can lie in the interval $x_c = \in (0.20; 0.80)$.

3.3 The dependence of the excess Gibbs energy on temperature

In relationships based on local compositions (Wilson, Uniquaq, NRTL, etc.), the temperature dependence is included in the exponents. If the NRTL equation is to be used in a broad temperature region, the interaction energies $(g_{ij}-g_{jj})$ and $(g_{ji}-g_{ii})$ are mostly considered to be linearly dependent on temperature. Sometimes, the parameter α_{12} is also considered to be temperature-dependent. Quadratic temperature dependence has been considered by Nagata and Yamada [55]. With such parameters, the compositions of the coexisting phases can be described very well. However, for quadratic temperature dependence already 6 adjustable parameters are needed. It is clear that modifying the NRTL-parameters in this way, and thus the NRTL-equation, takes all theoretical background away.

Novak shows that it is possible to force the NRTL model to go through the critical point of the binary liquid cyclohexane - methanol with linear temperature dependence of the parameters $(g_{12}-g_{22})$, $(g_{21}-g_{11})$, and α_{12} [53]. Bittrich *et al.* also show for five different binary liquids that it is possible to use the NRTL model in the critical region with linear temperature dependence of the parameters $(g_{12}-g_{22})$, $(g_{21}-g_{11})$, and a value for α_{12} near -1 [56]. However, both Novak and Bittrich do not have data points very close to the critical point and they do not check the limiting behaviour.

4 Results and discussion

4.1 Description of liquid-liquid equilibria with the classical NRTL model

In order to show the shortcomings of the classical NRTL model, the calculation of a phase boundary is discussed here. According to equation (3.2), the total Gibbs energy of mixing of a binary mixture can be written in the following way:

$$\frac{\Delta G}{RT} = x_1 \ln(x_1) + x_2 \ln(x_2) + \frac{G^E}{RT} \tag{4.1}$$

where	ΔG=	Gibbs energy of mixing	[J/mole]
	G^E=	Excess Gibbs energy	[J/mole]

The excess Gibbs energy is described by the classical NRTL model:

$$\frac{G^E}{RT} = x_1 x_2 \cdot \left\{ \frac{\tau_{21} G_{21}}{x_1 + x_2 G_{21}} + \frac{\tau_{12} G_{12}}{x_2 + x_1 G_{12}} \right\} \tag{4.2}$$

The coupling between the NRTL parameters in equation (4.2) and the interaction energies in equation (3.11) is given by:

$$\begin{aligned} \tau_{21} &= \frac{g_{21} - g_{11}}{RT} & \qquad \tau_{12} &= \frac{g_{12} - g_{22}}{RT} \\ G_{21} &= \exp(-\alpha_{12}\tau_{21}) & \qquad G_{12} &= \exp(-\alpha_{12}\tau_{12}) \end{aligned} \tag{4.3}$$

As an example, the liquid-liquid equilibria of the binary liquid acetic anhydride - heptane is analysed here. Phase-boundary data for this system are given by Nagarajan *et al.* [57]. The classical NRTL model is not able to describe the coexistence curve up to the critical region because critical fluctuations are neglected in classical equations. If all data points are taken into account during optimisation of the NRTL parameters, the result will be both bad in the classical region, *i.e.* far away from the critical point, and in the critical region. The coexistence curve in Figure (4.1) has been obtained by data regression to 6 points in the range 275 K – 310 K, which is more than 20°C away from the real critical point. The interaction energies $(g_{21} - g_{11})$ and $(g_{12} - g_{22})$ were taken with linear temperature dependence. The value of α_{12} was fixed at 0.2. The fit in the classical region is good. At higher temperatures, there is a large overshoot with respect to the experimental data points. Like all mean-field equations, the classical NRTL model predicts a critical temperature that is much higher than the experimental critical temperature, and a coexistence curve with the wrong critical curvature.

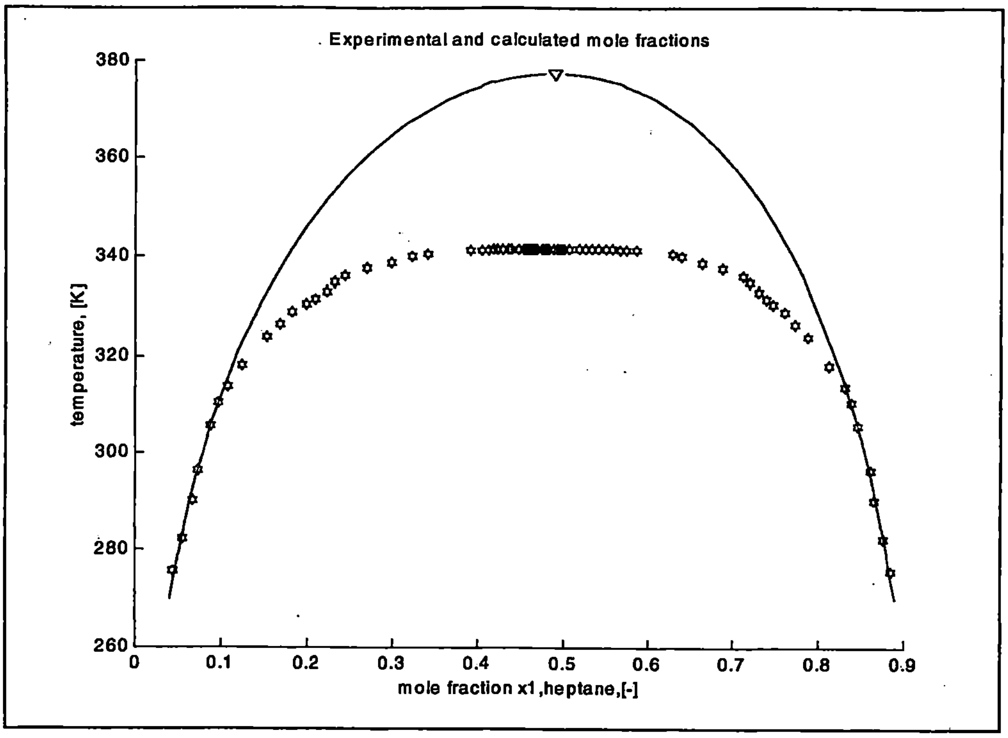

Figure 4.1: Experimental (blue stars) and calculated (red line) phase boundary with the classical NRTL model for acetic anhydride + cyclohexane

4.2 Crossover-NRTL model

In order to be able to describe the coexistence curve both in the classical and the critical regions, critical fluctuations must be introduced into the classical NRTL equation. Edison *et al.* give the procedure that must be applied to the NRTL equation [2]. The variables are made dimensionless in the following way:

$$\bar{T} = -\frac{T_c^{cl}}{T} \qquad \bar{x} = \frac{x}{x_c^{cl}} \qquad \Delta\tilde{G} = \frac{\Delta G}{RT}$$

$$\Delta\bar{T} = 1 - \frac{T_c^{cl}}{T} \qquad \Delta\bar{x} = \frac{x}{x_c^{cl}} - 1 \tag{4.4}$$

where T_c= classical critical temperature [K]
x_c= classical mole fraction at the critical point [-]
$\bar{T}$ = reduced temperature, reduced with classical T_c [-]
$\Delta\bar{T}$ = reduced temperature minus 1, reduced with classical T_c [-]
$\bar{x}$ = reduced mole fraction, reduced with classical x_c [-]
$\Delta\bar{x}$ = 1 minus reduced mole fraction, reduced with classical x_c [-]

The NRTL parameters τ_{21} and τ_{12} can be rewritten in these reduced variables. The interaction energies $(g_{21}-g_{11})$ and $(g_{12}-g_{11})$ are taken with a linear temperature dependence:

$$\tau_{21} = \tilde{a}(1-\tilde{b}\Delta\bar{T}) \qquad \tau_{12} = \tilde{c}(1-\tilde{d}\Delta\bar{T}) \tag{4.5}$$

The classical Gibbs energy of mixing is separated into a regular and a singular part in analogy with the Helmholtz energy in the Landau theory. This can be accomplished by expanding it around the classical consolute critical point:

$$\Delta\tilde{G}_{\mathrm{cl}}(\bar{T},\bar{x}) = \sum_{k=0}^{\infty} \frac{\Delta\tilde{G}_{\mathrm{cl}}^{(k)}(\bar{T},1)}{k!}(\bar{x}-1)^k \tag{4.6}$$

The terms of second and higher order in $\bar{x}$ are combined to form the critical or singular part, $\Delta\tilde{G}_{\mathrm{sing}}$. The regular part, $\Delta\tilde{G}_{\mathrm{reg}}$, consists of the terms of zero order and first order in $\bar{x}$:

$$\begin{aligned}\Delta\tilde{G}_{\mathrm{reg}} = {} & x\cdot\ln\left(\frac{x_{\mathrm{c}}}{1-x_{\mathrm{c}}}\right)+\ln(1-x_{\mathrm{c}})+ \\ & (x_{\mathrm{c}}^{2}+x-2xx_{\mathrm{c}})\cdot\left\{\frac{\tau_{21}G_{21}}{x_{\mathrm{c}}+(1-x_{\mathrm{c}})G_{21}}+\frac{\tau_{12}G_{12}}{1-x_{\mathrm{c}}+x_{\mathrm{c}}G_{12}}\right\}- \\ & (x-x_{\mathrm{c}})x_{\mathrm{c}}(1-x_{\mathrm{c}})\left\{\frac{\tau_{21}G_{21}(1-G_{21})}{\left(x_{\mathrm{c}}+(1-x_{\mathrm{c}})G_{21}\right)^{2}}+\frac{\tau_{12}G_{12}(G_{12}-1)}{\left(1-x_{\mathrm{c}}+x_{\mathrm{c}}G_{12}\right)^{2}}\right\}\end{aligned} \tag{4.7}$$

$$\begin{aligned}\Delta\tilde{G}_{\mathrm{sing}} = {} & x\cdot\ln\left(\frac{x}{1-x}\right)+\ln\left(\frac{1-x}{1-x_{\mathrm{c}}}\right)-x\cdot\ln\left(\frac{x_{\mathrm{c}}}{1-x_{\mathrm{c}}}\right)+ \\ & x\cdot(1-x)\cdot\left\{\frac{\tau_{21}G_{21}}{x+(1-x)G_{21}}+\frac{\tau_{12}G_{12}}{1-x+xG_{12}}\right\}- \\ & (x_{\mathrm{c}}^{2}+x-2xx_{\mathrm{c}})\cdot\left\{\frac{\tau_{21}G_{21}}{x_{\mathrm{c}}+(1-x_{\mathrm{c}})G_{21}}+\frac{\tau_{12}G_{12}}{1-x_{\mathrm{c}}+x_{\mathrm{c}}G_{12}}\right\}+ \\ & (x-x_{\mathrm{c}})x_{\mathrm{c}}(1-x_{\mathrm{c}})\left\{\frac{\tau_{21}G_{21}(1-G_{21})}{\left(x_{\mathrm{c}}+(1-x_{\mathrm{c}})G_{21}\right)^{2}}+\frac{\tau_{12}G_{12}(G_{12}-1)}{\left(1-x_{\mathrm{c}}+x_{\mathrm{c}}G_{12}\right)^{2}}\right\}\end{aligned} \tag{4.8}$$

Because the regular part contains only the *value* of the Gibbs energy of mixing and the *slope*, both at $x=x_c$, it will not be modified by the crossover transformation and will remain an analytic function of reduced temperature. The critical part will become a singular function after the effects of fluctuations are incorporated. According to equation (4.4), the mole fraction can be written as $x = x_{\mathrm{c}}(\Delta\bar{x}+1)$. In the classical theory, the square of the inverse correlation length, κ_{cl}^2, for the NRTL model is defined as:

$$\kappa_{\mathrm{cl}}{}^2 = \left(\frac{\partial^2 \Delta\tilde{G}_{\mathrm{sing}}}{\partial \Delta\bar{x}^2}\right) = \frac{x_{\mathrm{c}}{}^2}{x(1-x)} - 2x_{\mathrm{c}}{}^2 \cdot \left\{\frac{\tau_{21}G_{21}}{x+(1-x)G_{21}} + \frac{\tau_{12}G_{12}}{1-x+xG_{12}}\right\} -$$
$$2(x_{\mathrm{c}} - 2x_{\mathrm{c}}x) \cdot \left\{\frac{\tau_{21}G_{21}x_{\mathrm{c}}(1-G_{21})}{\left(x_{\mathrm{c}}+(1-x_{\mathrm{c}})G_{21}\right)^2} + \frac{\tau_{12}G_{12}x_{\mathrm{c}}(G_{12}-1)}{\left(1-x_{\mathrm{c}}+x_{\mathrm{c}}G_{12}\right)^2}\right\} + \tag{4.9}$$
$$2(x-x^2) \cdot \left\{\frac{\tau_{21}G_{21}x_{\mathrm{c}}{}^2(1-G_{21})^2}{\left(x_{\mathrm{c}}+(1-x_{\mathrm{c}})G_{21}\right)^3} + \frac{\tau_{12}G_{12}x_{\mathrm{c}}{}^2(G_{12}-1)^2}{\left(1-x_{\mathrm{c}}+x_{\mathrm{c}}G_{12}\right)^3}\right\}$$

Close to the critical point, the singular part of the Gibbs energy of mixing has to be transformed to take into account the effects of critical fluctuations. Edison *et al.* apply the transformation of Chen *et al.* [1] to the classical NRTL model. This transformation has been developed for the Helmholtz energy density of a one-component fluid near the liquid-vapour critical point, where the order parameter can be identified with the overall density. In incompressible liquid mixtures, the order parameter can be identified with the concentration *x*. Now, the reduced variables are expressed in terms of the real critical parameters, *i.e.* $\Delta\bar{x}$ and $\Delta\bar{T}$ are to be replaced by $\Delta\tilde{x}$ and $\Delta\tilde{T}$ respectively. The renormalised variables and the accompanying rescaling functions are given by:

$$\Delta\tilde{T} = \left(1 - \frac{T_{\mathrm{c}}}{T}\right) \qquad \Delta\tilde{x} = \left(\frac{x}{x_{\mathrm{c}}} - 1\right) \qquad \tau_{21} = \tilde{a}(1-\tilde{b}\Delta\tilde{T}) \qquad \tau_{12} = \tilde{c}(1-\tilde{d}\Delta\tilde{T})$$

$$\Delta\tilde{T}_{\mathrm{R}} = \Delta\tilde{T}\mathcal{T}\mathcal{U}^{-1/2} \qquad \Delta\tilde{x}_{\mathrm{R}} = \Delta\tilde{x}\mathcal{D}^{1/2}\mathcal{U}^{1/4} \tag{4.10}$$

$$\mathcal{T} = Y^{\frac{2\nu-1}{\nu\omega}} \qquad \mathcal{U} = Y^{\frac{1}{\omega}} \qquad \mathcal{D} = Y^{\frac{-\eta}{\omega}} \qquad \mathcal{K} = \frac{\nu}{\alpha\bar{u}\Lambda}\left(Y^{\frac{-\alpha}{\nu\omega}} - 1\right)$$

where	$\nu, \omega, \eta, \alpha =$	universal critical exponents	[-]
	$\tilde{x} =$	reduced mole fraction, reduced with real x_{c}	[-]
	$\Delta\tilde{x} =$	1 minus reduced mole fraction, reduced with real x_{c}	[-]
	$\tilde{T} =$	reduced temperature, reduced with real T_{c}	[-]
	$\Delta\tilde{T} =$	reduced temperature minus 1, reduced with real T_{c}	[-]
	$\Delta\tilde{x}_{\mathrm{R}}, \Delta\tilde{T}_{\mathrm{R}} =$	renormalised reduced variables	[-]

A kernel term must be added to the singular part of the Gibbs energy of mixing to include fluctuation-induced contributions. The reduced mole fraction $\Delta\tilde{x}$ and the reduced temperature $\Delta\tilde{T}$ in $\Delta\tilde{G}_{\mathrm{sing}}$ (Equation 4.8) have to be replaced by the renormalised ones (Equation 4.10):

$$\Delta\tilde{G}_{\mathrm{sing}} = \Delta\tilde{G}_{\mathrm{sing}}(\Delta\tilde{x} = \Delta\tilde{x}_{\mathrm{R}}, \Delta\tilde{T} = \Delta\tilde{T}_{\mathrm{R}}) - \frac{1}{2}c_t{}^2\Delta\tilde{T}^2\mathcal{K} \tag{4.11}$$

The function *Y* is a crossover function, which is implicitly defined through:

$$1-(1-\bar{u})Y=\bar{u}\left\{1+\left(\frac{\Lambda}{\kappa}\right)^2\right\}^{1/2}Y^{\frac{1}{\omega}} \tag{4.12}$$

The renormalised parameter κ^2 is obtained through $\kappa_{\mathrm{cl}}^{\,2}(\Delta\tilde{T},\Delta\tilde{x})$ by:

$$\kappa^2=\frac{Y^{\frac{1}{2\omega}}}{c_p^{\,2}}\kappa_{\mathrm{cl}}^{\,2}(\Delta\tilde{T}=\Delta\tilde{T}_{\mathrm{R}},\Delta\tilde{x}=\Delta\tilde{x}_{\mathrm{R}}) \tag{4.13}$$

To be able to calculate the liquid-liquid phase boundary, one has to calculate the activities of both components in both coexisting phases. These activities are defined by:

$$\begin{aligned}\ln(a_1)'&=\Delta\tilde{G}'+(1-x')\cdot\frac{d}{dx'}\left(\frac{\Delta G'}{RT}\right)=\Delta\tilde{G}_{\mathrm{reg}}{}'+\Delta\tilde{G}_{\mathrm{sing}}{}'(\Delta\tilde{T}_{\mathrm{R}},\Delta\tilde{x}_{\mathrm{R}})+\\&\quad(1-x')\cdot\frac{d}{dx'}\left(\Delta\tilde{G}_{\mathrm{reg}}{}'+\Delta\tilde{G}_{\mathrm{sing}}{}'(\Delta\tilde{T}_{\mathrm{R}},\Delta\tilde{x}_{\mathrm{R}})\right)\\[2ex]\ln(a_2)'&=\Delta\tilde{G}'-x'\cdot\frac{d}{dx'}\left(\frac{\Delta G'}{RT}\right)=\Delta\tilde{G}_{\mathrm{reg}}{}'+\Delta\tilde{G}_{\mathrm{sing}}{}'(\Delta\tilde{T}_{\mathrm{R}},\Delta\tilde{x}_{\mathrm{R}})-\\&\quad x'\cdot\frac{d}{dx'}\left(\Delta\tilde{G}_{\mathrm{reg}}{}'+\Delta\tilde{G}_{\mathrm{sing}}{}'(\Delta\tilde{T}_{\mathrm{R}},\Delta\tilde{x}_{\mathrm{R}})\right)\end{aligned} \tag{4.14}$$

where a_i' = activity of component i in phase $'$ [-]
x' = mole fraction of component 1 in phase $'$ [-]

The calculation of the derivative of $\Delta\tilde{G}_{\mathrm{sing}}(\Delta\tilde{T}_{\mathrm{R}},\Delta\tilde{x}_{\mathrm{R}})$ to the unrenormalised variable x is rather complex. To calculate this derivative, the derivative of the crossover function Y to the unrenormalised variable x is needed. This derivative can be calculated by implicit differentiation of the crossover function as given in equation Appendix A.

4.3 Errors in the Crossover-NRTL model of Edison *et al.*

Unfortunately, the model of Edison as described in his paper [2] cannot be used for data regression and for the description of the phase boundary because there are some errors in it.
Edison describes the liquid-liquid equilibria of the binary liquid acetic anhydride - heptane [2]. The equilibrium data for this binary liquid have been measured by Nagarajan *et al.* [57]. These data can be analysed with the following extended Wegner expansion:

$$\Delta\tilde{x}^{\pm} = \pm B_0 \left|\frac{T-T_c}{T}\right|^{\beta}\left\{1+B_1\left|\frac{T-T_c}{T}\right|^{\Delta_s}\right\}+d_{\mathrm{sing}}\left|\frac{T-T_c}{T}\right|^{1-\alpha}+d_{2\beta}\left|\frac{T-T_c}{T}\right|^{2\beta}+d_1\left|\frac{T-T_c}{T}\right|+\ldots.. \qquad (4.15)$$

where B_0, B_1, d_{sing}, $d_{2\beta}$, d_1= amplitudes [-]

The relations for the amplitudes B_0 and B_1 of the power laws in equation (4.15) are given by [58]:

$$B_0 = 0.534\left(\frac{c_t^{\,0.5}}{\bar{u}\Lambda}\right)\frac{(\bar{u}\Lambda)^{0.5}}{c_\rho} \qquad B_1 = 2.98\left(\frac{c_t^{\,0.5}}{\bar{u}\Lambda}\right)^{2\Delta_s}(1-\bar{u}) \qquad (4.16)$$

After data regression of the data set to the extended Wegner expansion (4.15) in the temperature range $|\Delta\tilde{T}|$<0.01, one obtains B_0=1.58 and B_1=-1.05. Physically realistic values for c_t, $\bar{u}$ and Λ are positive. Therefore, for the amplitude B_1 to be negative, $\bar{u}$ must be larger than 1. However, Edison gets $\bar{u}$=0.555 after optimisation of his crossover-NRTL model to the data set measured by Nagarajan *et al.*.

Edison *et al.* correctly state that the number of parameters of the crossover-NRTL model can be reduced by two by applying the conditions of incipient immiscibility at the real consolute critical point:

$$\left(\frac{\partial^2\Delta\tilde{G}}{\partial x^2}\right)\Bigg|_{x=x_c,T=T_c} = \left(\frac{\partial^3\Delta\tilde{G}}{\partial x^3}\right)\Bigg|_{x=x_c,T=T_c} = 0 \qquad (4.17)$$

According to Edison, these two equations should result in universal values for the NRTL equation, $\tilde{a}$=1.3474 and $\tilde{c}$=0.94366. Edison uses these "universal" NRTL parameters for different binary liquids. However, at the critical point, T equals T_c and, therefore, $\Delta\tilde{T}$=0, τ_{21} = $\tilde{a}$ and τ_{12} = $\tilde{c}$ (4.10). The conditions in equation (4.17) depend on $\tilde{a}$, $\tilde{c}$, and x_c. This means that $\tilde{a}$ and $\tilde{c}$ do not have universal values at all because they depend on the mole fraction x_c at the critical point.

Other errors in Edison's model are some missing factors x_c^2 in the derivatives of κ^2 with respect to $\Delta\tilde{T}$ and $\Delta\tilde{x}$ and the omission of the parameters c_t (4.11) in the kernel term and c_ρ^2 in the relation for κ^2 (4.13). The importance of the parameters c_t and c_ρ will be dealt with in paragraph (4.4). The errors mentioned above were found by comparing the Crossover-NRTL model of Edison *et al.* with a much simpler model, the Two-Term Landau Expansion.

4.4 Simplified Two-Term Landau expansion reformulated for the NRTL model

The optimisation of the NRTL parameters and the crossover parameters and the calculation of the phase boundary for the NRTL model are in general rather complicated. This calculation is much easier for the 2T-Landau expansion. The 2T-Landau expansion has been introduced in Chapter 1.

The Crossover-NRTL model needs good estimates for the crossover parameters $\bar{u}$ and Λ, and for the NRTL parameters $\tilde{b}$ and $\tilde{d}$, otherwise, the model will return infeasible solutions. The capability of the Landau model to give estimates for these parameters is investigated in this paragraph and in the following paragraph.

When the kernel term is neglected and the order parameter is defined as $M = c_p \Delta\tilde{x}$, the coexistence curve is symmetric with respect to the critical point. In this case the conditions for phase equilibrium are given by:

$$\left(\frac{\partial \Delta \tilde{G}_{\text{sing}}}{\partial M}\right)_t' = \left(\frac{\partial \Delta \tilde{G}_{\text{sing}}}{\partial M}\right)_t'' = 0 \tag{4.18}$$

Only one of the relations in equation (4.18) serves as a constraint during data regression because of the symmetry of the coexistence curve. The order parameter of the one branch can be calculated from the order parameter of the other branch:

$$M' = -M'' \qquad \Rightarrow \qquad x'' = 2x_c - x' \tag{4.19}$$

When the kernel term and the implicit dependence of Y on M are neglected, it is possible to calculate the analytical solution of equation (4.18) in the two-phase region:

$$M^2 = \frac{-6tT}{u^* u \Lambda \mathcal{D}\mathcal{U}} \qquad \kappa^2 = -2tY^{\frac{2\nu-1}{\Delta_s}} \tag{4.20}$$

The advantage of this simplified 2T-Landau expansion is that the calculation of the phase boundary is very simple. However, the model cannot account for the asymmetry of the coexistence curve with respect to x_c, because the order parameter $M = c_p \Delta\tilde{x}$ is equal in magnitude at both branches of the coexistence curve (but different sign). The phase boundary for the binary liquid acetic anhydride - cyclohexane, calculated with this simplified 2T-Landau model, is given in Figure (4.2). The calculated phase boundary for the binary liquid nitrobenzene - octane, which is more symmetric, is given in Figure (4.3). It is clear from Figure (4.2) and from Figure (4.3) that the simplified 2T-Landau model is not able to represent asymmetric coexistence curves. The model cannot reproduce the correct diameter of the coexistence curve. Of course, simplifying an expansion with only two leading terms reduces the range of validity. Actually, this simplified 2T-Landau model is only valid very close to the critical point. For binary liquids with a very symmetric coexistence curve, this model is a good approximation within a restricted temperature range.

The couplings between the crossover-NRTL model and the simplified 2T-Landau theory are the system-dependent amplitudes c_t and c_p. The amplitudes c_t and c_p are given by:

$$c_t = \frac{\tilde{G}_{12}(\tilde{a},\tilde{b},\tilde{c},\tilde{d})}{\sqrt{\tilde{G}_{04}(\tilde{a},\tilde{c})}}\sqrt{u^*\bar{u}\Lambda} \qquad c_\rho = \sqrt[4]{\frac{\tilde{G}_{04}(\tilde{a},\tilde{c})}{u^*\bar{u}\Lambda}} \tag{4.21}$$

where $\tilde{G}_{12} =$ partial derivative of the Gibbs energy of mixing one time to $\Delta\tilde{T}$ and two times to $\Delta\tilde{x}$, evaluated at the critical point. This property is called a_0 in the Landau theory. [-]

$\tilde{G}_{04}$ = partial derivative of the Gibbs energy of mixing four times to $\Delta\tilde{x}$, evaluated at the critical point. This property is called u_0 in the Landau theory. [-]

The derivative $\tilde{G}_{12}$ is evaluated at the critical point and it depends on the NRTL parameters $\tilde{a}$, $\tilde{b}$, $\tilde{c}$, and $\tilde{d}$, as indicated in equation (4.21). The derivative $\tilde{G}_{04}$ is also evaluated at the critical point and it depends on the values of $\tilde{a}$ and $\tilde{c}$, which can be calculated from equation (4.17).
The optimised crossover parameters, obtained with the simplified 2T-Landau model, for the binary liquid nitrobenzene - octane are given in Table (4.1) together with the crossover parameters for the Crossover-NRTL model. According to Table (4.1), the simplified 2T-Landau expansion is able to give good estimates for c_ρ and $\bar{u}$ when, for example, c_t and Λ are fixed. This perfect symmetric model is only valid very close to the critical point. The results in Table (4.1) are obtained for the temperature range $|\Delta\tilde{T}|<0.01$. To fix c_t, in order to get estimates for c_ρ and $\bar{u}$, an estimate for c_t is needed. In this work, all calculated values for c_t lie between 0.43 and 0.88. Also, 0.5 seems to be a good estimate for c_t. It is not possible to calculate the independent values of $\tilde{b}$ and $\tilde{d}$ from c_t (4.21) because there is only one relation and there are two unknown variables.

The κ_{cl}^2 in the Landau theory is calculated by taking the second derivative of $\Delta\tilde{G}_{\mathrm{sing}}$ to M. The only difference with the calculation of κ_{cl}^2 in Edison's model is the factor $1/c_\rho^2$ in relation (4.13). The kernel term in the Landau theory contains a factor c_t^2 in front of $\Delta\tilde{T}$ (4.11), which is not present in Edison's model. Edison did not forget about these parameters but he fixed them at 1. It follows from the Landau theory that this simplification is not correct. The Landau theory is based on the so-called Landau variables, the order parameter M and the temperature-like variable t. It is a general model to describe the phase transition in crossing the critical point. The Landau variables are related to the physical variables $\Delta\tilde{x}$ and $\Delta\tilde{T}$ by the parameters c_t and c_ρ. It is clear that the application of the crossover theory to the NRTL model is meaningless when the parameters c_t and c_ρ are not taken into account.

3.5 Two-Term Landau expansion

The first asymmetric term $1/3!\tilde{G}_{13}\Delta\tilde{T}\Delta\tilde{x}^3$ in the Landau expansion can be accounted for by the following redefinition of the order parameter:

$$M = c_\rho(\Delta\tilde{x} - d_1\Delta\tilde{T}) \qquad \text{with} \qquad d_1 = -\frac{\tilde{G}_{13}(\tilde{a},\tilde{b},\tilde{c},\tilde{d})}{\tilde{G}_{04}(\tilde{a},\tilde{c})} \tag{4.22}$$

where $\tilde{G}_{13}$ = partial derivative of the Gibbs energy of mixing one time to $\Delta\tilde{T}$ and three times to $\Delta\tilde{x}$, evaluated at the critical point [-]

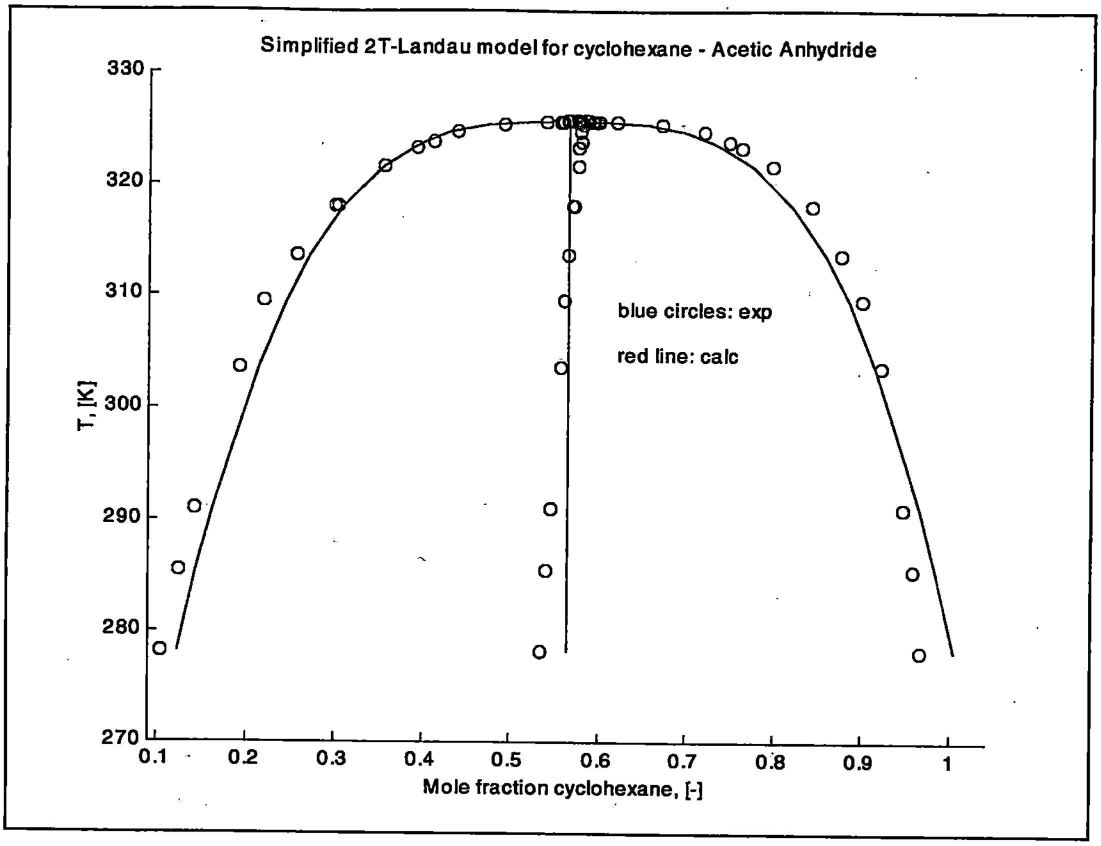

Figure 4.2: Calculated and experimental phase boundary for the binary liquid acetic anhydride – cyclohexane. The calculated values were obtained for the simplified 2T-Landau model neglecting the kernel term and the implicit dependence of *Y* on *M*.

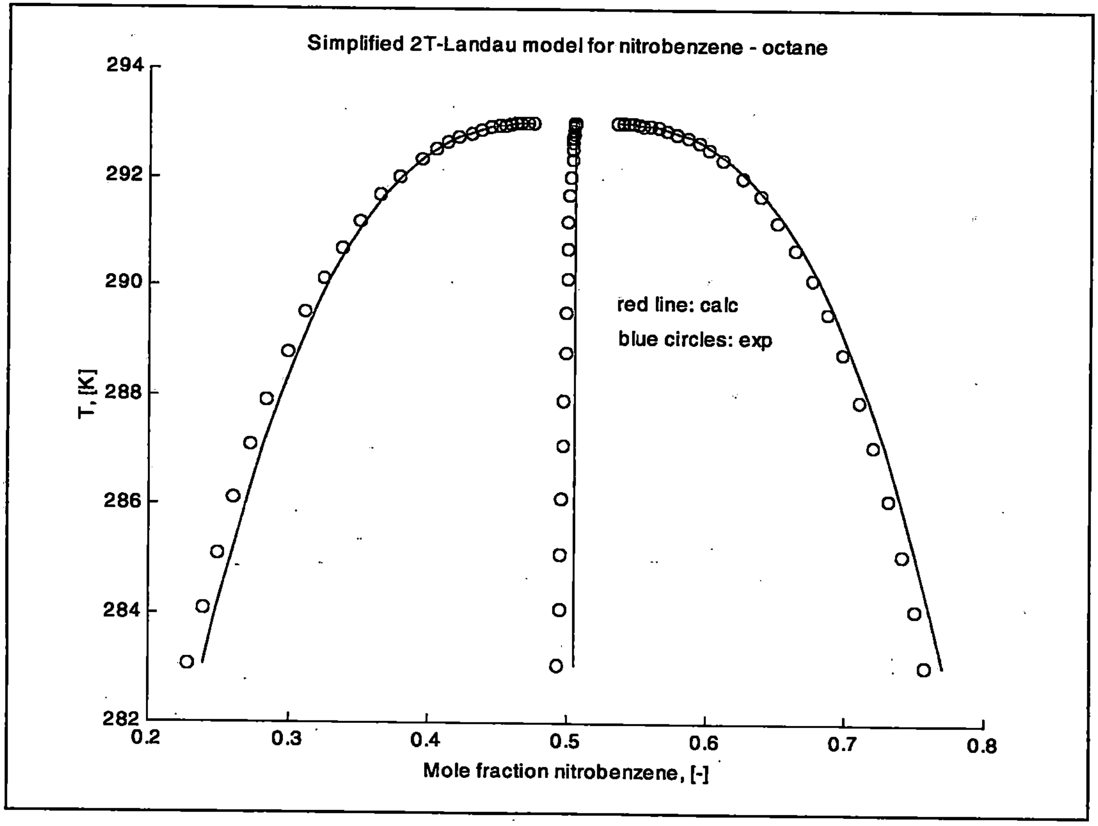

Figure 4.3: Calculated and experimental phase boundary for the binary liquid nitrobenzene - octane. The calculated values were obtained for the 2T-Landau model neglecting the kernel term and the implicit dependence of *Y* on *M*.

This first asymmetric term is of higher order than the two terms in the simplified 2T-Landau expansion. The 2T-Landau model can be expanded in terms of the order parameter in equation (4.22):

$$\begin{aligned}\Delta\tilde{G}_{\text{sing}} = {} & \frac{1}{2!}c_t c_\rho \Delta\tilde{T}\Delta\tilde{x}^2\mathcal{T}\mathcal{D} + \frac{1}{4!}u^*\bar{u}\Lambda c_\rho{}^4\Delta\tilde{x}^4\mathcal{D}^2\mathcal{U} - \frac{1}{3!}u^*\bar{u}\Lambda c_\rho{}^4 d_1\Delta\tilde{T}\Delta\tilde{x}^3\mathcal{D}^2\mathcal{U} + \ldots \\ & - c_t c_\rho{}^2 d_1\Delta\tilde{T}^2\Delta\tilde{x}\mathcal{T}\mathcal{D} + \frac{1}{2!}c_t c_\rho{}^2 d_1{}^2\Delta\tilde{T}^3\mathcal{T}\mathcal{D} + \frac{1}{2!}u^*\bar{u}\Lambda c_\rho{}^4 d_1{}^2\Delta\tilde{T}^2\Delta\tilde{x}^2\mathcal{D}^2\mathcal{U} + \ldots \\ & - \frac{1}{3!}u^*\bar{u}\Lambda c_\rho{}^4 d_1{}^3\Delta\tilde{T}^3\Delta\tilde{x}\mathcal{D}^2\mathcal{U} + \frac{1}{4!}u^*\bar{u}\Lambda c_\rho{}^4 d_1{}^4\Delta\tilde{T}^4\mathcal{D}^2\mathcal{U} + \ldots\ldots\end{aligned} \tag{4.23}$$

The last four terms are of higher order than $1/3!\tilde{G}_{13}\Delta\tilde{T}\Delta\tilde{x}^3$. The fourth term, $-c_t c_\rho{}^2 d_1\Delta\tilde{T}^2\Delta\tilde{x}\mathcal{T}\mathcal{D}$, is of the same order as $1/3!\tilde{G}_{13}\Delta\tilde{T}\Delta\tilde{x}^3$, however, it was not present in the original Landau expansion. Another difference between the expansion in equation (4.23) and the original 2T-Landau expansion is that the term $1/3!\tilde{G}_{13}\Delta\tilde{T}\Delta\tilde{x}^3$ in the original Landau expansion had to be rescaled in the normal way, *i.e.* by applying equation (4.10) to $\Delta\tilde{x}$ and $\Delta\tilde{T}$. In equation (4.23), $\Delta\tilde{T}$ in $1/3!\tilde{G}_{13}\Delta\tilde{T}\Delta\tilde{x}^3$ is rescaled like the order parameter. Therefore, writing the order parameter like equation (4.22) is not totally correct but it has the advantage that the first non-symmetric term can be accounted for, whereas the Landau expansion remains symmetric in the order parameter *M*. Still only one of the relations in equation (4.18) serves as a constraint during data regression because of the symmetry. The order parameter of the one branch follows from the order parameter of the other branch:

$$M' = -M'' \qquad \Rightarrow \qquad x'' = 2x_c + 2x_c d_1\Delta\tilde{T} - x' \tag{4.24}$$

However, it is not possible to calculate the analytical solution of equation (4.18) in the two-phase region. The kernel term and the implicit dependence of *Y* on the order parameter *M* have not been neglected in the calculations of the phase boundary for this 2T-Landau model. The experimental and calculated phase boundaries for the binary liquid nitrobenzene - octane are given in Figure (4.4). The experimental and the calculated diameter of the coexistence curve are also given in Figure (4.4). The redefinition of the order parameter like equation (4.22) improves the fit considerably. The NRTL parameters $\tilde{b}$ and $\tilde{d}$ can be calculated from c_t and d_1. Because only the first asymmetric term is taken into account, the values of $\tilde{b}$ and $\tilde{d}$ are only rough approximations for the parameters of the Crossover-NRTL model. The obtained NRTL parameters and crossover parameters for the binary liquid nitrobenzene - octane, as calculated by the 2T-Landau model and the Crossover-NRTL model are given in Table (4.1).

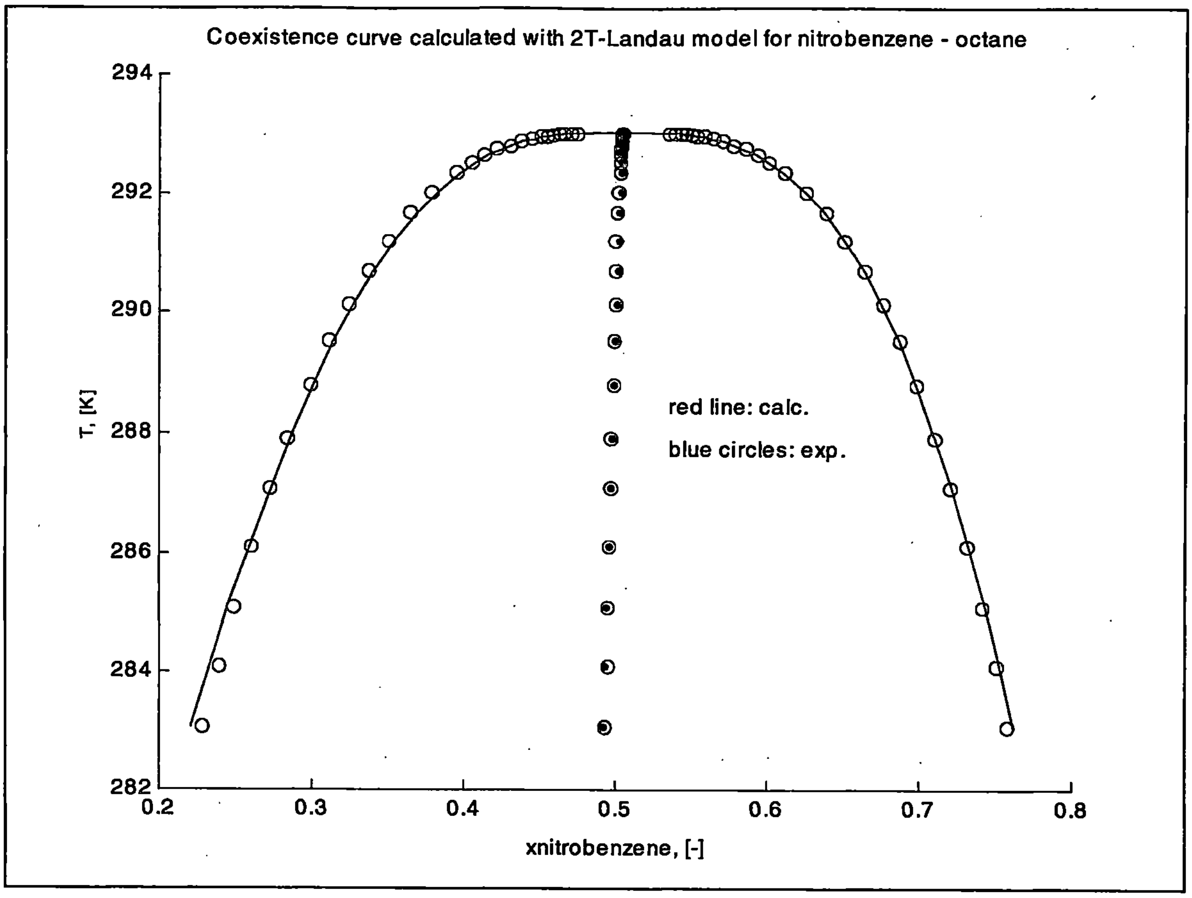

Figure 4.4: Calculated and experimental phase boundary for the binary liquid nitrobenzene - octane. Calculations were performed for the 2T-Landau model, with the order parameter defined by Equation (4.22), *i.e.* with an asymmetric correction. The kernel term and the implicit dependence of *Y* on *M* have not been neglected in this calculation.

Table 4.1: Comparison between Landau models and crossover-NRTL

	Range $\lvert\Delta\tilde{T}\rvert < 0.01$	Range $\lvert\Delta\tilde{T}\rvert < 0.036$	Range $\lvert\Delta\tilde{T}\rvert < 0.036$
Model	2T-Landau without d*Y*/d*M* and kernel term	2T-Landau with first asymmetric term, d*Y*/d*M*, and kernel term	Crossover-NRTL
A	1 fixed	1 fixed	1 fixed
$\tilde{u}$	0.5074	0.4619	0.3430
$\tilde{b}$	-	3.894	3.515
$\tilde{d}$	-	-0.7637	0.5595
c_t	0.5 fixed	0.4382	0.5014
c_ρ	1.842	1.723	1.856
χ^2	2.710	12.63	0.3130
d_1	-	0.7548	0.4570

The 2T-Landau expansion with the first non-symmetric term can be applied to represent the experimental phase equilibria in a wider range in temperature than the simplified 2T-Landau model. Therefore, it is possible to extract an approximation for the temperature dependence of the NRTL parameters from it. The whole data set is used for the data regression to the 2T-Landau expansion. This corresponds to a temperature range $|\Delta\tilde{T}|$<0.036. It is clear from Table (4.1) that only taking the first asymmetric term into account is not enough to give a good representation (very high value of χ^2) or a reliable estimate for $\tilde{b}$ and $\tilde{d}$ in the Crossover-NRTL model. The sign of $\tilde{d}$ is incorrect. The value for $\tilde{b}$ is a rather good estimate.

4.6 Calculation of the coexistence curve for different binary liquids with the Crossover-NRTL model

Unfortunately, there are few systems available in the literature that have been experimentally studied in an extended temperature range, including the critical region, with high accuracy. Studies focused on the critical region often have very accurate data but they usually cover only a narrow temperature range. Data sets with an extended range in temperature mostly have less accurate data and/or no data in the critical region.

Gopal *et al.* measured the phase-boundary of the binary liquid acetic anhydride - cyclohexane [59,60]. Their data set has a temperature range of about 50°C. However, the accuracy of the data is lower than required for the present analysis, specially in the critical region. Gopal *et al.* measured the transition temperature of more than 40 samples. The samples with $x_{C_6H_{12}}$=0.576$_2$ and $x_{C_6H_{12}}$=0.579$_5$ had the same highest phase separation temperature of T_c=325.718 K, whereas the samples with $x_{C_6H_{12}}$=0.568$_4$ and $x_{C_6H_{12}}$=0.565$_3$ had phase separation temperatures 0.5 and 1.0 mK lower than T_c respectively. Gopal *et al.* plotted the data close to T_c on an enlarged scale and they drew a smooth curve through the data giving x_c=0.574$_5$±0.001. It is clear that this determination of x_c is not so precise because of the flatness of the coexistence curve in the critical region.

The limiting slopes of the two branches of the coexistence curve in a log-log plot of $\Delta\tilde{T}$ versus $\Delta\tilde{x}$ should equal the Ising value of the universal exponent β=0.3255. The value of x_c can be changed within experimental error to get the correct limiting slope in the log-log plot. Notwithstanding the uncertainty quoted by Gopal *et al.*, the value obtained in the present work is x_c= 0.5815. A possible explanation for the discrepancy can be found in the gravity effects, that clearly distort their experimental results for $|1-T_c/T|<10^{-4}$ [59].

The coexistence curve, calculated with the Crossover-NRTL model, for the binary liquid acetic anhydride – cyclohexane on a normal scale and on a log-log scale is given in Figures (4.5) and (4.6). The optimised NRTL parameters and the crossover parameters are given in Tables (4.3) and (4.4). The data in the range $|1-T_c/T|<10^{-4}$ were not taken into account in the optimisation. The fit is rather good, both in the critical region and the classical region. There is a small deviation between the experimental data points and the calculated phase boundary in the right branch of the classical region. However, it is a nice fit for such a large temperature range. The limiting slopes of the two branches of the coexisting curve in the log-log plot assume the correct value in approaching the critical point. Farther away from the critical point, the slopes of the two branches of the coexistence curve, *i.e.* the effective exponents β of the two branches, assume different values because the distance x-x_c from the critical point is different for both branches.

Wims *et al.* measured liquid-liquid equilibria for the binary liquid nitroethane - 3-methylpentane [61]. The range of the temperature of the phase-boundary data of Wims *et al.* is too small to obtain physically realistic values for the crossover parameters $\bar{u}$ and Λ and for the NRTL parameters $\tilde{b}$ and $\tilde{d}$. Therefore, two different data sets have to be combined. Data farther away from the critical point are given by Khosla *et al.* [62].

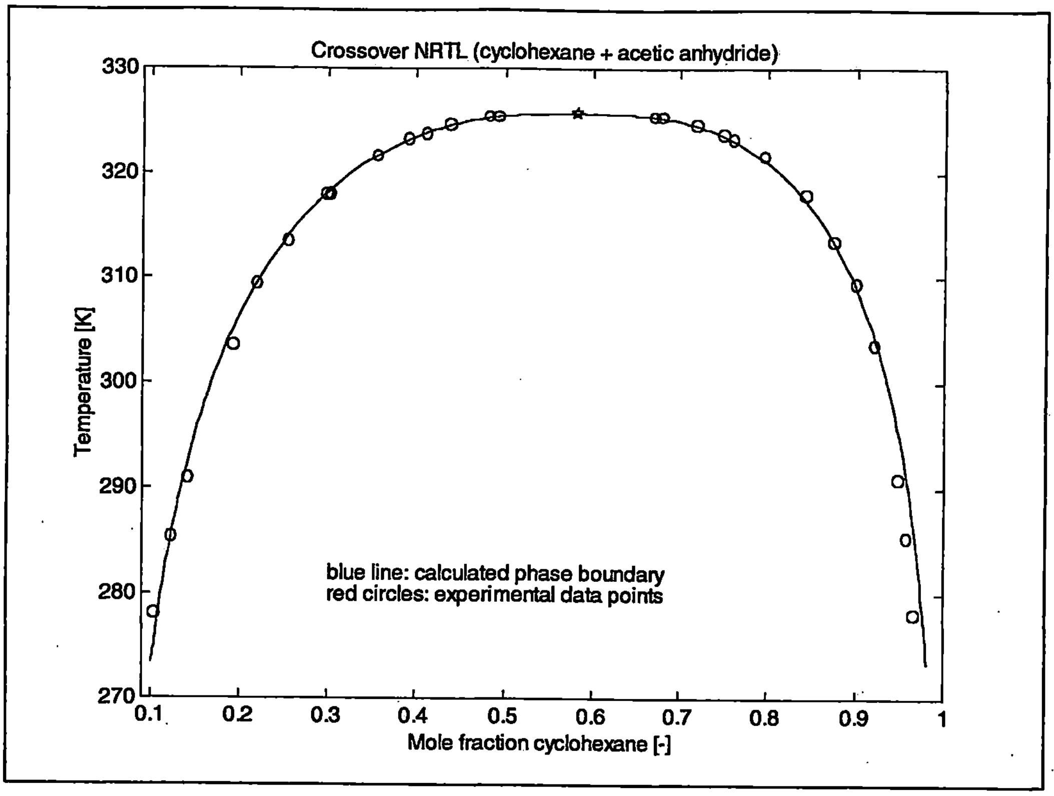

Figure 4.5: Calculated and experimental phase boundaries for the binary liquid cyclohexane - acetic anhydride

Great care has to be taken to combine data sets measured by different authors. Samples might differ in purity and it is well known that the critical temperature is very sensitive to impurities. Both Wims *et al.* and Khosla *et al.* mention their measured critical temperature, mole fraction at the critical point and the purity of the samples. These values are given in Table (4.2).

Table 4.2: Purities and critical parameters

	Purity [w%] $C_2H_5NO_2$	Purity [w%] CH_3-CH-$(C_2H_5)_2$	x_c [mol/mol]	T_c [K]
Wims *et al.* [61]	~100	99.99	0.5000±0.001	299.608±0.001
Khosla *et al.* [62]	99.96-99.98	99.99	0.500±0.001	299.600±0.001

Inspite of the high purity of all employed chemicals, the difference between the two critical temperatures is too large to use data of both sets near the critical point. In the present analysis, the data near the critical point from Wims *et al.* and the data farther away from the critical point from Khosla *et al.* are used. Far away from the critical point the difference between the critical temperatures is not important.

Both authors give their phase-boundary data in terms of coexisting densities. However, mole fractions are needed for the NRTL equation. Wims *et al.* recalculate their densities to mole fractions by assuming that there is no volume-change of mixing, without checking the validity of this approximation. Actually, it is clear that neglecting mixing effects is not justified because partial miscible binary liquids show non-ideal behaviour per definition.

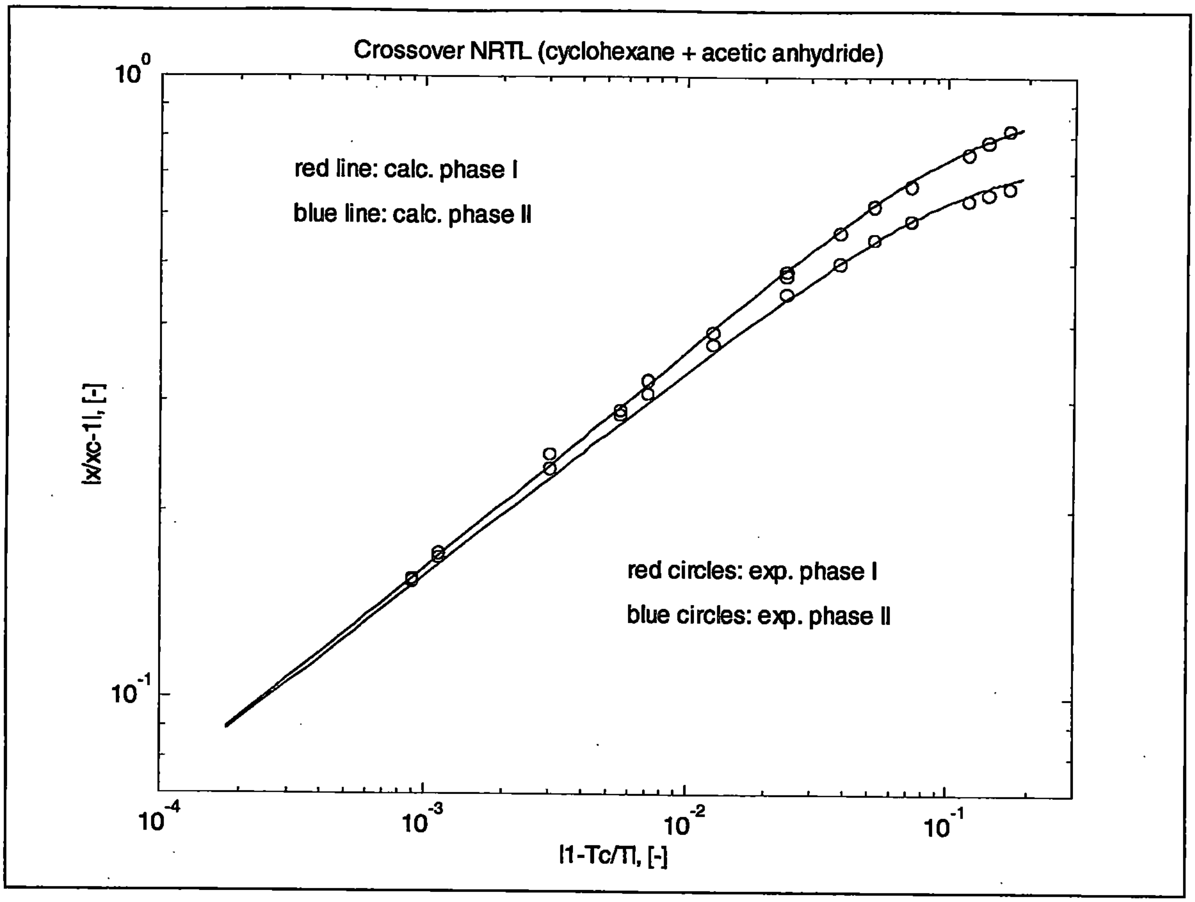

Figure 4.6: Calculated and experimental phase boundary for the binary liquid cyclohexane - acetic anhydride
red circles: exp phase I

blue circles: exp phase II

Handa *et al.* give excess volumes for the binary liquid nitroethane - 3-methylpentane for three different temperatures [63]. They fit their excess-volume data to the following equation:

$$V^{E}[\mathrm{cm^3/mol}] = x(1-x)\sum_{i=0}^{3} v_i(T)(1-2x)^i \tag{4.25}$$

where V^E = excess volume [m^3/mole]

The graphical result is given in Figure (4.7). It is clear that the portion of the subcritical curve (red curve) in the mole-fraction range 0.3 < $x_{\text{nitroethane}}$ < 0.7 has no significance because of the partial miscibility. The temperature dependence of the excess volumes is rather small. In the range 298.596 K - 303.150 K, the excess volume changes only by a few percents. Therefore, the mean value of the curves in the range 298.596 K - 303.150 K can serve as a rough approximation for the excess volumes for the whole temperature range of the combined data sets of Wims *et al.* and Khosla *et al.*.

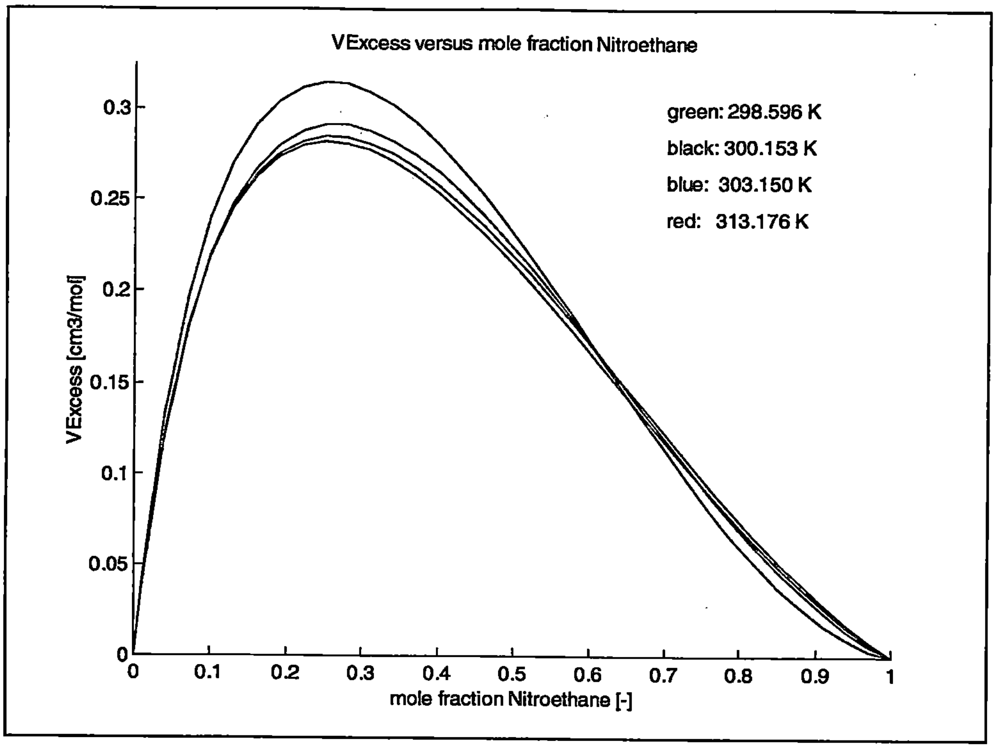

Figure 4.7: Excess volumes for the binary liquid nitroethane - 3-methylpentane at different temperatures

The mole fractions are calculated by the following relations:

$$V^i = V_i^{\mathrm{E}} + \sum x_j{}^i V_j \qquad \frac{1}{\rho^i} = \frac{V_i^{\mathrm{E}}}{\sum x_j{}^i M_j} + \sum \frac{x_j{}^i M_j}{\sum x_j{}^i M_j} \frac{1}{\rho_j}$$

$$x_{NB}{}^i = \frac{M_{\mathrm{3MP}} - \dfrac{\rho^i M_{\mathrm{3MP}}}{\rho_{\mathrm{3MP}}} - \rho^i V_i^{\mathrm{E}}}{\dfrac{\rho^i M_{\mathrm{NB}}}{\rho_{\mathrm{NB}}} - \dfrac{\rho^i M_{\mathrm{3MP}}}{\rho_{\mathrm{3MP}}} - M_{\mathrm{NB}} + M_{\mathrm{3MP}}} \tag{4.26}$$

where i = phase i
j = component j
V^i = molar volume of phase i [cm^3/mole]
V_j = molar volume of pure j [cm^3/mole]
V_i^E = excess molar volume of phase i [cm^3/mole]
ρ_j = mass density of pure j [g/cm^3]
ρ^i = mass density of phase i [g/cm^3]
M_{3MP} = molar mass of 3-methylpentane [g/mole]

After taking into account the excess volumes, the mole fraction of nitroethane in the 3-methylpentane-rich phase changes by 1.1% near the critical point to 3.8% 10°C away from the critical point and the mole fraction of nitroethane in the nitroethane-rich phase changes by 1.0% near the critical point to 0.2% 10°C away from the critical point. The changes of the mole fraction in the 3-methylpentane-rich and the nitroethane-rich phase are different because of the skewness of the curves in Figure (4.7). The phase boundary for the binary liquid nitroethane - 3-methylpentane on a normal scale and on a log-log scale is given in Figure (4.8) and Figure (4.9). The optimised NRTL parameters and the crossover parameters are given in Tables (4.3) and (4.4).

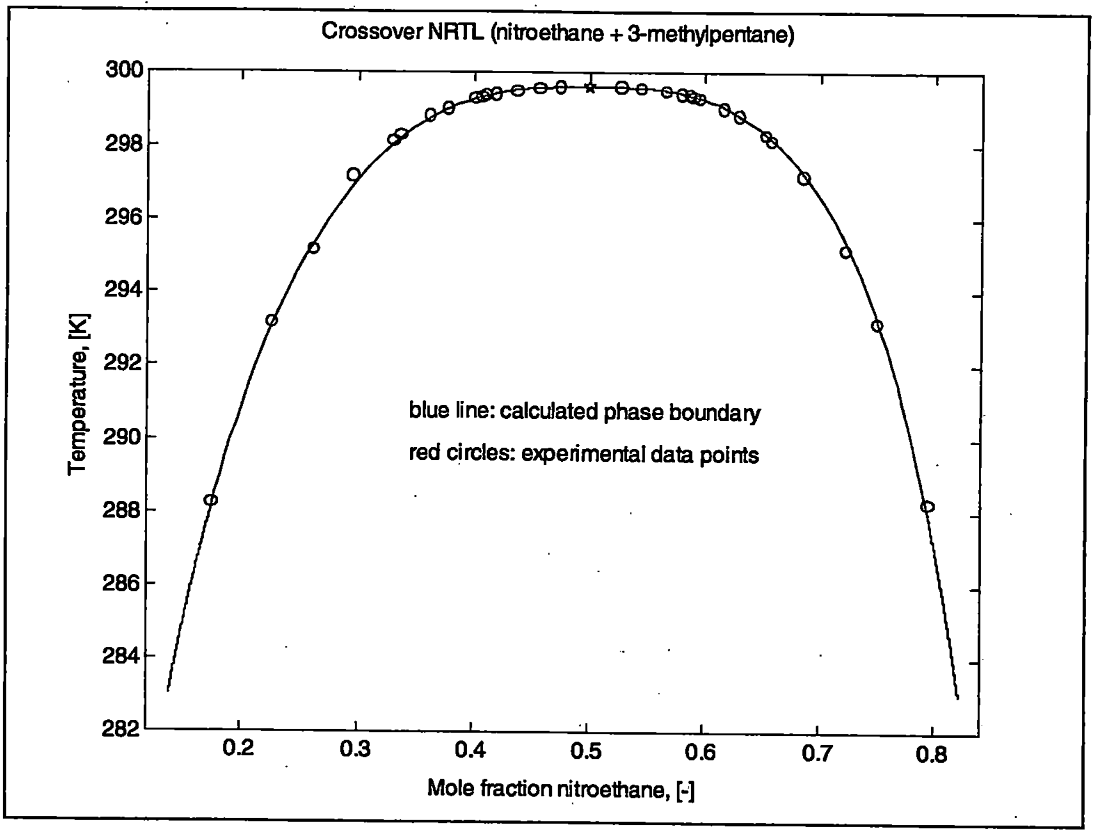

Figure 4.8: Calculated and experimental phase boundaries for the binary liquid nitroethane - 3-methylpentane

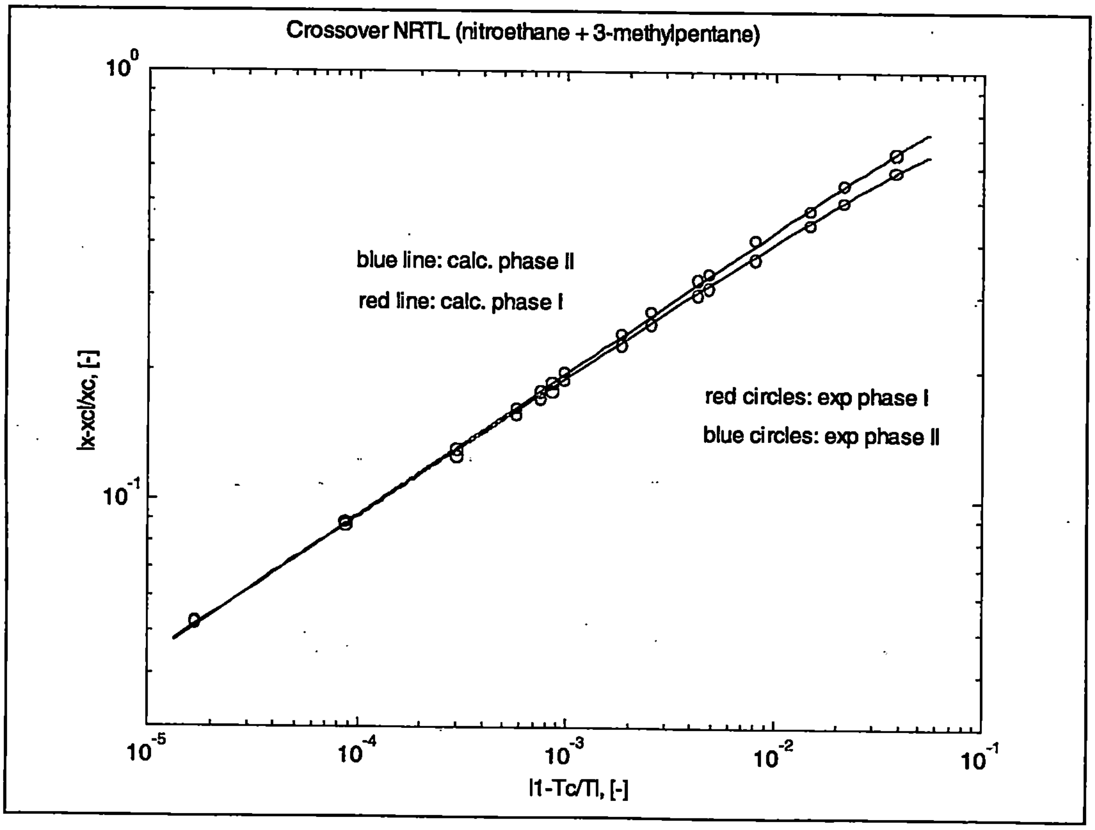

Figure 4.9: Calculated and experimental phase boundaries for the binary liquid nitroethane - 3-methylpentane

The fit is good, both in the critical and the classical regions. The limiting slopes of the two branches of the coexistence curve in the log-log plot assume the correct value in approaching the critical point. Farther away from the critical point, the slopes of the two branches of the coexistence curve assume different values because the distance x-x_c from the critical point is different for both branches. However, the difference is less pronounced than that for the system acetic anhydride – cyclohexane because the latter system is more asymmetric with respect to x_c.

Five other liquid-liquid systems, measured by An *et al.* [64-68], have been analysed. The systems consist of nitrobenzene and one of the five different linear alkanes, pentane, octane, decane, dodecane, and tetradecane. The data points are very accurate. Unfortunately, the temperature range is too small to make contact with the classical region. The higher the chain length of the linear alkanes, the more asymmetric the coexistence curve. The Crossover-NRTL model has no difficulties with describing these asymmetric systems. As an example, the coexistence curve for the binary liquid nitrobenzene (C_6H_5-NO_2) – tetradecane ($C_{14}H_{30}$) is given in Figures (4.10) and (4.11). The coexistence curves of the other systems are given in Appendix C.

Critical mole fractions and critical temperatures were changed within experimental error to get a better fit. The optimised NRTL parameters and the crossover parameters are given in Tables (4.3) and (4.4). Again, the asymmetry of the coexistence curves is evident in the difference of the slopes of the coexisting branches in the log-log plots of $\Delta\tilde{x}$ versus $\Delta\tilde{T}$.

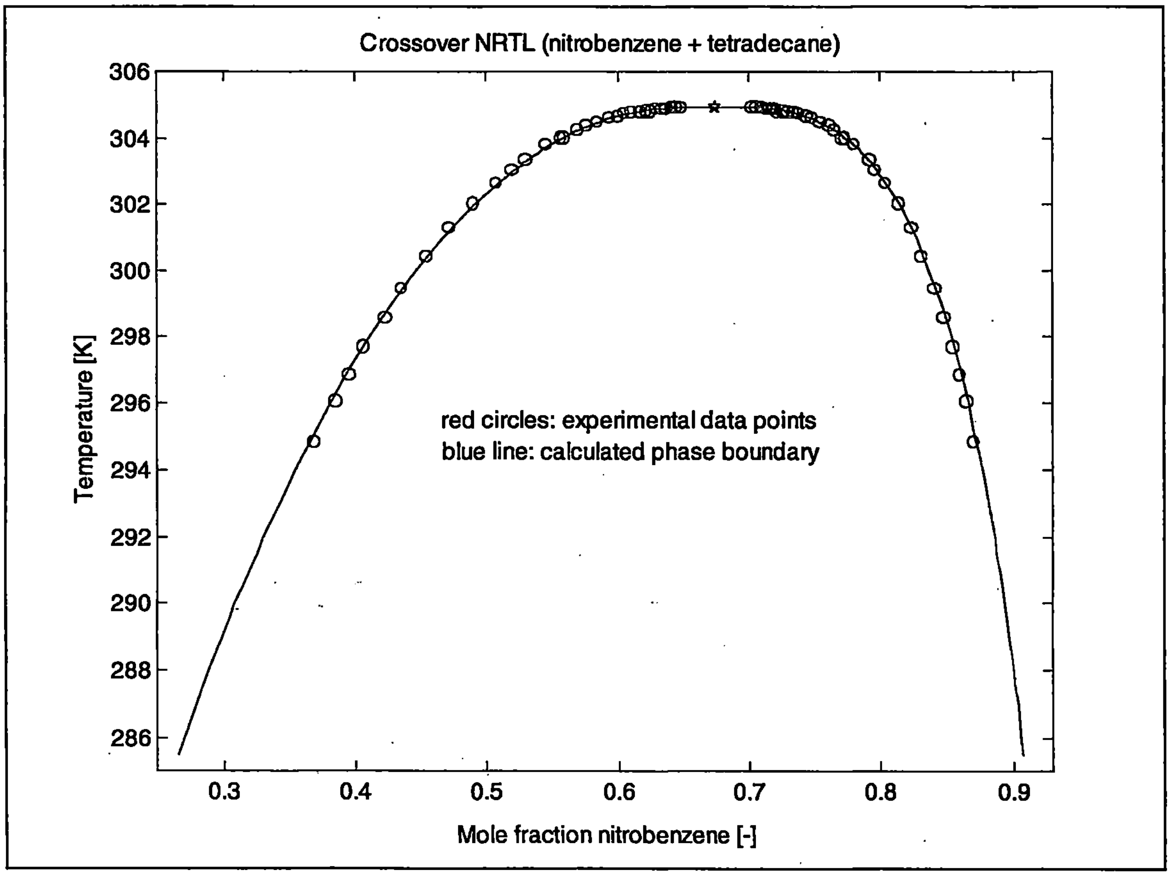

Figure 4.10: Calculated and experimental phase boundaries for the binary liquid nitrobenzene - tetradecane

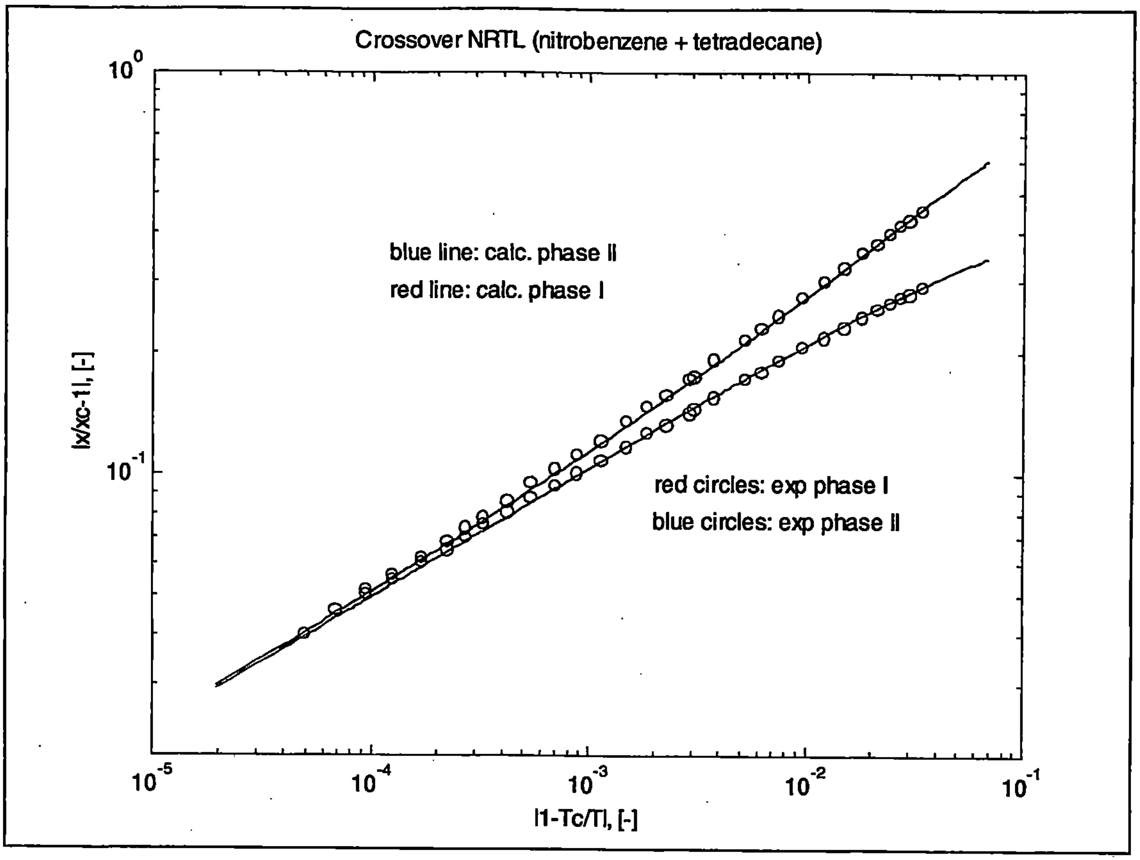

Figure 4.11: Calculated and experimental phase boundaries for the binary liquid nitrobenzene - tetradecane

Table 4.3: Crossover parameters and Ginzburg numbers

Parameter	A	$\bar{u}$	c_p	c_t	*Ginzburg Number*
acetic anhydride – cyclohexane	0.4519	0.4630	2.484	0.8829	$1.6\cdot10^{-3}$
nitroethane – 3-methylpentane	1.552	0.4512	1.540	0.7189	$2.1\cdot10^{-2}$
nitrobenzene – pentane	1 fixed	0.3571	1.486	0.4387	$9.1\cdot10^{-3}$
nitrobenzene – octane	1 fixed	0.3430	1.856	0.5014	$7.4\cdot10^{-3}$
nitrobenzene – decane	1 fixed	0.3250	2.186	0.5286	$6.3\cdot10^{-3}$
nitrobenzene – dodecane	1 fixed	0.3193	2.527	0.5578	$5.7\cdot10^{-3}$
nitrobenzene – tetradecane	1 fixed	0.2631	3.015	0.5592	$3.9\cdot10^{-3}$

Table 4.4: NRTL parameters

	$\tilde{a}$	$\tilde{c}$	$\tilde{b}$	$\tilde{d}$
acetic anhydride – cyclohexane	0.6066	1.714	3.790	4.979
nitroethane – 3-methylpentane	1.137	1.150	3.662	0.3667
nitrobenzene – pentane	1.944	0.4071	2.451	-0.7823
nitrobenzene – octane	1.110	1.177	3.515	0.5595
nitrobenzene – decane	0.6555	1.660	5.760	0.6627
nitrobenzene – dodecane	0.2883	2.086	12.63	0.7860
nitrobenzene – tetradecane	-0.01604	2.466	-286.2	0.4953

Group statistics have been used to show how the phase boundaries, calculated from the Crossover-NRTL model, compare to the accompanying experimental data. The group statistics typically used are based on the percent deviation of a property, %Δx:

$$\%\Delta x = 100\left(\frac{x_{\text{exp}} - x_{\text{calc}}}{x_{\text{exp}}}\right) \tag{4.27}$$

The group statistics used are summarised in equation (4.28):

$$AAD = \frac{1}{N}\sum_{i=1}^{N}\left|\%\Delta x_i\right| \qquad BIAS = \frac{1}{N}\sum_{i=1}^{N}\left(\%\Delta x_i\right)$$
$$SDV = \sqrt{\frac{1}{N-1}\sum_{i=1}^{N}\left(\%\Delta x_i - BIAS\right)^2} \qquad RMS = \sqrt{\frac{1}{N}\sum_{i=1}^{N}\left(\%\Delta x_i\right)^2} \tag{4.28}$$

The *AAD* is the average absolute deviation of a data set. High values of the *AAD* indicate either systematic or large random differences between the data and the Crossover-NRTL model. The Bias is the average deviation of a set of data. Large positive or negative values of the *BIAS* indicate systematic differences between the data and the crossover-NRTL model. The *SDV* represents the standard deviation of a data set. This value gives an indication of the systematic or random dispersion of the data set around the *BIAS* value. Finally, the *RMS* represents the root mean square of the deviations. This parameter provides another indication of the systematic or random dispersion of the data from the Crossover-NRTL model. The Crossover-NRTL model is considered to be representative for a data set when all four statistical parameters are near zero [69,70]. In general, the results, given in Table (4.5), are satisfactory. However, the group statistics and χ^2 for the fit of the phase boundary of the binary liquid acetic anhydride - cyclohexane are somewhat high. The χ^2 is expressed in the experimental uncertainties for the mole fractions and the temperature given by Gopal *et al.*. The small deviation between the experimental data points and the calculated phase boundary in the right branch of the classical region cannot be the only reason for this high χ^2. The claimed experimental uncertainties are probably to low.

Table 4.5: Group statistics and χ^2 of the different fits

	AAD [%]	*BIAS* [%]	*SDV* [%]	*RMS* [%]	χ^2
acetic anhydride- cyclohexane	0.6844	0.2779	1.1777	1.2029	18.9
nitroethane - 3-methylpentane	0.2975	-0.05261	0.5825	0.5189	4.13
nitrobenzene - pentane	0.1615	0.05782	0.1594	0.3064	1.45
nitrobenzene - octane	0.07979	-0.03411	0.1260	0.1213	0.313
nitrobenzene - decane	0.1627	-0.1105	0.2617	0.2757	1.64
nitrobenzene - dodecane	0.1036	0.01316	0.1813	0.1896	1.08
nitrobenzene - tetradecane	0.1523	-0.07076	0.2233	0.2443	2.01

4.7 Significance of the NRTL parameters and the crossover parameters

4.7.1 Calculation of the phase boundary

It has been mentioned in Chapter 2 that the NRTL model has many possible roots. Either one or two pairs of coexisting mole fractions are thermodynamically stable. Therefore, after calculation of the phase boundary, the stability of the solution should be checked. As an example the classical Gibbs energy of mixing for the binary liquid nitroethane - 3-methylpentane is given here. This graphical analysis is good enough because the crossover procedure only changes the shape of the profile of the classical Gibbs energy of mixing and it does not introduce new maxima or minima. The classical Gibbs energy of mixing for different temperatures as a function of the mole fraction is given in Figure (4.12). The values of $\tilde{a}$ and $\tilde{c}$ that force the coexistence curve through the real critical point are used. It is clear that the only possible solution is the stable solution, which minimises the Gibbs energy of mixing. The stars represent the spinodal curve.

4.7.2 NRTL interaction energies

The coexistence curves for the five binary liquids as a function of the carbon number of the linear alkanes are given in Figures (4.13), (4.14) and (4.15). The availability of the coexistence curves of nitrobenzene and different linear alkanes enables the study of the significance of the obtained NRTL parameters.

Mixing is an entropically driven process; configurations with a random molecular distribution have higher probability than ordered states. The other contribution to the Gibbs-energy-of-mixing, the enthalpic term, depends on the difference between like-molecules interactions (*i-i* and *j-j*) and unlike (*i-j*) interactions. For partially miscible liquids, these contributions compete and form a Gibbs-energy-of-mixing pattern like the one in Figure (4.12).

The influence of the chain length of the linear alkanes on the *entropy* change of mixing with non-polar molecules is qualitatively represented by Flory-Huggins theory in terms of the volume fraction. Consequently, the larger the carbon chain, the smaller the critical mole fraction of the hydrocarbon (Figure 4.13). The enthalpy of mixing will be determined by the fact that apolar alkane molecules will screen the dipole-dipole interactions of nitrobenzene, which has a dipole moment of 3.97 Debye [71]. The linear alkanes are apolar. Long-chain alkanes will exhibit a higher screening effect than small alkanes, with a concomitant increase in the enthalpy of the mixture and, therefore, a larger miscibility gap with nitrobenzene, *i.e.* a higher critical temperature (Figure 4.15).

The binary liquid nitrobenzene - octane has the most symmetric coexistence curve and the lowest phase separation temperature (Figure 4.15). For the NRTL equation, symmetric systems are those where τ_{12} equals τ_{21}, *i.e.* systems where the interaction-energy differences g_{12}-g_{22} and g_{21}-g_{11} are the same. The interaction-energy differences are given in Table (4.7). The interaction-energy differences are almost the same for the mixture nitrobenzene – octane. Therefore, the system nitrobenzene – octane forms the breaking point in the homologue series of mixtures nitrobenzene - alkane. This difference is evidenced in the slope of the coexistence-curve diameter and in the critical solution temperature. According to Figure (4.15), for the binary liquid nitrobenzene - pentane the diameter, $x_{d,\mathrm{nitrobenzene}}$, shifts to lower values as the critical point is approach, while the diameter for the binary liquids with higher alkanes than octane have the opposite tendency. The diameter of the coexistence curve for nitrobenzene – octane is almost vertical. The critical solution temperatures of all systems are higher than that of the system nitrobenzene – octane.

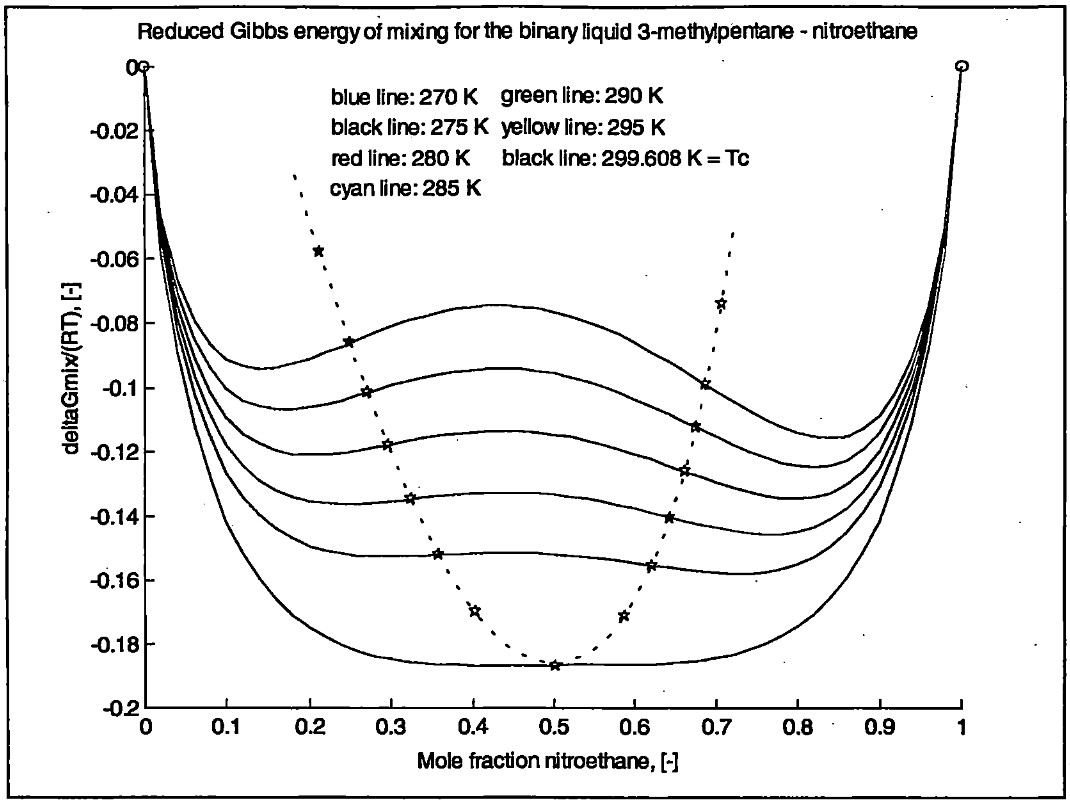

Figure 4.12: Gibbs energy of mixing for the binary liquid nitroethane - 3-methylpentane

The molecular sizes of the alkanes and nitrobenzene can be estimated from the liquid densities [72]. The calculated sizes of nitrobenzene and the different alkanes, as given in Table (4.6), are obtained assuming that molecules are spherical. The effective size of the long-chain molecules will differ from the sizes mentioned in Table (4.6) because those molecules can not be regarded as spherical. Roughly speaking, a molecule nitrobenzene is of the same size as a molecule pentane. Nitrobenzene and octane have slightly different sizes. Other effects, like difference in polarity and differences in number of possible conformations will compensate this source of asymmetry in the coexistence curve.

Table 4.6: Molecular sizes [Å]	
nitrobenzene	3.51
propane	3.19
butane	3.40
pentane	3.58
hexane	3.74
heptane	3.90
octane	4.04
nonane	4.17
decane	4.29
tetradecane	4.73

The interaction energies of the NRTL model are taken with a linear temperature dependence, resulting in the following (classical) relations for the local mole fractions (2.7):

$$x_{21} = \frac{x_2 \exp\left(-\alpha_{12}(g_{21}-g_{11})/RT\right)}{x_1 + x_2 \exp\left(-\alpha_{12}(g_{21}-g_{11})/RT\right)} = \frac{x_2 \exp\left(-\alpha_{12}\tilde{a}(1-\tilde{b}\Delta\tilde{T})\right)}{x_1 + x_2 \exp\left(-\alpha_{12}\tilde{a}(1-\tilde{b}\Delta\tilde{T})\right)}$$

$$x_{12} = \frac{x_1 \exp\left(-\alpha_{12}(g_{12}-g_{22})/RT\right)}{x_2 + x_1 \exp\left(-\alpha_{12}(g_{12}-g_{22})/RT\right)} = \frac{x_1 \exp\left(-\alpha_{12}\tilde{c}(1-\tilde{d}\Delta\tilde{T})\right)}{x_2 + x_1 \exp\left(-\alpha_{12}\tilde{c}(1-\tilde{d}\Delta\tilde{T})\right)} \qquad (4.29)$$

The subscript 1 in equation (4.29) belongs to nitrobenzene and the subscript 2 to the linear alkane. The local mole fractions for two different temperatures are given in Table (4.7), together with the differences between the overall mole fractions and the local mole fractions of the alkane-rich phase.

The interaction-energy differences g_{12}-g_{22} and g_{21}-g_{11} in equation (4.29) can be separated into a temperature-independent part and a temperature-dependent part:

$$\frac{g_{21}-g_{11}}{RT} = \tilde{a} - \tilde{a}\tilde{b}\left(1-\frac{T_c}{T}\right) \quad \Rightarrow \quad g_{21}-g_{11} = \tilde{a}\tilde{b}RT_c + R\tilde{a}(1-\tilde{b})T$$

$$\frac{g_{12}-g_{22}}{RT} = \tilde{c} - \tilde{c}\tilde{d}\left(1-\frac{T_c}{T}\right) \quad \Rightarrow \quad g_{12}-g_{22} = \tilde{c}\tilde{d}RT_c + R\tilde{c}(1-\tilde{d})T \qquad (4.30)$$

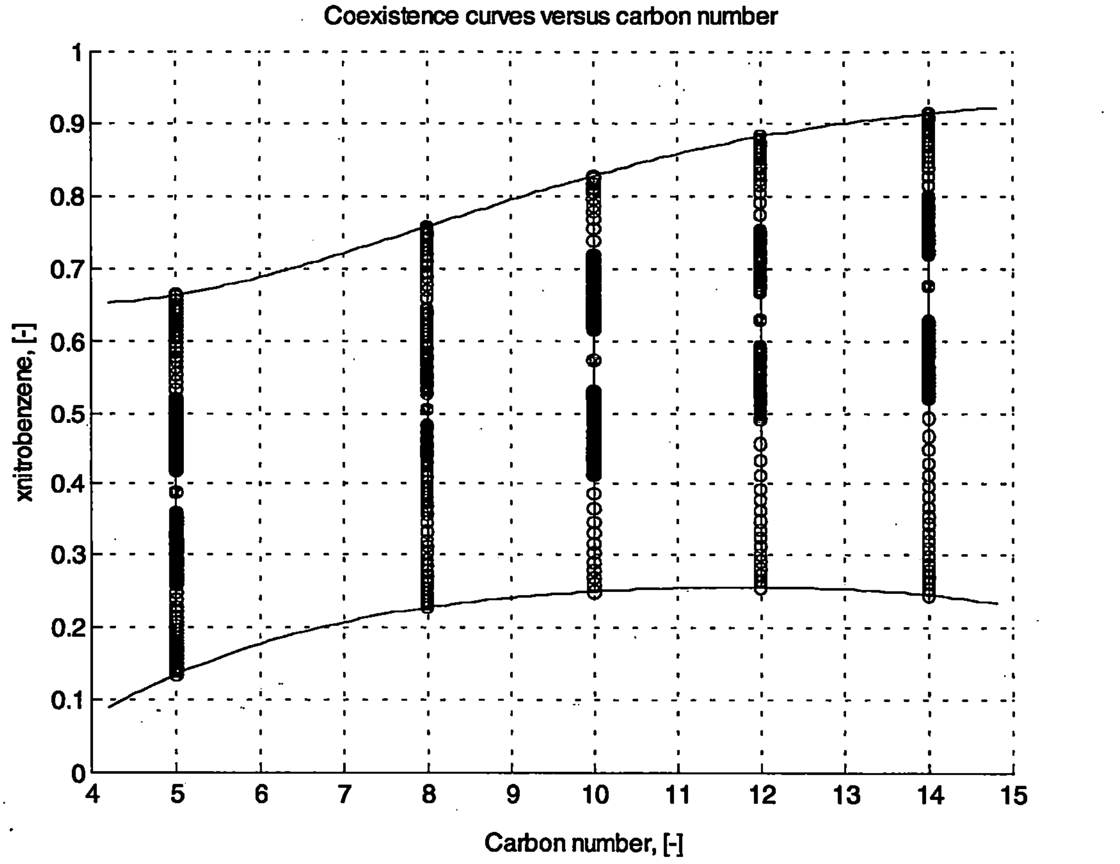

Figure 4.13: Different coexistence curves as a function of the carbon number of the linear alkanes, view from above

These two parts are given in Table (4.8). Several things become clear from Table (4.7) and Table (4.8). The differences x_1'-x_{12} and x_2'-x_{21} respectively increase and decrease with the chain length of the linear alkanes at constant temperature. The prime indicates the alkane-rich phase. These differences represent the differences between the overall mole fractions and the local mole fractions. The differences between the interaction energies, g_{12}-g_{22} and g_{21}-g_{11}, respectively increase and decrease with increasing carbon number at T=285 K.

The differences x_1'-x_{12} and x_2'-x_{21} are in agreement with the interaction-energy differences g_{12}-g_{22} and g_{21}-g_{11}. For example, when the difference g_{12}-g_{22} increases, this means that it costs a molecule 2 (alkane) at the centre of a cell more energy to be in the vicinity of a molecule 1 (nitrobenzene). Therefore, the cell will reduce its energy by minimising the number of molecules 1 in its vicinity, *i.e.* the difference x_1'-x_{12} increases. Also, the alkanes have more difficulty with being close to nitrobenzene with increasing carbon number. On the other hand, nitrobenzene has less difficulty with being close to the alkanes with increasing carbon number. In other words, the mean *local* concentration of nitrobenzene around an alkane central molecule is smaller than the *average* nitrobenzene concentration ("unfavored" solvation), and the longer the length of the carbon-chain the higher that difference. This is due to the fact that both the alkane-nitrobenzene and the alkane-alkane interaction increase with carbon number of the alkane, the latter being more pronounced. Therefore, solvation of alkane by nitrobenzene becomes less favoured as the carbon number increases. On the other hand, the mean *local* concentration of alkane around a nitrobenzene central molecule is also smaller than the *average* alkane concentration, but in this case the difference becomes smaller as the carbon number increases. The explanation is that while nitrobenzene-nitrobenzene interactions are always the same, nitrobenzene-alkane interactions increase with chain length and, consequently, the latter become relatively more relevant in the solvation process.

It can be concluded that the total interaction-energy differences monotonically increase or decrease with increasing carbon number.

Another thing that becomes clear is that the separate temperature-independent and the temperature-dependent parts of the interaction energy-differences do not monotonically increase or decrease with increasing carbon number. This cannot be explained so easily because the effects of difference in sizes of the molecules, difference in number of possible conformations, and difference in polarity have to be decoupled.

It follows from Table (4.7) that the difference x_1'-x_{12} increases with increasing temperature. The difference x_2'-x_{21} increases with increasing temperature for nitrobenzene - pentane and nitrobenzene - octane, is almost temperature independent for nitrobenzene - decane, and decreases with temperature for mixtures of nitrobenzene and the higher alkanes.

Also, the NRTL parameters $\tilde{a}$, $\tilde{b}$, $\tilde{c}$, and $\tilde{d}$ and the accompanying interaction energies give an indication of the "relationship" between the molecules in the solution. They show whether the molecules prefer to be close to each other or not, which is closely related to partial miscibility. The behaviour of the separate temperature-independent and temperature-dependent parts of the interaction-energy differences is too complex to explain here.

Table 4.7: Mole fractions and corresponding local mole fractions

System	T [K]	x_{12} [-]	x_{21} [-]	x_1' [-]	x_2' [-]	$x_1'-x_{12}$ [-]	$x_2'-x_{21}$ [-]
nitrobenzene – pentane	285.000	0.136	0.792	0.146	0.854	0.010	0.062
	297.104	0.369	0.517	0.388	0.612	0.019	0.095
nitrobenzene – octane	285.000	0.206	0.704	0.248	0.752	0.042	0.048
	293.052	0.446	0.440	0.505	0.495	0.049	0.055
nitrobenzene – decane	285.000	0.208	0.698	0.269	0.731	0.061	0.033
	295.963	0.492	0.394	0.574	0.426	0.082	0.032
nitrobenzene – dodecane	285.000	0.196	0.707	0.273	0.727	0.077	0.020
	300.368	0.529	0.357	0.630	0.370	0.101	0.013
nitrobenzene – tetradecane	285.000	0.176	0.726	0.262	0.738	0.086	0.012
	304.940	0.559	0.325	0.675	0.325	0.116	-0.001

Table 4.8: interaction-energy diff. at T=285 K for nitrobenzene – *n*-alkane

System	$\tilde{a}\tilde{b}RT_c$ [kJ/mole]	$R\tilde{a}(1-\tilde{b})$ [J/(mole K)]	$\tilde{c}\tilde{d}RT_c$ [kJ/mole]	$R\tilde{c}(1-\tilde{d})$ [J/(mole K)]	$g_{21}-g_{11}$ [kJ/mole]	$g_{12}-g_{22}$ [kJ/mole]
nitrobenzene – pentane	11.77	-23.45	-0.7867	6.033	5.086	0.9326
nitrobenzene – octane	9.506	-23.21	1.605	4.311	2.891	2.833
nitrobenzene – decane	9.291	-25.94	2.707	4.655	1.897	4.034
nitrobenzene – dodecane	9.094	-27.88	4.095	3.712	1.148	5.152
nitrobenzene – tetradecane	11.64	-38.30	3.097	10.35	0.7231	6.046

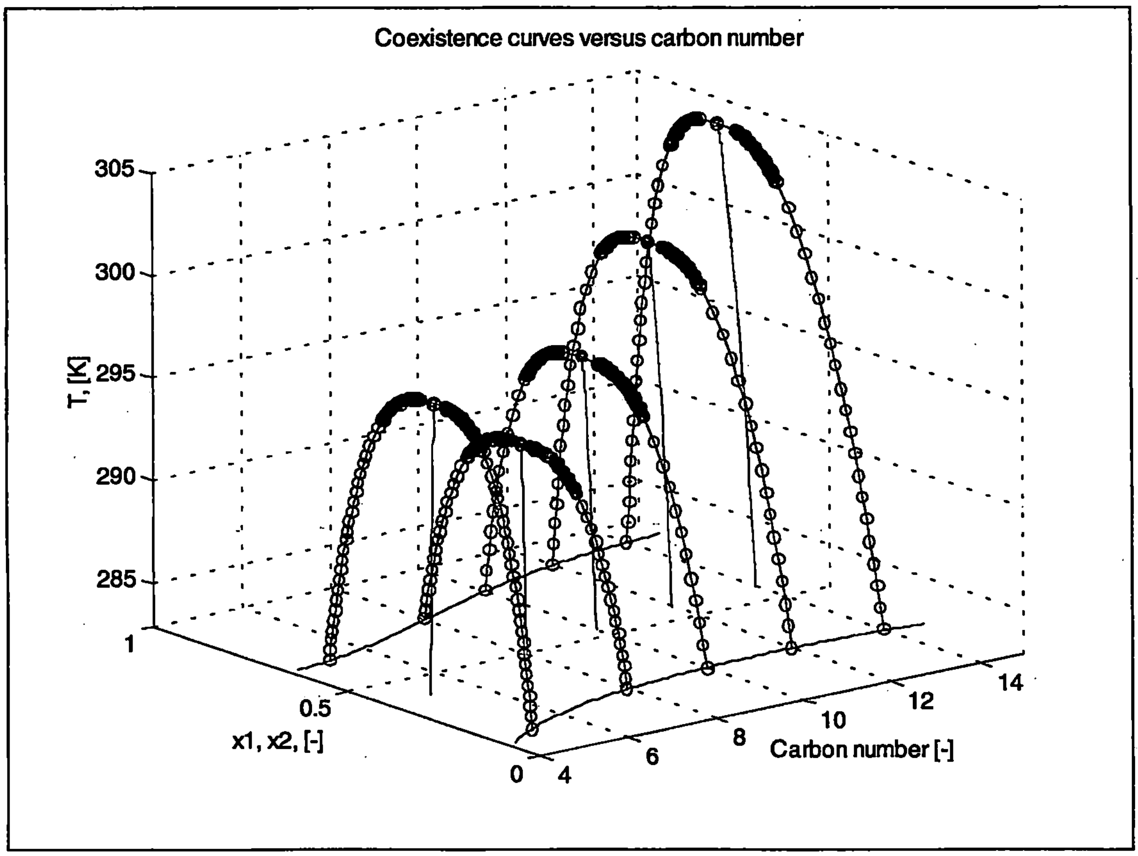

Figure 4.14: Different coexistence curves as a function of the carbon number of the linear alkanes, 3D-view

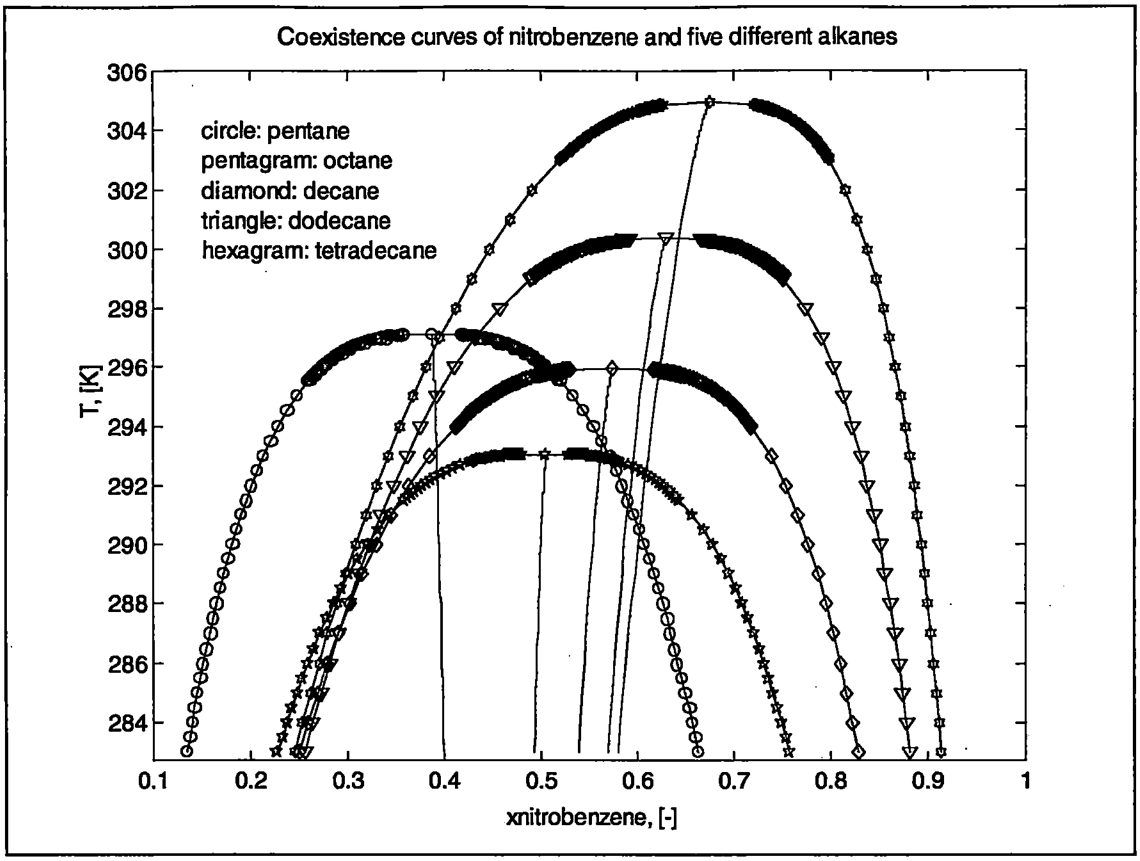

Figure 4.15: Different coexistence curves as a function of the carbon number of the linear alkanes, front view

4.7.3 Crossover parameters

To relate the physical features of the five binary liquids, given by An *et al.*, to the crossover parameters, the significance of the crossover parameters must first be clarified.

The crossover transformation is controlled by the ratio Λ/κ or $\xi/\xi_D = q_D\xi$ and by the rescaled coupling constant $\bar{u}$. The crossover parameter Λ is an ultraviolet cutoff wavenumber of the long-range critical fluctuations. It is a measure of the wavenumber for which fluctuations become microscopic. Λ can be written in the following way:

$$\Lambda = q_D v_0^{1/3} = \frac{v_0^{1/3}}{\xi_D} \qquad (4.31)$$

where $q_D =$ actual cutoff wavenumber, characterising a discrete structure of matter with spacing, $\xi_D = 1/q_D$ $[m^{-1}]$

$v_0 =$ average molecular volume $[Å^3]$

Only fluctuations of length scales larger than ξ_D will affect the thermodynamic behaviour. In simple fluids Λ is always of order unity since the natural microscopic cutoff is determined by the size of the molecules [73]. Λ=1 means that the microscopic cutoff corresponds to the average distance between molecules at the critical concentration. The binary fluids that are considered in this work are all simple fluids and, therefore, Λ is fixed at 1 in most cases.

The amplitudes c_t and c_p depend on the range of intermolecular interactions, since they can be written in terms of the amplitude of the power law of the correlation length in the one-phase region:

$$c_t = \frac{v_0^{\frac{2}{3}}}{\left(\bar{\xi}_0^+\right)^2} = a_0\sqrt{\frac{u^*\bar{u}\Lambda}{u_0}} \qquad c_p = \bar{\xi}_0^+ \frac{a_0^{\frac{1}{2}}}{v_0^{\frac{1}{3}}} = \left(\frac{u_0}{u^*\bar{u}\Lambda}\right)^{1/4} \tag{4.32}$$

where $\bar{\xi}_0^+ =$ mean-field correlation-length amplitude [Å]

The values of c_t and c_p increase with increasing carbon number of the linear alkanes. According to equation (4.30), c_t is inversely related to the range of intermolecular forces. If c_t=1, the range of intermolecular interactions equals the average intermolecular distance. The values for c_t in this work are smaller than 1, which means that the average intermolecular distance is smaller than the range of intermolecular interactions.

The amplitude $\bar{\xi}_0^+$ is proportional to the average molecular interaction diameter σ of the mixture. The only contribution to σ that changes when the chain length of the alkanes is increased is $\sigma_{n\text{-alkane}}$ because $\sigma_{\text{nitrobenzene}}$ is the same in the different binary liquids. Some molecular interaction diameters for linear alkanes are given in Table (4.9) showing that longer linear alkanes have a higher molecular interaction diameter. To get a c_t that increases with the carbon number, $v_0^{1/3}$ must increase faster with increasing carbon number than σ does, as can be concluded from comparison of Tables (4.6) and (4.9).

Table 4.9: Molecular interaction diameters [Å]

σ_i	Data from Flynn *et al.* [74]	Data from Svehla [75]
propane	5.061	5.118
butane	4.997	4.687
pentane	5.769	5.784
hexane	5.909	5.949
octane	7.451	
nonane	8.448	

The rescaled coupling constant is given by:

$$\bar{u} = \frac{u_0}{u^*\Lambda c_p^{\,4}} = \frac{u_0 c_t^{\,2}}{u^*\Lambda a_0^{\,2}} \tag{4.33}$$

The larger the range of interactions, the smaller $\bar{u}$ [76]. This is in agreement with the values for $\bar{u}$ given in Table (4.3) and the molecular interaction diameters given in Table (4.9). Actually, Λ and $\bar{u}$ cannot be decoupled for simple mixtures. However, Λ is fixed at 1 and, therefore, the product $\Lambda\bar{u}$ equals $\bar{u}$.

The Ginzburg number gives an indication of the region where the fluctuations are negligible and the classical theory is valid:

$$|\Delta\tilde{T}| \gg N_{\mathrm{G}} = \frac{u_0 v_0^2}{64\pi^2 a_0^4 \left(\bar{\xi}_0^+\right)^6} \approx 0.0314\left(\frac{\bar{u}\Lambda}{\sqrt{c_t}}\right)^2 \tag{4.34}$$

This Ginzburg criterion is based on the susceptibility $\tilde{\chi}$. The Ginzburg numbers for the five binary liquids are given in Table (4.3). The Ginzburg numbers decrease with increasing carbon number. This means that the stronger interactions of the longer alkanes extend the range where the classical NRTL model is valid. Close to the critical point, large fluctuations in the concentration are thermally excited at low cost in energy. However, the stronger the interactions in the fluid, the more energy it costs to excite the fluctuations, *i.e.* the range where fluctuations are important shrinks.

4.8 Comparison of the Crossover-NRTL model and a Wegner expansion

The validity of the Crossover-NRTL model in the critical region can be tested by comparing its results with an extended Wegner expansion. The data near the critical point should asymptotically obey the following power law:

$$\Delta\tilde{x}^{\pm} = \pm B_0\left|\frac{T-T_{\mathrm{c}}}{T}\right|^{\beta} \tag{4.35}$$

This simple power law only holds at and near the critical point. If one moves away from the critical point, this simple power law is not enough to describe the coexistence curve and terms that correct the power law for lack of scaling are needed. The extended Wegner expansion for the coexistence curve is given by equation (4.15). The amplitudes in equation (4.15) are given in equation (4.16). This expansion is valid in the range $|\Delta\tilde{T}| \leq 0.01$. Equation (4.15) was optimised to the phase boundary data to get B_0 and B_1. These amplitudes were also calculated with the relations in equation (4.16) for the crossover-NRTL model. The results are given in Table (4.9). It is clear from Table (4.9) that the crossover-NRTL model predicts the right amplitude B_0 of the leading scaling term in the extended Wegner expansion for the coexistence curve. The largest error between B_0 calculated from the crossover-NRTL model and B_0 calculated from the Wegner expansion is 2.6%. The values for the amplitude of the first correction-to-scaling term are totally different. The crossover-NRTL model predicts a much higher B_1 than the Wegner expansion does. As the critical point is approached, the universal scaled asymptotic critical behaviour (4.34) is recovered from the crossover-NRTL model. Far away from the critical point, the classical NRTL model is recovered. This means that, in going from the critical point to the classical limit, the classical NRTL model, with its own temperature dependence, becomes more and more important. Therefore, the Crossover-NRTL will predict its own characteristic values of B_1. All values for B_1 mentioned in Table (4.9) are positive which is common for simple fluids, which have $\bar{u} \leq 1$.

Table 4.10: Comparison of Wegner expansion and crossover-NRTL				
	Wegner expansion applied to experimental data		Crossover-NRTL (Equation (4.16))	
	B_0	B_1	B_0	B_1
acetic anhydride – cyclohexane			1.44	1.86
nitroethane – 3-methylpentane	1.83	0.209	1.83	0.358
nitrobenzene – pentane	1.80	0.056	1.79	0.665
nitrobenzene – octane	1.53	0.192	1.51	0.763
nitrobenzene – decane	1.33	0.298	1.31	0.855
nitrobenzene – dodecane	1.18	0.367	1.16	0.905
nitrobenzene – tetradecane	1.03	0.628	1.00	1.21

4.9 Calculation of the effective exponent β_{eff}

The asymptotic crossover behaviour implies that the coexistence curve asymptotically close to the critical temperature will diverge according to a power law with critical exponent β =0.3255. It is generally believed that farther away from the critical point, the critical exponent will cross over to its classical value β =0.5. This is a crossover from asymptotic singular critical behaviour to asymptotic classical or analytic critical behaviour. The real behaviour of the exponents for simple fluids can be studied with effective exponents. One can define the effective exponent β_{eff} as:

$$\beta_{\mathrm{eff}} = \left(\frac{d \ln(\Delta \tilde{x})}{d \ln(\Delta \tilde{T})} \right) \tag{4.36}$$

The crossover behaviour of this exponent for the system nitrobenzene - octane is shown in Figure (4.16). It is clear from Figure (4.16) that the effective exponent β approaches the Ising value when the temperature approaches the critical temperature. For higher temperatures, there is a tendency to the classical exponent β =0.5. However, for $\Delta\tilde{T}$ >10^{-2} the value of β_{eff} decreases. The explanation for this behaviour is the following. Asymptotic crossover behaviour by itself is not sufficient to describe the thermodynamic crossover behaviour in simple fluids, since the classical theory does not become valid until one reaches temperatures and mole fractions so far away from the critical point that an asymptotic critical description will no longer be applicable. In other words, before classical critical behaviour is reached, regular effects cannot be neglected anymore and β_{eff} decreases. This is a common phenomenon for simple fluids with short-range interactions where ξ is large, while ξ_D is of the order of molecular size.

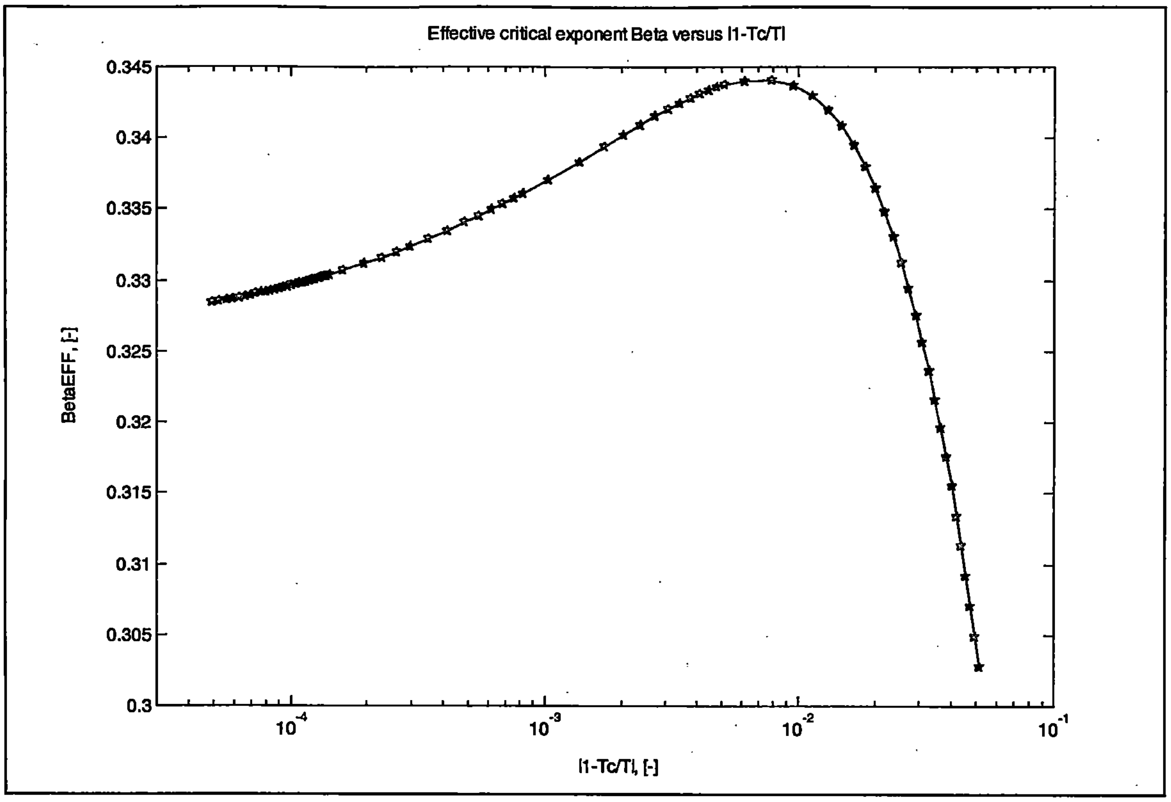

Figure 4.16: Effective exponent β_{eff} for the binary liquid nitrobenzene - octane

4.10 Calculation of the heat capacity C_{px} for the binary mixture 3-methylpentane - nitroethane

In order to describe a real system completely, both the phase boundary and the heat capacity C_{px} have to be described. This heat capacity can be predicted from the Crossover-NRTL model and the optimised NRTL parameters and crossover parameters. In literature there is hardly any system for which both the phase-boundary data and the C_{px} -data are available. For the binary liquid 3-methylpentane - nitroethane, both phase-boundary data and C_{px} -data are available [61,62,77]. The calculation of the phase boundary was given in paragraph 4.6. Sanchez *et al.* have measured the heat capacity at constant p and $x=x_c$ [77].

The heat capacity of mixing at constant pressure and constant composition can be calculated with equation (4.37):

$$\frac{\Delta C_{px}}{R}=\left(\frac{\partial \Delta H/R}{\partial T}\right)_{px}=-T\left(\frac{\partial^2 \Delta G/R}{\partial T^2}\right)_{px}=-T\left(\frac{\partial^2 T\Delta\tilde{G}_{\mathrm{reg}}}{\partial T^2}+\frac{\partial^2 T\Delta\tilde{G}_{\mathrm{sing}}}{\partial T^2}\right)_{px} \qquad (4.37)$$

where ΔC_{px} = heat capacity of mixing at constant p and constant composition [J/(mole·K)]
ΔH = enthalpy of mixing [J/mole]

This heat capacity is the analogue of the isochoric heat capacity C_V for a one-component fluid. A derivative of a density with respect to a field with one field and one density constant is taken along a path asymptotically parallel to the coexistence curve and diverges weakly. Such derivatives diverge with an exponent α along the weak path, in the coexistence surface *intersecting the critical line.* They remain finite in the classical case. In general, properties that diverge strongly in one-component fluids only diverge weakly in binary mixtures of constant composition or constant molar density of one of the components.

The calculation of C_{px} is rather difficult because of the dependence of the crossover variable Y on the temperature. Part of the calculation is given in Appendix B. This heat capacity can be calculated for the one-phase region above the critical point and for the two branches of the coexistence curve below the critical point.

In simple liquid mixtures there is a strong coupling between $\bar{u}$, Λ, and c_t and it is difficult to obtain the independent value of Λ from optimisation of the crossover-NRTL model to phase-boundary data. Therefore, for simple mixtures Λ is mostly fixed at 1, which is good enough for simple mixtures [78]. However, if different thermodynamic properties are to be calculated, the independent value of Λ has to be obtained. Therefore, it is needed to put a new constraint to the optimisation problem of the coexistence curve. For example, the constraint that the leading amplitude of the scaling law for the supercritical heat capacity, A_0^+, has to equal the amplitude of the experimental data points, *i.e.* the value of A_0^+ given by Sanchez *et al.* This procedure was followed in this work. The optimised NRTL parameters and optimised crossover parameters are given in Table (4.3).

In order to describe the singular behaviour of the specific heat capacity resulting from the critical fluctuations, it is needed to make sure that the equation does represent the specific heat capacity in the absence of critical fluctuations. The NRTL equation is a excess Gibbs model that can be used to describe the liquid-liquid phase boundary. However, it is no fundamental thermodynamic equation and it cannot describe caloric properties like C_{px}. Following a suggestion of Edison *et al.* the NRTL equation can be transformed into a fundamental thermodynamic equation by adding an analytic background function to the regular part of the Gibbs energy of mixing (Equation 4.7):

$$\tilde{\mu}_0(\Delta\tilde{T}) = \sum_{j=0}^{4} \tilde{\mu}_j (\Delta\tilde{T})^j \qquad (4.38)$$

The parameters $\tilde{\mu}_0$ and $\tilde{\mu}_1$ are related to the zero points of energy and entropy and do not change the value of any measurable quantity. The coefficients $\tilde{\mu}_2$, $\tilde{\mu}_3$, *and* $\tilde{\mu}_4$ for the binary liquid nitroethane - 3-methylpentane are 10.021, 10.226, and -130.61 respectively. The results for the supercritical C_{px}/R are given in Figure (4.17) on a normal scale and in Figure (4.18) on a log-log scale.

The extended NRTL equation yields exactly the same phase boundary as the original NRTL equation while it is also capable of representing caloric properties.

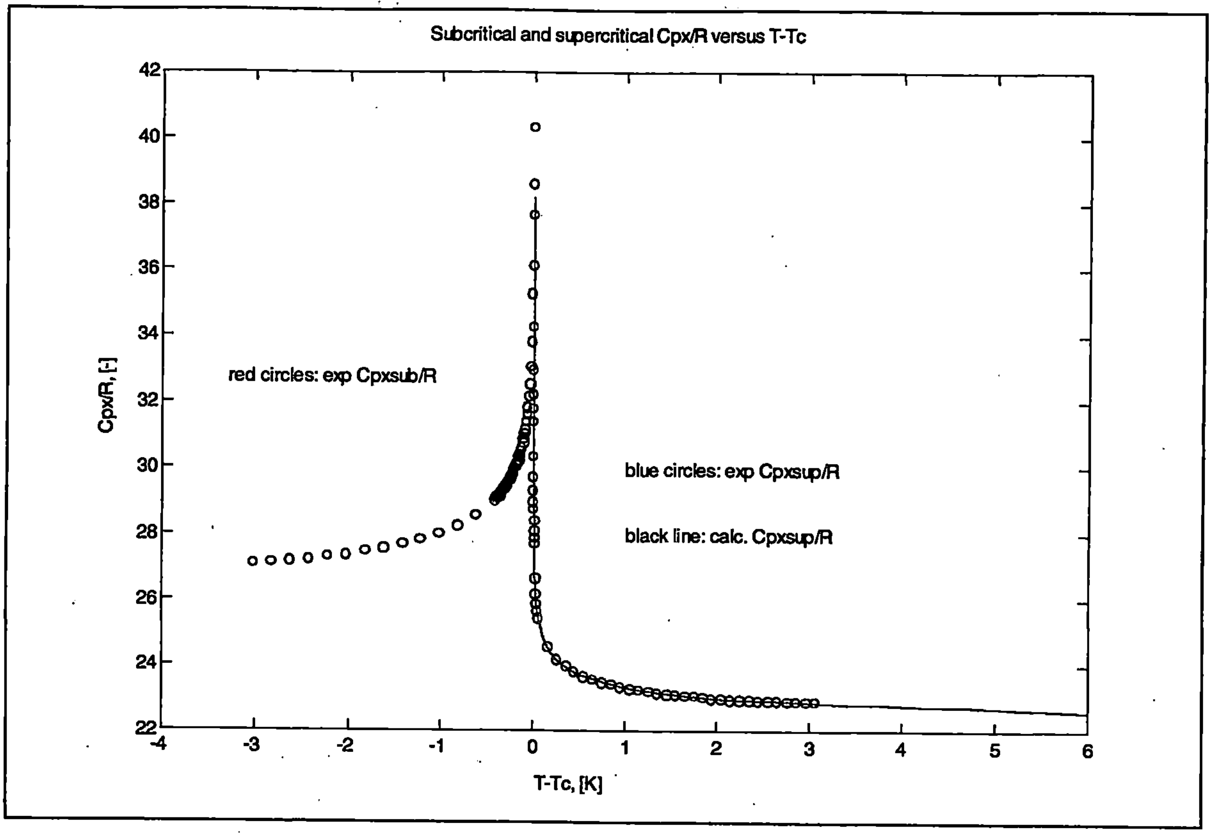

Figure 4.17: Supercritical heat capacity C_{px}, predicted with the Crossover-NRTL model and a caloric background

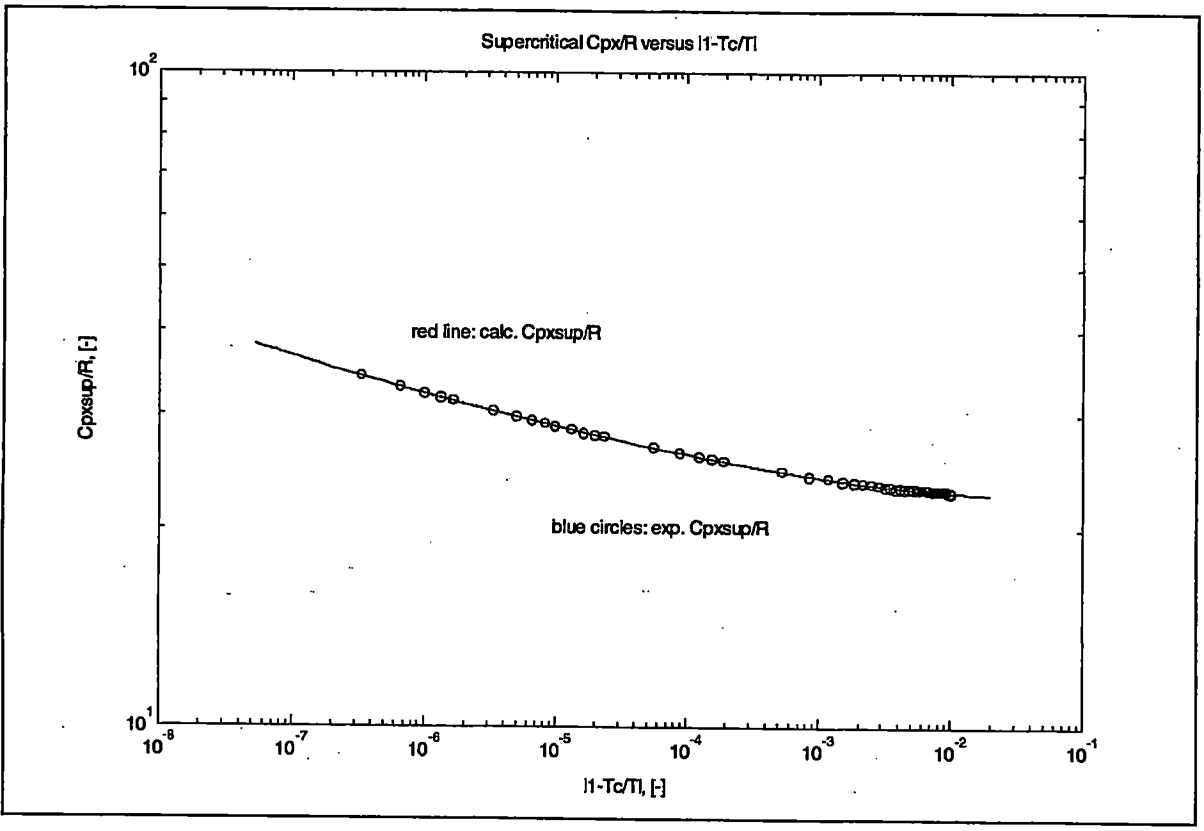

Figure 4.18: Supercritical heat capacity C_{px}, predicted with the Crossover-NRTL model and a caloric background

Sanchez *et al.* optimised the following extended Wegner expansion to their C_{px}/R-data [77]:

$$
\begin{aligned}
\frac{C_{px}^{\ +}}{R} &= \frac{A_0^{\ +}}{\alpha}\left|\frac{T-T_c}{T}\right|^{-\alpha}\left(1+A_1^{\ +}\left|\frac{T-T_c}{T}\right|^{\Delta_1}+\ldots\right)+B+E\left(\frac{T-T_c}{T}\right)+\ldots \\
\frac{C_{px}^{\ -}}{R} &= \frac{A_0^{\ -}}{\alpha}\left|\frac{T-T_c}{T}\right|^{-\alpha}\left(1+A_1^{\ -}\left|\frac{T-T_c}{T}\right|^{\Delta_1}+\ldots\right)+B+E\left(\frac{T-T_c}{T}\right)+\ldots
\end{aligned}
\qquad (4.39)
$$

where $+/-$ = one-phase region (+) or two-phase region (-)
B = background heat capacity far from the critical temperature [-]
$A_0^{+/-}$ = amplitude of the leading divergence of C_{px} [-]
$A_1^{+/-}$ = amplitude of the first correction-to-scaling term of C_{px} [-]
Δ_1 = universal exponent for the first correction term [-]
E = amplitude of the linear background term, which arises from the regular part of the Gibbs energy [-]

Unfortunately, they do not give the experimental data points. Sanchez *et al.* use several fitting procedures. Their 'best' fit, *i.e.* the fit with the lowest χ^2, has an optimised exponent $\alpha = 0.1192$. However, the exponent α has a universal value and cannot be optimised. Therefore, the results of the fit with the universal exponent $\alpha = 0.110$ are taken (fit 15). These results are given in Table (4.11), together with the values of the supercritical reduced heat capacity C_{px}/R, calculated with the Crossover-NRTL model. It can be concluded that the Crossover-NRTL model predicts the correct divergence of the supercritical heat capacity.

Table 4.11: Comparison between experimental and calculated C_{px}/R

	A_0^+	A_1^+	B	E
C_{px}/R experimental	3.41	0.460	16.65	30.26
C_{px}/R calculated	3.42	0.503	16.61	30.27

The calculation of the heat capacity in the two-phase region is a little bit more complicated. C_{px} in the two-phase region is composed of two terms. The first is the heat supplied to raise the temperature of each of the phases at constant pressure and temperature, without allowing the composition of the phases to change. This part is given by the sum of the amounts of each phase times the heat capacities of each phase. The second part is related to the changes in the amount and the composition of each phase and to the difference of the partial molar heat contents in both phases [10].

$$
C_{px} = \underbrace{fC_p{}' + (1-f)C_p{}''}_{\text{Part 1}} + \underbrace{T\left\{ f\left(\frac{\partial^2 G}{\partial x^2}\right)'\left(\frac{dx}{dT}\right)'^{2} + (1-f)\left(\frac{\partial^2 G}{\partial x^2}\right)''\left(\frac{dx}{dT}\right)''^{2}\right\}}_{\text{Part 2}} \qquad (4.40)
$$

where f = factor arising from the lever rule [-]

The primes in equation (4.40) indicate the phase. The calculation of the derivative

$\left(\partial^2 G/\partial x^2\right)$ is analogous to the calculation of $\left(\partial^2 G/\partial T^2\right)$, which is given in Appendix B. The derivative *(dx/dT)* is calculated in a numerical way from the results of the calculation of the coexistence curve. The amplitude of the leading divergence of the subcritical C_{px}, A_0^-, calculated with the crossover-NRTL model equals 5.83. It is known that the leading amplitude below the critical point is two times larger than the one above the critical point for the crossover model of Chen *et al.* [78]. The ratio in this work equals 1.7. From this ratio it is clear that there is something wrong in the calculation of the subcritical heat capacity. Because of the lack of time, results for the subcritical C_{px} will not be given here.

5 Description of the Matlab® programs and subroutines

5.1 Program Datdemo

The optimisation procedures have been written in Matlab®, version 5.3. The optimisation routine *fmincon* has been used. *Fmincon* finds, if possible, the minimum of a constrained multivariable function *f(x)*:

$$\min_{x} f(x) \quad \text{subject to} \quad \begin{aligned} c(x) &\le 0 \\ c_{eq}(x) &= 0 \\ A\cdot x &\le b \\ A_{eq}\cdot x &= b_{eq} \\ LB \le x &\le UB \end{aligned} \tag{5.1}$$

The variables x, b, b_{eq}, LB, and UB are vectors, A and A_{eq} are matrices, $c(x)$ and $c_{eq}(x)$ are functions that return vectors, and $f(x)$ is a function that returns a scalar. The functions $f(x)$, $c(x)$, and $c_{eq}(x)$ can be non-linear. The vectors LB and UB define a set of lower and upper bounds on the vector of design variables, x, so that the solution is always in the range $LB \le x \le UB$. The vector $c(x)$ and the vector $c_{eq}(x)$ respectively consist of the non-linear inequality and the non-linear equality constraints of the problem. The matrices A and A_{eq} consist of the linear inequality and linear equality constraints. Linear constraints play no role in the optimisation processes in this work.

In this work, the vector of design variables x consists of the temperatures, mole fractions of both phases, crossover Y's of both phases, the NRTL parameters $\tilde{b}$ and $\tilde{d}$, and the crossover parameters $\bar{u}$ and/or Λ. One of the advantages of the optimisation routine *fmincon* over the more common optimisation procedures is that it is not needed to calculate the propagated error. The temperature is a free variable in this optimisation procedure. The crossover Y's are also independent variables. They need not to be iterated from the crossover function in an inner loop. During optimisation, Matlab® changes the values of the mole fractions, the temperatures, and the parameters to minimise the objective function and the constraint violation. In the common optimisation procedures, the crossover Y's have to be iterated for every change in the parameters. When the estimates for the mole fractions and the parameters are not good enough, the crossover function has no physically realistic solution. In the critical region, the spinodal curve is very close to the phase boundary. When one of the mole fractions crosses the spinodal curve during optimisation, the condition of material stability is violated and κ^2 becomes negative. For negative values of κ^2, which are physically meaningless, there is no solution for the crossover function. That means that the calculation of the crossover Y's is very sensitive to the first estimates of the parameters. The great advantage of the routine *fmincon* in Matlab® is that one can let Y be a free variable. When there is no solution for the crossover function for the given set of parameters, the procedure chooses another set of parameters.

The main program, Datdemo, and its accompanying subroutines are given in Appendix D, E, and F for the Crossover-NRTL model, the 2T-Landau expansion and the simplified 2T-Landau expansion respectively. These three models were defined in Chapter 4. The program starts with reading in the data set. The first, the second, and the third column of the data set respectively represent the mole fraction of component 1 in phase 1, x_1, the mole fraction of component 1 in phase 2, x_2, and the temperature, T.

After reading in the data, the program calculates the NRTL parameters $\tilde{a}$ and $\tilde{c}$ with the subroutine NRTLPar for the given values of α_{12} and x_c from the conditions of incipient immiscibility (4.17).

The user has to define estimates for the parameters that have to be optimised. The program also needs estimates for the mole fractions of both phases, the accompanying temperature, and the accompanying crossover values Y. The mole fractions and the temperature of the data set can be used as estimates for the final solution. However, estimates for the crossover Y's have to be calculated. The subroutine Bisection calculates these crossover Y's from the crossover function and the initial estimates for the parameters.

The estimates for x_1, x_2, T, Y_1, Y_2, and the parameters are combined in the subroutine VarToVector to form the design vector. The optimisation process optimises the vector of variables by minimising the objective function given in subroutine FitFun and the NRTL and crossover constraints given in subroutine Constraints. The objective function is minimised with the Levenberg-Marquardt optimisation routine. This routine is a modification of the well-known Gauss-Newton optimisation routine. The Levenberg-Marquardt method uses a search direction that is a cross between the Gauss-Newton direction and the steepest descent. The Levenberg-Marquardt method often needs more function evaluations than the Gauss-newton method but this poorer efficiency is compensated for by the increased robustness of the method.

5.2 Subroutine Bisection

Bisection calculates estimates for the crossover variable Y. This subroutine is the same for the Crossover-NRTL model, the 2T-Landau expansion and the simplified 2T-Landau expansion. It is given in Appendix D. The crossover function (4.12) is an implicit function of Y. The estimates for Y are calculated with use of the estimates for the NRTL parameters $\tilde{b}$ and $\tilde{d}$ and the estimates for the crossover variables $\bar{u}$ and Λ. The objective function to be minimised is given by:

$$f_Y = 1-(1-\bar{u})Y - \bar{u}\left(1+\frac{\Lambda^2}{\kappa^2}\right)^{1/2} Y^{1/\omega} \tag{5.2}$$

The bisection root solver needs two starting values for Y. It analyses the sign of the objective function f_Y at both starting values for Y. When the product of the objective functions at the two starting values is negative, the root lies between those two starting points. If the product is positive, the root does not lie between the two starting points and two other starting values have to be chosen. A physically realistic solution for Y lies between 0 and 1. The subroutine Bisection starts with the two starting values Y_0 and $Y_0+0.001=Y_1$. If the product of the objective functions is positive, the new starting values for Y are Y_1 and $Y_1+0.001=Y_2$. For larger values of Y, *i.e.* for points farther away from the critical point, there are several possible solutions to the crossover function. Therefore, the choice of Y_0 must be taken care of. The subroutine Bisection gives different starting values, Y_0, for different ranges of $\Delta\tilde{T}$. The farther away from the critical point, the larger Y_0. When the product of the objective functions is negative and not complex, the bisection root solver finds the root in the following way:

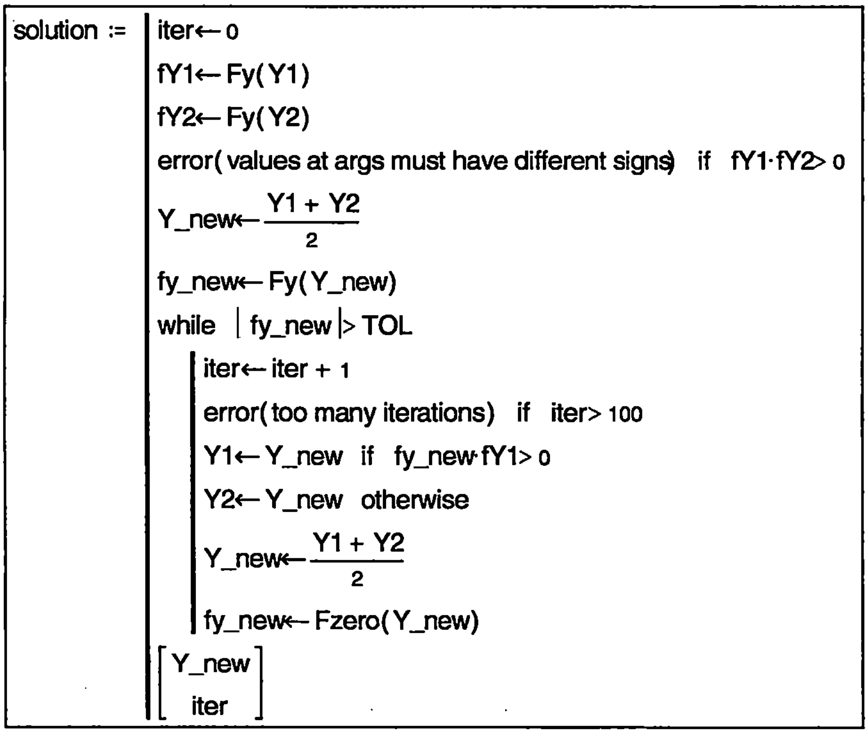

```
solution :=  iter ← 0
             fY1 ← Fy(Y1)
             fY2 ← Fy(Y2)
             error(values at args must have different signs)  if  fY1·fY2 > 0
             Y_new ← $\frac{Y1 + Y2}{2}$
             fy_new ← Fy(Y_new)
             while  |fy_new| > TOL
                 iter ← iter + 1
                 error(too many iterations)  if  iter > 100
                 Y1 ← Y_new  if  fy_new·fY1 > 0
                 Y2 ← Y_new  otherwise
                 Y_new ← $\frac{Y1 + Y2}{2}$
                 fy_new ← Fzero(Y_new)
             $\begin{bmatrix} Y\_new \\ iter \end{bmatrix}$
```

Each data point in each phase has its own distance from the critical point and, therefore, its own *Y*.

5.3 Subroutine FitFun

This subroutine defines the objective function. The objective function $\chi^2(x)$, which has to be minimised, is given by:

$$\chi^2(x_{i,p,\mathrm{calc}},T_{i,\mathrm{calc}})=\frac{1}{N-M}\sum_{j=1}^{L}\frac{w_j N}{N_j}\left\{\sum_{p=1}^{P}\sum_{i=1}^{N_j}\frac{\left(x_{i,p,\exp}-x_{i,p,calc}\right)^2}{\sigma_x^2}+\sum_{i=1}^{N_1}\frac{\left(T_{i,\exp}-T_{i,\mathrm{calc}}\right)^2}{\sigma_T^2}\right\} \tag{5.3}$$

where	N =	total number of data points	[-]
	N_j =	number of type *i* data points	[-]
	M =	number of parameters to be optimised	[-]
	w_j =	weight factor that can be applied to type *j* data points	[-]
	P =	number of coexisting phases	[-]
	$x_{i,p,\mathrm{exp/calc}}$ =	experimental or calculated mole fraction belonging to data point *i* and phase *p*	[-]
	$T_{i,\mathrm{exp,calc}}$ =	experimental or calculated temperature belonging to data point *i*	[K]
	σ_x =	standard deviation of the experimental mole fractions	[-]
	σ_T =	standard deviation of the experimental mole temperatures	[K]

This subroutine is somewhat different for the Crossover-NRTL model, the 2T-Landau expansion, and the simplified 2T-Landau expansion. Therefore it is given in Appendix D, E, and F for the different models separately.

The standard deviations of the mole fractions and the temperature have to be supplied by the user. The weight factor was not used in this work. The optimisation converges much faster if Matlab® does not have to determine the partial derivatives of all constraints to all variables in a numerical way. When the user supplies the analytical derivatives of the objective function, they should be presented in the following way:

$$G_{\chi^2} = \begin{bmatrix} \dfrac{\partial \chi^2}{\partial T} \\ \dfrac{\partial \chi^2}{\partial Y_1} \\ \cdots \end{bmatrix} \tag{5.4}$$

5.4 Subroutine Constraints

This subroutine is given in Appendix D, E, and F for the Crossover-NRTL model, the 2T-Landau expansion, and the simplified 2T-Landau expansion respectively.

The phase-boundary constraints and the crossover constraints are defined in this subroutine. The phase-boundary constraints can be calculated from the activities of both components in both phases (3.3, 4.14). The difference between the activities of component i in both phases must equal zero. Another equality constraint is given by the crossover function. The right side minus the left side of the crossover function must equal zero. The subroutine Constraints also supplies inequality constraints. The values of these constraints must be smaller than 0. When the optimisation procedure comes across a negative value for κ^2, the optimisation procedure will become much more difficult, often terminating with an infeasible solution. An inequality constraint is $-\kappa^2$. The property κ^2 must be positive. Also, the non-linear equality constraints and the non-linear inequality constraints are given by:

$$\begin{aligned} c_{\mathrm{eq}_{1,j}} &= \ln(a_{\mathrm{comp}_j,\mathrm{phase}_1}) - \ln(a_{\mathrm{comp}_j,\mathrm{phase}_2}) \\ c_{\mathrm{eq}_{2,i}} &= 1-(1-\bar{u})Y_{\mathrm{phase}_i} - \bar{u}\left(1+\left(\frac{\Lambda}{\kappa_{\mathrm{phase}_i}}\right)^2\right)^{1/2} Y_{\mathrm{phase}_i}{}^{1/\omega} \\ c_i &= -\kappa^2{}_{\mathrm{phase}_i} \end{aligned} \tag{5.5}$$

It is possible to determine the constraints for the phase boundary as indicated in equation (4.14). However, they can also be calculated in a much simpler way. See Appendix A. The optimisation converges much faster if Matlab® does not have to determine the partial derivatives of all constraints to all variables numerically. The analytical derivatives of the non-linear equality and inequality constraints should be presented in the following way:

$$GC_{\mathrm{eq}}=\begin{bmatrix} \frac{\partial c_{\mathrm{eq}_{1,1}}}{\partial T} & \frac{\partial c_{\mathrm{eq}_{1,1}}}{\partial T} & \frac{\partial c_{\mathrm{eq}_{2,1}}}{\partial T} & \frac{\partial c_{\mathrm{eq}_{2,2}}}{\partial T} \\ \frac{\partial c_{\mathrm{eq}_{1,2}}}{\partial Y_1} & \frac{\partial c_{\mathrm{eq}_{1,2}}}{\partial Y_1} & \frac{\partial c_{\mathrm{eq}_{2,1}}}{\partial Y_1} & \cdots\cdot \\ \frac{\partial c_{\mathrm{eq}_{1,1}}}{\partial Y_2} & \frac{\partial c_{\mathrm{eq}_{1,2}}}{\partial Y_2} & \cdots\cdot & \cdots\cdot \\ \cdots\cdot & \cdots\cdot & \cdots\cdot & \cdots\cdot \end{bmatrix} \qquad GC=\begin{bmatrix} \frac{\partial c_{1,1}}{\partial T} & \frac{\partial c_{1,2}}{\partial T} \\ \frac{\partial c_{1,1}}{\partial Y_1} & \frac{\partial c_{1,2}}{\partial Y_1} \\ \frac{\partial c_{1,1}}{\partial Y_2} & \frac{\partial c_{1,2}}{\partial Y_2} \\ \cdots\cdot & \cdots\cdot \end{bmatrix} \qquad (5.6)$$

GC$_{\mathrm{eq}}$ is the matrix of the partial derivatives of the non-linear equality constraints to the variables in the design vector. *GC* is the matrix of the partial derivatives of the non-linear inequality constraints to all variables in the design vector.

5.5 Subroutine VarToVector

The subroutine VarToVector converts the variables into the design vector. The boundaries for the vector can also be given in this subroutine. The default lower and upper bounds are minus infinity and plus infinity. Without lower and upper bounds, the optimisation problem often cannot find a feasible solution. It is not difficult to give physically realistic lower and upper bounds. For example, the mole fractions and the crossover *Y*s must lie between 0 and 1. When these bounds are not stringent enough, one can reduce the range by making the lower bound 0.95 times the experimental property and the upper bound 1.05 times the experimental property. A disadvantage of these stringent bounds is that the optimisation process converges much slower. However, in most cases a feasible solution is found. The Matlab® code of VarToVector is given in Appendix D.

5.6 Subroutine VectorToVar

This subroutine extracts the variables from the design vector. The Matlab® code of VectorToVar is given in Appendix D.

5.7 Subroutine NRTLPar

NRTLPar calculates the NRTL parameters $\tilde{a}$ and $\tilde{c}$ from the conditions of incipient immiscibility, as given by equation (4.17). The Matlab® code of NRTLPar is given in Appendix D.

5.8 Program Coex

The program Coex calculates the coexistence curve using the optimised parameters $\bar{u}$, Λ, $\tilde{b}$, and $\tilde{d}$. It extrapolates the coexistence curve to the classical region.

5.9 Program Cpx and CpxTwoPhase

These programs calculate the heat capacity at constant pressure and constant composition, $x=x_c$, in the one-phase region above the critical point and in the two-phase region below the critical point. The program needs mole fractions and accompanying crossover variables Y's for different temperatures. The mole fractions and the crossover Y's in the two-phase region below the critical point are calculated with the program Coex, The mole fraction in the one-phase region above the critical point is fixed at its critical value x_c. The crossover variable Y can be calculated with the subroutine Bisection. The Matlab® code of these programs is not given here because it is too voluminous.

6 Conclusions

This graduation work consists of a study of crossover theory and of the applicability and modelling of the Crossover Non-Random Two Liquid model for the description of liquid-liquid equilibria both in the classical and the critical regions. The NRTL equation is a so-called excess Gibbs energy model, which accounts for the non-ideality of the mixture. The classical NRTL model by itself is not able to describe both the classical and critical regions. It is a typical mean-field equation, which cannot account for the critical fluctuations that are so important in a broad region around the critical point. The classical NRTL equation should only be applied in the region where it is valid, *i.e.* far from the critical point. As soon as the equation is applied to that part of the coexistence curve where critical fluctuations become important, the result will be both bad in the classical region and in the region where fluctuations become important.

In this work the crossover model of Chen *et al.* is applied to the Non-Random Two Liquid equation in order to introduce critical fluctuations. The main part of the procedure has been given by Edison *et al.*. Edison's model contains some fundamental errors. These errors kept my own model, written in Matlab®, from converging. Basic error's in Edison's model were some missing factors x_c^2 in the derivatives of κ^2 to the unrenormalised variables $\Delta\tilde{x}$ and $\Delta\tilde{T}$. Another error is the wrong assumption of universality of the parameters $\tilde{a}$ and $\tilde{c}$ for the Crossover-NRTL equation. These parameters depend on the non-randomness parameter α_{12} and the mole fraction at the critical point, x_c.

The remaining errors were found by comparing the crossover NRTL model to a simplified 2T-Landau expansion (without kernel term and implicit dependence of the crossover variable Y on the order parameter M) and a normal 2T-Landau expansion (with kernel term and implicit dependence of Y on M). Edison omitted the system-dependent amplitudes c_t and c_ρ that give the coupling between the general Landau variables and the physical variables. After correcting these errors, the model returned physically realistic feasible solutions.

The simplified 2T-Landau expansion can give first estimates for the crossover parameters in the optimisation routine for the Crossover-NRTL model. The normal 2T-Landau expansion can also give estimates for the NRTL parameters $\tilde{b}$ and $\tilde{d}$. However, the latter estimates are not particularly good.

Edison's program was written in Fortran® code. The programs and accompanying subroutines in this work are written in Matlab® code. My optimisation routine, written in Matlab® code, is much more flexible than Edison's original program. In the new program, the temperature, mole fractions, and crossover Y's are independent variables during optimisation. Therefore, the propagated error in the measured property and the inner loop for the calculation of the crossover Y's from the crossover function need not to be calculated.

The corrected Crossover-NRTL model describes the coexistence curve both in the classical region far away from the critical point and in the critical region very well. The corrected Crossover-NRTL model reduces to the asymptotic scaling laws with the correct universal critical exponents near the critical point and to the classical NRTL equation far away from the critical point. The Crossover-NRTL model is also able to describe rather asymmetric coexistence curves. Taking the critical fluctuations into account causes the calculated coexistence curve to become flatter and the critical point to be lower than expected from classical mean-field theory.

The Crossover-NRTL model contains two system-dependent parameters $\tilde{a}$ and $\tilde{c}$, which can be determined from the conditions of incipient immiscibility at the consolute critical point. Two other NRTL parameters $\tilde{b}$ and $\tilde{d}$ have to be optimised by data regression. For simple fluids, the crossover parameters $\bar{u}$ and Λ are too much correlated to be calculated independently. Therefore, Λ is fixed at 1 in most cases. In these cases the crossover parameter $\bar{u}$ has to be optimised by data regression.

The predictive capabilities of the crossover NRTL model were tested by comparison of a derived thermodynamic property with data taken from literature. For the calculation of the heat capacity C_{px}, an independent value of the crossover parameter Λ is needed. The determination of this independent crossover parameter is not so easy because there is a strong correlation between $\bar{u}$ and Λ for simple mixtures. The temperature range of the available phase-boundary data was too small and the mixture too simple to determine the independent Λ. However, an estimate for Λ could be found by forcing the leading amplitude of the power law for the supercritical C_{px} to be equal to the one calculated from the experimental data points during optimisation of the Crossover-NRTL model to the phase-boundary data. This procedure did not influence the χ^2 of the fit.

The supercritical heat capacity C_{px} can be described by adding a caloric background term to the regular part of the Gibbs energy of mixing. This extension of the NRTL model yields exactly the same phase boundary as the original NRTL model while it is also capable of representing caloric properties. Analysis of the calculated supercritical C_{px} with an extended Wegner expansion and comparison with data taken from literature show that the extended Crossover-NRTL model predicts the correct divergence near the critical point.

The asymptotic behaviour of the coexistence curve was analysed by plotting it on a log-log scale and by calculating the effective exponent β_{eff}. For the analysed systems, the exponent β_{eff} equals the corresponding Ising exponent asymptotically close to the critical point. As the distance to the critical point is increased, β_{eff} first increases towards the mean field value but, before reaching that limit, it drops steeply, indicating that for simple fluids the crossover from Ising-like behaviour to mean-field critical behaviour is not completed within the critical domain.

A short survey of the significance of the crossover parameters $\bar{u}$ and Λ, the NRTL parameters $\tilde{b}$ and $\tilde{d}$ and the Ginzburg number is given. The NRTL parameters are related to the interaction energies and show whether molecules of different types "like" each other or not, which is expressed in the local mole fractions. The significance of the crossover parameters has to do with the range of interactions between the molecules. The crossover parameters are representative for simple fluids.

7 Recommendations

The results of the crossover-NRTL model seem to be very promising. However, there are few data sets with both accurate data in the critical region and an extended range in temperature. The validity of the Crossover-NRTL model should be tested with data sets with extended temperature ranges. Except for the data set acetic anhydride – cyclohexane, the ranges are a little bit too small to test the validity in the classical region.

In the present work, the C_{px} values in the subcritical region could not be represented adequately. The calculations of the thermal response function in the 2-phase region, usually split into a frozen phase-equilibrium response and material relaxation to the new equilibrium state, need to be improved.

The calculation of C_{px} was only a prediction from the NRTL parameters and crossover parameters that were calculated from data regression of the crossover-NRTL model to the coexistence curve. A better value for Λ and $\bar{u}$, and maybe a better representation of the coexistence curve can be obtained by optimising the NRTL parameters and crossover parameters to both heat-capacity data and phase-boundary data at the same time.
One recommendation with respect to the modelling. The Gibbs energy of mixing is separated into a regular and a singular part by expanding it around the consolute critical point. This results in voluminous expressions. Giving repeating terms a new name can reduce the sizes of these expressions. This will also reduce the calculation time during optimisation.

8 Literature

[1] Z. Y. Chen, A. Abbaci, S. Tang, J. V. Sengers, *Phys. Rev. A*, **42** (1990), page 4470

[2] T. A. Edison, M. A. Anisimov, J. V. Sengers, *Fluid Phase Equilibria*, **150-151** (1998), page 429

[3] A. Lesne, *Renormalization methods: Critical Phenomena, Chaos, Fractal Structures*, 1998, (J. Wiley, New York)

[4] *Critcal Phenomena, Proc. of a Conference held in Washington D. C.*, NBS Misc. Publ. 273, M. S. Green, J. V. Sengers, eds., National Bureau of Standards, Washington D. C., 1986

[5] J. V. Sengers, *Progress in Liquid Physics*, Chapter 4, C. A. Croxton, ed. (Wiley, Chichester, U. K., 1978), page 103

[6] J. M. H. Levelt Sengers, Thermodynamics of solutions near the solvent's critical point, In: *Supercritical Fluid Technology:* Reviews in Modern Theory and Applications, eds. T. J. Bruno, J. F. Ely, (CRC, London)

[7] S. Tang, J. V. Sengers, Z. Y. Chen, *Physica A*, **179** (1991), page 344

[8] R. B. Griffiths, *J. Chem. Phys.*, **43** (1965a), page 1958

[9] R. B. Griffiths, *Phys. Rev. Lett.*, **14** (1965b), page 623

[10] J. S. Rowlinson, *Liquids and liquid Mixtures*, 2nd ed., Butterworths, London, 1969

[11] G. S. Rushbrooke, *J. Chem. Phys.*, **43** (1965), page 3439

[12] D. A. Liberman, *J. Chem. Phys.*, **44** (1966), page 419

[13] J. V. Sengers, Kritische verschijnselen in gassen en vloeistoffen, College Bijzondere Onderwerpen Theoretische Natuurkunde, 1974, Delft

[14] G. S. Rushbrooke, *J. Chem. Phys.*, **39** (1963), page 842

[15] M. E. Fisher, *J. Math. Phys.*, **5** (1964), page 944

[16] N. D. Mermin, J. J. Rehr, *Phys. Rev. Lett.*, **26** (1971), page 1155

[17] P. Schofield, *Phys. Rev. Lett.*, **22** (1969), page 606

[18] J. M. H. Levelt Sengers, *From the Van der Waals equation to the scaling laws*, North-Holland Publishing Co., *Physica*, **73** (1973), page 106

[19] J. M. H. Levelt Sengers, *Supercritical Fluids*, (1994), page 3

[20] R. B. Griffiths, J. C. Wheeler, *Phys. Rev. A*, **2** (1970), page 1047

[21] J. V. Sengers, J.M. H. Levelt Sengers, *Ann. Rev. Phys. Chem.*, **37** (1986), page189

[22] R. L. Scott, (1977), In: M. L. McGlashan (Ed.), *Chemical Society Specialist*

[23] J. M. H. Levelt Sengers, *Physica*, **82A** (1976), page 319

[24] F. Wegner, *Phys. Rev. B*, **5** (1972), page 4529

[25] M. Ley-Koo, M. S. Green, (1976)

[26] G. R. Golner, E. K. Riedel, *Phys. Rev. Lett.*, **34**, (1975), page 856

[27] K. G. Wilson, J. Kogut, *Phys. Rev.*, **12C** (1974), page 75

[28] K. G. Wilson, *Rev. Mod. Phys.*, **55** (1983), page 583

[29] P. C. Albright, J. V. Sengers, J. F. Nicoll, M. Ley-Koo, *Intern. J. Thermophys.*, **7** (1986), page 75

[30] A. Z. Patashisnkii, V. L. Pokrovskii, *Fluctuation Theory of Phase Transitions* (Pergamon, New York, 1979)

[31] M. A. Anisimov, S. B. Kiselev, J. V. Sengers, S. Tang, *Physica A*, **188** (1992), page 487

[32] S. Tang, J. V. Sengers, *J. Supercritical Fluids*, **4** (1991), page 209

[33] J. F. Nicoll, J. K. Bhattacharjee, *Phys. Rev. B*, **23** (1981), page 389

[34] J. F. Nicoll, *Phys. Rev. A*, **24** (1981), page 2203

[35] J. Nicoll, P. C. Albright, *Phys. Rev. B*, **31** (1985), page 4576

[36] P. C. Albright, J. V. Sengers, J. F. Nicoll, M. Ley-Koo, *Int. J. Thermophys.*, **7** (1986), page 75

[37] P. C. Albright, Z. Y. Chen, J. V. Sengers, *Phys. Rev. B*, **36** (1987), page 877

[38] Z. Y. Chen, P. C. Albright, J. V. Sengers, *Physica A*, **41**, (1990), page 3161

[39] J. V. Sengers, *Effects of Critical Fluctuations on the Thermodynamic and Transport Properties of Supercritical Fluids*

[40] J. C. Le Guillou, J. Zinn-Justin, *Phys. Rev. B*, **21** (1980), page 3796

[41] A. D. Bruce, D. J. Wallace, *J. Phys. A*, **9** (1976), page 1117

[42] S. Tang, J. V. Sengers, Z. Y. Chen, *Physica A*, **179** (1991), page 344

[43] M. Ley-Koo, M. S. Green, *Phys. Rev. A*, **23**, (1981), page 2650

[44] F. C. Zhang, R. K. P. Zia, *J. Phys. A*, **15** (1982), page 3303

[45] K. E. Newman, E. K. Riedel, *Phys. Rev. B*, **30** (1984), page 6615

[46] G. X. Jin, *Ph. D. Thesis*, Institute of Physical Science and Technology, Univ. of Maryland: College Park MD, 1993

[47] A. Kostrowicka Wyczalkowska, M. A. Anisimov, J. V. Sengers, *Fluid Phase Equilibria*, **158-160** (1999), page 523

[48] A. van Pelt, G. X. Jin, J. V. Sengers, Paper presented at the 12th Symposium on Thermophysical Properties, June 19-24, 1994, Boulder, Colorado, USA

[49] G. M. Wilson, *J. Am. Chem. Soc.*, **86** (1964), page 127

[50] H. Renon, J. M. Prausnitz, *AIChE J.*, **14(1)** (1968), page 135

[51] R. L. Scott, *J. Chem. Phys.*, **25** (1956), page 193

[52] E. A. Guggenheim, Mixtures, Clarendon Press, Oxford, 1952

[53] J. P. Novák, J. Matouš, J. Pick, Liquid-Liquid Equilibria, Elsevier, 1987

[54] J. M. Marina, D. Tassios, *Ind. Eng. Chem. Process Des. Dev.*, **12** (1973), page 271

[55] I. Nagata, T. Yamada, *J. Chem. Eng. Data*, **18** (1973), page 87

[56] H.-J. Bittrich, D. A. Lempe, K. Reinhardt, J.-U. Wüstling, *Fluid Phase Equilibria*, **126** (1996), page 115

[57] N. Nagarajan, A. Kumar, E. S. R. Gopal, *J. Phys. Chem.*, **84** (1980), page 2883

[58] J. Jacob, A. Kumar, M. A. Anisimov, A. A. Povodyrev, J. V. Sengers, *Phys. Rev. E*, **58(2)** (1998), page 2188

[59] E. S. R. Gopal, P. Chandra Sekhar, G. Ananthakrishna, R. Ramachandra, S. V. Subramanyam, *Proc. R. Soc. Lond.*, **A 350** (1976), page 91

[60] S. C. Greer, personal communications

[61] M. Wims, D. McIntyre, F. Hynne, *J. Chem. Phys.*, **50(2)** (1969), page 616

[62] M. P. Khosla, B. Widom, *J. Colloid Interface Sci.*, **76** (1980), page 375

[63] Y. P. Handa, C. M. Knobler, R. L. Scott, *J. Chem. Thermodynamics*, **9** (1977), page 451

[64] X. An, P. Li, H. Zhao, Weiguo Shen, *J. Chem. Thermodynamics*, **30** (1998), page 1049

[65] X. An, F. Jiang , H. Zhao, C. Chen, Weiguo Shen, *J. Chem. Thermodynamics*, **30** (1998), 751

[66] X. An, H. Zhao, F. Jiang, Weiguo Shen, *J. Chem. Thermodynamics*, **30** (1998), page 21
[67] X. An, H. Zhao, F. Jiang, C. Mao, Weiguo Shen, *J. Chem. Thermodynamics*, **29** (1997), page 1047
[68] X. An, F. Jiang, H. Zhao, Weiguo Shen, *J. Chem. Thermodynamics*, **30** (1998), page 1181
[69] A. Van Pelt, J. V. Sengers, *J. Supercritical Fluids*, **8(2)** (1995), page 81
[70] R. T. Jacobson, S. G. Penoncello, E. W. Lemmon, preprint
[71] W. Maassen van den Brink, H. van Bekkum, Lecture Notes Organische Chemie, ST308, 1997, TUDelft, Faculty of Applied Sciences, Subfaculty of Chemical Technology and Material Sciences
[72] D. R. Lide, Handbook of Chemistry and Physics, 79th Ed., CRC Press LLC, Boca Raton, 1998
[73] A. A. Povodyrev, M. A. Anisimov, J. V. Sengers, *Physica A*, **264** (1999), page 345
[74] L. W. Flynn, G. Thodos, *AIChE J.*, **8** (1962), page 362
[75] R. A. Shevla, NASA Tech. Rep. R-132, Lewis Research Center, Cleveland, Ohio, 1962
[76] M. A. Anisimov, J. V. Sengers, Critical and Crossover Phenomena in Fluids and Fluid Mixtures, preprint
[77] G. Sanchez, M. Meichle, C. W. Garland, *Phys. Rev. A*, **28** (1983), page 1647
[78] M. A. Anisimov, J. V. Sengers, personal communications

9 Nomenclature

Greek

α_p = isobaric expansivity [K^{-1}]

α = universal critical exponent for the power law of the isochoric heat capacity along the supercritical part for the critical isochore [-]

α' = universal critical exponent for the power law of the isochoric heat capacity along the coexistence curve [-]

α'' = universal critical exponent for the power law of the isochoric heat capacity along the subcritical part of the critical isochore [-]

α_{12} = non-randomness parameter [-]

β = critical exponent for the power law of the coexistence curve [-]

β_{eff} = effective critical exponent for the coexistence curve [-]

γ_i' = activity coefficient of component *i* in phase ' [-]

γ = universal critical exponent for the power law of the susceptibility along the critical isochore [-]

γ' = universal critical exponent for the power law of the susceptibility along the coexistence curve [-]

Γ_0 = amplitude of the leading term for the power law for K_T along the critical isochore [-]

Γ_0' = amplitude of the leading term for the power law for K_T along the coexistence curve [-]

δ = universal critical exponent for the chemical potential and the pressure along the critical isotherm [-]

Δ = chemical-potential difference, μ_1-μ_2 [J/mole]

Δ_a = crossover exponent [-]

Δ_1 = universal exponent for the first correction term [-]

η = universal critical exponent [-]

θ = variable that controls the phase transition

θ_p = universal critical exponent [-]

θ_μ = universal critical exponent [-]

κ = variable characterising the distance from the critical point [-]

κ_{cl} = variable characterising the distance from the critical point in the classical theory [-]

λ = scaling parameter in a homogeneous relation [-]

Λ = maximum cutoff wavenumber [-]

Λ = thermal or De Broglie wavelength [m]

μ_i = chemical potential of component *i* [J/mole]

$\tilde{\mu}$ = reduced chemical potential [-]

$\Delta\tilde{\mu}$ = reduced difference in chemical potential [-]

$\tilde{\mu}_0(\Delta\tilde{T})$ = analytic background function of $\Delta\tilde{T}$ subject to the condition that at the critical point, $\Delta\tilde{\mu}=0$ [J/mole]

ν = universal critical exponent for the power law of the correlation length [-]

ξ = correlation length [Å]

$\bar{\xi}_0^{(+)}$ = mean-field correlation-length amplitude [Å]

ξ_D = characteristic length [Å]

ρ_c = molar critical density [mole/m^3]

ρ_j = mass density of pure *j* [g/cm^3]

ρ^i = mass density of phase *i* [g/cm^3]

ρ = molar density [mol/m^3]

$\tilde{\rho}$ = reduced molar density [-]

$\Delta\tilde{\rho}$ = reduced molar density minus 1 [-]
σ_x = standard deviation of the experimental mole fractions [-]
σ_T = standard deviation of the experimental temperatures [K]
σ_i = molecular interaction diameter of component *i* [Å]
τ_{21} = NRTL parameter [-]
τ_{12} = NRTL parameter [-]
$\phi(\vec{r})$ = position-dependent order parameter [-]
χ = symmetrised isothermal compressibility or susceptibility [mol^2/(J·m^3)]
χ^2 = objective function [-]
ω_c = critical exponent [-]

Latin

a_0 = Landau amplitude [-]
a_ρ = exponent in homogeneous relation [-]
a_T = exponent in homogeneous relation [-]
$a(\phi(\vec{r}))$ = position-dependent Helmholtz energy density [-]
$a(x/x_0)$ = scaling function [-]
a_i' = activity of component *i* in phase ′ [-]
$\tilde{a}$ = NRTL parameter [-]
A = Helmholtz energy of a system consisting of *N* molecules in a volume *V* with potential energy U_N [J]
A = Helmholtz energy [J/mole]
$A^{(0)}$ = Helmholtz energy of the reference system [J]
$A^{(1)}$ = Helmholtz energy of the perturbation [J]
A_0^+ = amplitude for the leading term of the power law for C_V along the supercritical isochore [-]
$A_{0\,\mathrm{I}}^-$ = amplitude for the leading term of the power law for C_V along the coexistence curve [-]
$A_{0\,\mathrm{II}}^-$ = amplitude for the leading term of the power law for C_V along the subcritical isochore [-]
$\tilde{A}_0(\Delta\tilde{T})$ = mechanical background, analytic in temperature [-]
$\tilde{A}_{ij}$ = partial derivative of the Helmholtz energy density, *i* times to $\Delta\tilde{T}$ and *j* times to $\Delta\tilde{x}$, evaluated at the critical point. [-]
$\Delta\tilde{A}_{\mathrm{sing}}$ = singular part of the reduced Helmholtz energy [-]
$\Delta\tilde{A}_{\mathrm{R}}$ = renormalised singular part of the reduced Helmholtz energy [-]
$\Delta\tilde{A}_{\mathrm{R,symm}}$ = renormalised singular part of the reduced Helmholtz energy for a symmetrical system [-]
$\tilde{b}$ = NRTL parameter [-]
B = background heat capacity far from the critical temperature [-]
B_0 = amplitude for the leading term of the power law for the coexisting densities/ mole fractions [-]
B_1 = amplitude for the first correction-to-scaling term for the coexisting densities/ mole fractions [-]
c = system-dependent coefficient that accounts for mixing of variables [-]
$c(x)$ = vector with inequality constraints
$c_{\mathrm{eq}}(x)$ = vector with equality constraints
$\tilde{c}$ = NRTL parameter [-]
c_0 = system-dependent coefficient related to the square of a so-called short-range correlation length [-]
c_t = system-dependent amplitude [-]
c_ρ = system-dependent amplitude [-]
C_p = isobaric heat capacity [J/(mole·K)]

C_{px} = isobaric heat capacity at constant composition [J/(mole·K)]
$C_{p\Delta}$ = isobaric heat capacity at constant chemical potential difference [J/(mole·K)]
C_v = isochoric heat capacity [J/(mole·K)]
$\Delta\tilde{C}_V$ = jump in the reduced heat capacity [-]
ΔC_{px} = heat capacity of mixing at constant *p* and constant composition [J/(mole·K)]
$\tilde{d}$ = NRTL parameter [-]
d_{sing}, $d_{2\beta}$, d_1 = amplitudes in the extended Wegner expansion for the coexistence curve [-]
D_0 = amplitude for the leading term of the power law for the reduced pressure/reduced chemical potential difference [-]
$\mathcal{D}$ = rescaling function [-]
E = amplitude for the linear background term, which arises from the regular part of the Gibbs energy [-]
f = factor arising from the lever rule [-]
g_{ij} = interaction energy between an *i-j* pair of molecules [J/mole]
g_{ii} = interaction energy between an *i-i* pair of molecules [J/mole]
$g^{(i)}$ = Gibbs energy of a cell containing molecule *i* at its centre [J/mole]
$g_{\text{pure}}^{(i)}$ = Gibbs energy of a cell containing pure *i* [J/mole]
G^E = Excess Gibbs energy [J/mole]
G^{id} = Gibbs energy of an ideal mixture [J/mole]
G_i = Gibbs energy of pure *i* [J/mole]
G_{21} = NRTL parameter [-]
G_{12} = NRTL parameter [-]
$\tilde{G}_{ij}$ = partial derivative of the Gibbs energy of mixing *i* times to $\Delta\tilde{T}$ and *j* times to $\Delta\tilde{x}$, evaluated at the critical point. [-]
ΔG = Gibbs energy of mixing [J/mole]
$\Delta\tilde{G}_{\text{sing}}$ = singular part of the reduced Gibbs energy of mixing [-]
$\Delta\tilde{G}_{\text{reg}}$ = regular part of the reduced Gibbs energy of mixing [-]
$h(x/x_0)$ = scaling function [-]
$h(\phi(\vec{r}))$ = position dependent ordering field
ΔH = enthalpy of mixing [J/mole]
k_B = Boltzman constant [J/K]
K_T = isothermal compressibility [Pa^{-1}]
K_{sx} = adiabatic compressibility at constant composition [Pa^{-1}]
K_{Tx} = isothermal compressibility at constant composition [Pa^{-1}]
$K_{T\Delta}$ = isothermal compressibility at constant chemical potential difference [Pa^{-1}]
$\mathcal{K}$ = rescaling function [-]
LB = Lower bounds on design vector
M = order parameter in the Landau theory [-]
M = number of parameters to be optimised [-]
M_i = molar mass of component *i* [g/mole]
N = number of components [-]
N = total number of data points [-]
N_i = number of type *i* data points [-]
N_G = Ginzburg number [-]
p = pressure [Pa]
p_c = critical pressure [Pa]
P = number of coexisting phases [-]
$\tilde{p}_{\text{sing}}$ = singular part of the reduced pressure [-]
q_D = actual cutoff wavenumber, characterising a discrete structure of matter with spacing, $\xi_D=1/q_D$ [m^{-1}]
$\vec{r}$ = variable indicating position dependence
R = universal gas constant [J/(mole·K)]
S = (molar) entropy [J/(mole·K)]

t = temperature-like variable in the Landau theory [-]

T = temperature [K]

T_c = critical temperature [K]

$\tilde{T}$ = reduced temperature [-]

$\Delta\tilde{T}$ = 1 minus reduced temperature [-]

$\bar{T}$ = reduced temperature, reduced with classical T_c [-]

$\Delta\bar{T}$ = reduced temperature minus 1, reduced with classical T_c [-]

$T_{i,\mathrm{exp,calc}}$ = experimental or calculated temperature belonging to data point i [-]

$\mathcal{T}$ = rescaling function [-]

u_0 = Landau amplitude [-]

u_i = irrelevant scaling field [-]

u^* = fixed-point coupling constant, 0.472 [-]

$\bar{u}$ = ratio of the actual coupling constant of the system over u^* [-]

u_t = scaling field, analytic functions of $\tilde{\mu}$ and $\tilde{T}$ [-]

u_h = scaling field, analytic functions of $\tilde{\mu}$ and $\tilde{T}$ [-]

$\mathcal{U}$ = rescaling function [-]

$U_N^{(0)}$ = potential energy of the reference system with N molecules [J]

$U_N^{(1)}$ = potential energy of the perturbation for a system N molecules [J]

UB = upper bounds on design vector

v_0 = average molecular volume [Å^3]

V^i = molar volume of phase i [cm^3/mole]

V_j = molar volume of pure j [cm^3/mole]

V_i^E = excess molar volume of phase i [cm^3/mole]

V = volume [m^3]

$\mathcal{V}$ = rescaling function [-]

w_j = weight factor that can be applied to type j data points [-]

x = scaling variable [-]

x_0 = help variable in scaling law for the coexistence curve [-]

x_i = overall mole fraction of component i [-]

x_{ij} = local mole fraction of molecule i in the immediate neighbourhood of molecule j [-]

$x_{i,p,\mathrm{exp/calc}}$ = experimental or calculated mole fraction belonging to data point i and phase p [-]

x_c = real mole fraction at the critical point [-]

$\bar{x}$ = reduced mole fraction, reduced with classical x_c [-]

$\tilde{x}$ = reduced mole fraction, reduced with real x_c [-]

$\Delta\bar{x}$ = 1 minus reduced mole fraction, reduced with classical x_c [-]

$\Delta\tilde{x}$ = 1 minus reduced mole fraction, reduced with real x_c [-]

$\%\Delta x$ = percent deviation of a property [%]

Y = crossover variable [-]

Z_N = Grand canonical partition function [-]

Appendix A

Calculation of $\mathrm{d}Y/\mathrm{d}\Delta\tilde{x}$ and $\mathrm{d}Y/\mathrm{d}\Delta\tilde{T}$ by implicit differentiation

$$1-(1-\bar{u})Y=\bar{u}\left(1+\frac{\Lambda^2}{\kappa^2(\Delta\tilde{T}_R,\Delta\tilde{x}_R)}\right)^{\frac{1}{2}}Y^{\frac{1}{\omega}}\rightarrow$$

$$F(Y,\kappa^2)=Y=\frac{1-\bar{u}\left(1+\frac{\Lambda^2}{\kappa^2(\Delta\tilde{T}_R,\Delta\tilde{x}_R)}\right)^{\frac{1}{2}}Y^{\frac{1}{\omega}}}{1-\bar{u}}$$

$$\frac{\partial F(Y,\kappa^2)}{\partial Y}=F_Y=-\frac{\bar{u}}{(1-\bar{u})Y\omega}\left(1+\frac{\Lambda^2}{\kappa^2(\Delta\tilde{T}_R,\Delta\tilde{x}_R)}\right)^{\frac{1}{2}}Y^{\frac{1}{\omega}}$$

$$\frac{\partial F(Y,\kappa^2)}{\partial\kappa^2}=F_{\kappa^2}=\frac{\bar{u}}{2(1-\bar{u})}\left(1+\frac{\Lambda^2}{\kappa^2(\Delta\tilde{T}_R,\Delta\tilde{x}_R)}\right)^{-\frac{1}{2}}Y^{\frac{1}{\omega}}\frac{\Lambda^2}{(\kappa^2)^2}$$

$$\frac{dY}{d\Delta\tilde{x}}=\frac{dF(Y,\kappa^2)}{d\Delta\tilde{x}}=\frac{\partial F(Y,\kappa^2)}{\partial\kappa^2}\frac{d\kappa^2}{d\Delta\tilde{x}}+\frac{\partial F(Y,\kappa^2)}{\partial Y}\frac{dY}{d\Delta\tilde{x}}$$

$$\frac{d\kappa^2}{d\Delta\tilde{x}}=\frac{\partial\kappa^2}{\partial\Delta\tilde{x}}\frac{d\Delta\tilde{x}}{d\Delta\tilde{x}}+\frac{\partial\kappa^2}{\partial Y}\frac{dY}{d\Delta\tilde{x}}\rightarrow$$

$$\frac{dY}{d\Delta\tilde{x}}=\frac{\left(\frac{F_{\kappa^2}}{1-F_Y}\right)\frac{\partial\kappa^2}{\partial\Delta\tilde{x}}}{1-\left(\frac{F_{\kappa^2}}{1-F_Y}\right)\frac{\partial\kappa^2}{\partial Y}}\qquad\frac{dY}{d\Delta\tilde{T}}=\frac{\left(\frac{F_{\kappa^2}}{1-F_Y}\right)\frac{\partial\kappa^2}{\partial\Delta\tilde{T}}}{1-\left(\frac{F_{\kappa^2}}{1-F_Y}\right)\frac{\partial\kappa^2}{\partial Y}}$$

Calculation of the phase boundary

The chemical potentials off phase 1 and phase 2 are given by:

$$\Delta\mu_1 = \Delta G + (1-x_1)\left(\frac{\partial \Delta G}{\partial x_1}\right)_{Tp} \qquad \Delta\mu_2 = \Delta G + (1-x_2)\left(\frac{\partial \Delta G}{\partial x_2}\right)_{Tp} = \Delta G - x_1\left(\frac{\partial \Delta G}{\partial x_1}\right)_{Tp} \tag{A.1}$$

These relations can be simplified by subtracting $\Delta\mu_1$ and $\Delta\mu_2$. The natural logarithm of the activity equals $\Delta\mu/(RT)$:

$$\frac{\Delta\mu_1 - \Delta\mu_2}{RT} = \left(\frac{\partial \Delta\tilde{G}}{\partial x_1}\right)_{Tp} \qquad \ln a_i = \frac{\Delta\mu_i}{RT} = \frac{\mu_i - \mu_i{}^*}{RT} \tag{A.2}$$

Phase equilibrium requires the chemical potentials or activities of component *i* in both phases to be equal:

$$\ln(a_1)' = \ln(a_1)'' \qquad \ln(a_2)' = \ln(a_2)'' \qquad \ln\left(\frac{a_1}{a_2}\right)' = \ln\left(\frac{a_1}{a_2}\right)'' \tag{A.3}$$

The prime in (A.3) refers to the phase. The last relation in (A.3) in terms of $\Delta\mu_i$ reads:

$$\Delta\mu_1' - \Delta\mu_2' = \Delta\mu_1'' - \Delta\mu_2'' \tag{A.4}$$

Comparing (A.2) and (A.4) results in:

$$\left(\frac{\partial \Delta\tilde{G}_{Sing}}{\partial x_1}\right)'_{Tp} = \left(\frac{\partial \Delta\tilde{G}_{Sing}}{\partial x_1}\right)''_{Tp} \tag{A.5}$$

Now, (A.1) can be simplified to:

$$\begin{aligned} &\Delta\tilde{G}_{Reg}{}' + \Delta\tilde{G}_{Sing}{}' + (1-x_1')\left(\frac{\partial \Delta\tilde{G}_{Reg}{}'}{\partial x_1} + \frac{\partial \Delta\tilde{G}_{Sing}{}'}{\partial x_1}\right)_{Tp} = \\ &\Delta\tilde{G}_{Reg}{}'' + \Delta\tilde{G}_{Sing}{}'' + (1-x_1'')\left(\frac{\partial \Delta\tilde{G}_{Reg}{}''}{\partial x_1} + \frac{\partial \Delta\tilde{G}_{Sing}{}''}{\partial x_1}\right)_{Tp} \end{aligned} \tag{A.6}$$

$$A(x_1' - x_1'') + (\Delta\tilde{G}_{Sing}' - \Delta\tilde{G}_{Sing}'') + (x_1'' - x_1')\left\{A + \left(\frac{\partial \Delta\tilde{G}_{Sing}}{\partial x_1}\right)_{Tp}\right\} = 0 \Rightarrow$$

$$(\Delta\tilde{G}_{Sing}' - \Delta\tilde{G}_{Sing}'') + (x_1'' - x_1')\left(\frac{\partial \Delta\tilde{G}_{Sing}}{\partial x_1}\right)_{Tp} = 0 \qquad \text{(A.7)}$$

Relation (A.5) and the last relation in (A.7) form the simplified conditions for phase equilibrium.

Appendix B

Calculation of $\mathrm{d}^2(\Delta G/R)/\mathrm{d}T^2$

$$\frac{d^2(\Delta G/R)}{dT^2}=$$

$$T\left(\frac{\partial \Delta T}{\partial T}\right)^2\left\{\frac{\partial^2\Delta\tilde{G}_{\mathrm{reg}}}{\partial \Delta T^2}+\frac{d}{d\Delta T}\left(\left.\frac{\partial\Delta\tilde{G}_{\mathrm{sing}}}{\partial\Delta T}\right|_{Y,\Delta x_R}\right)+\frac{d}{d\Delta T}\left(\frac{\partial\Delta\tilde{G}_{\mathrm{sing}}}{\partial Y}\right)\frac{dY}{d\Delta T}+\left(\frac{\partial\Delta\tilde{G}_{\mathrm{sing}}}{\partial Y}\right)\frac{d^2Y}{d\Delta T^2}\right\}$$

$$\frac{d}{d\Delta T}\left(\left.\frac{\partial\Delta\tilde{G}_{\mathrm{sing}}}{\partial\Delta T}\right|_{Y,\Delta x_R}\right)=\left.\frac{\partial^2\Delta\tilde{G}_{\mathrm{sing}}}{\partial\Delta T^2}\right|_{Y,\Delta x_R}+\frac{\partial}{\partial Y}\left(\left.\frac{\partial\Delta\tilde{G}_{\mathrm{sing}}}{\partial\Delta T}\right|_{Y,\Delta x_R}\right)\frac{dY}{d\Delta T}$$

$$\frac{\partial}{\partial Y}\left(\left.\frac{\partial\Delta\tilde{G}_{\mathrm{sing}}}{\partial\Delta T}\right|_{Y,\Delta x_R}\right)=\left.\frac{\partial}{\partial Y}\left\{\left.\frac{\partial\Delta\tilde{G}_{\mathrm{sing}}}{\partial\Delta T}\right|_{Y,\Delta x_R}\right\}\right|_{\Delta T_R,\Delta x_R}+\frac{\partial}{\partial\Delta T_R}\left\{\left.\frac{\partial\Delta\tilde{G}_{\mathrm{sing}}}{\partial\Delta T}\right|_{Y,\Delta x_R}\right\}\frac{\partial\Delta T_R}{\partial Y}+\ldots.$$

$$\frac{\partial}{\partial x_R}\left\{\left.\frac{\partial\Delta\tilde{G}_{\mathrm{sing}}}{\partial\Delta T}\right|_{Y,\Delta x_R}\right\}\frac{\partial\Delta x_R}{\partial Y}$$

$$\frac{d}{d\Delta T}\left(\frac{\partial\Delta\tilde{G}_{\mathrm{sing}}}{\partial Y}\right)=\left.\frac{\partial}{\partial\Delta T}\left\{\frac{\partial\Delta\tilde{G}_{\mathrm{sing}}}{\partial Y}\right\}\right|_{Y,\Delta x_R}+\frac{\partial^2\Delta\tilde{G}_{\mathrm{sing}}}{\partial Y^2}\frac{dY}{d\Delta T}$$

$$\frac{d^2Y}{d\Delta T^2}=\frac{(1-\alpha)\dfrac{\partial\kappa^2}{\partial Y}\dfrac{d}{d\Delta T}\left(\alpha\dfrac{\partial\kappa^2}{\partial\Delta T}\right)-\alpha\dfrac{\partial\kappa^2}{\partial\Delta T}\dfrac{d}{d\Delta T}\left(1-\alpha\dfrac{\partial\kappa^2}{\partial Y}\right)}{\left(1-\alpha\dfrac{\partial\kappa^2}{\partial Y}\right)^2}$$

$$\frac{d}{d\Delta T}\left(\alpha\frac{\partial\kappa^2}{\partial\Delta T}\right)=\alpha\left\{\left.\frac{\partial\kappa^2}{\partial\Delta T}\right|_{Y,\Delta xR}+\frac{\partial^2\kappa^2}{\partial\Delta T\partial Y}\frac{dY}{d\Delta T}\right\}+\frac{\partial\kappa^2}{\partial\Delta T}\left\{\left.\frac{\partial\alpha}{\partial\Delta T}\right|_{Y,\Delta xR}+\frac{\partial\alpha}{\partial Y}\frac{dY}{d\Delta T}\right\}$$

$$\frac{\partial^2\kappa^2}{\partial\Delta T\partial Y}=\left.\frac{\partial}{\partial Y}\left\{\frac{\partial\kappa^2}{\partial\Delta T}\right\}\right|_{\Delta T_R,\Delta x_R}+\frac{\partial^2\kappa^2}{\partial\Delta T\partial\Delta T_R}\frac{\partial\Delta T_R}{\partial Y}+\frac{\partial^2\kappa^2}{\partial\Delta T\partial\Delta x_R}\frac{\partial\Delta x_R}{\partial Y}$$

$$\left.\frac{\partial\alpha}{\partial\Delta T}\right|_{Y,\Delta xR}=\frac{(1-F_Y)\dfrac{\partial F_{\kappa^2}}{\partial\Delta T}-F_{\kappa^2}\dfrac{\partial}{\partial\Delta T}(1-F_Y)}{(1-F_Y)^2}\qquad\frac{\partial\alpha}{\partial Y}=\frac{(1-F_Y)\dfrac{\partial F_{\kappa^2}}{\partial Y}-F_{\kappa^2}\dfrac{\partial}{\partial Y}(1-F_Y)}{(1-F_Y)^2}$$

Appendix C

Calculated phase bounderies

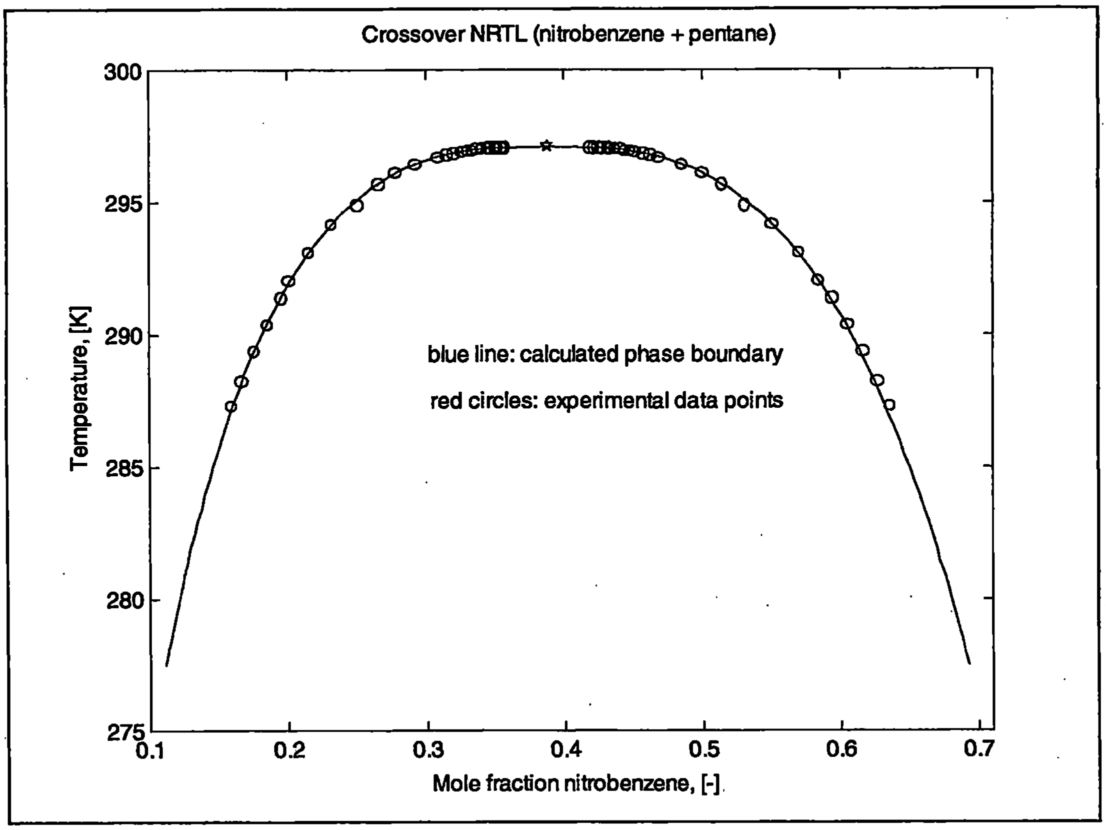

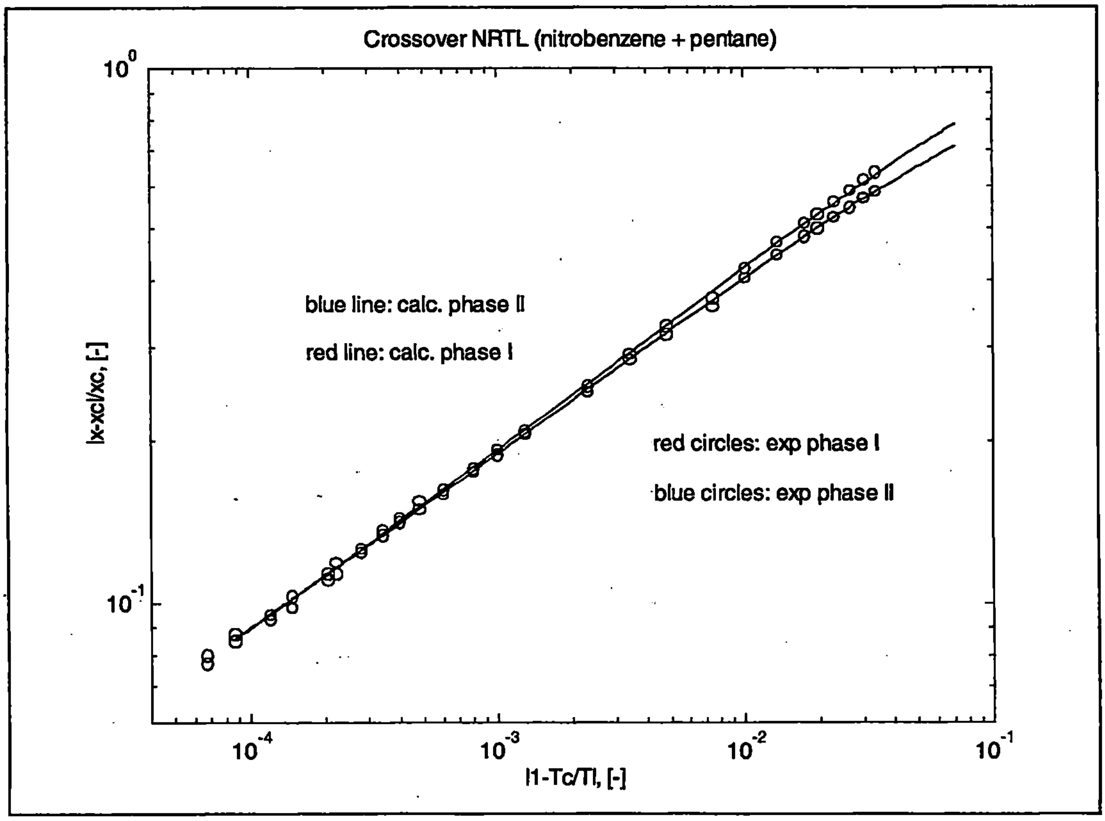

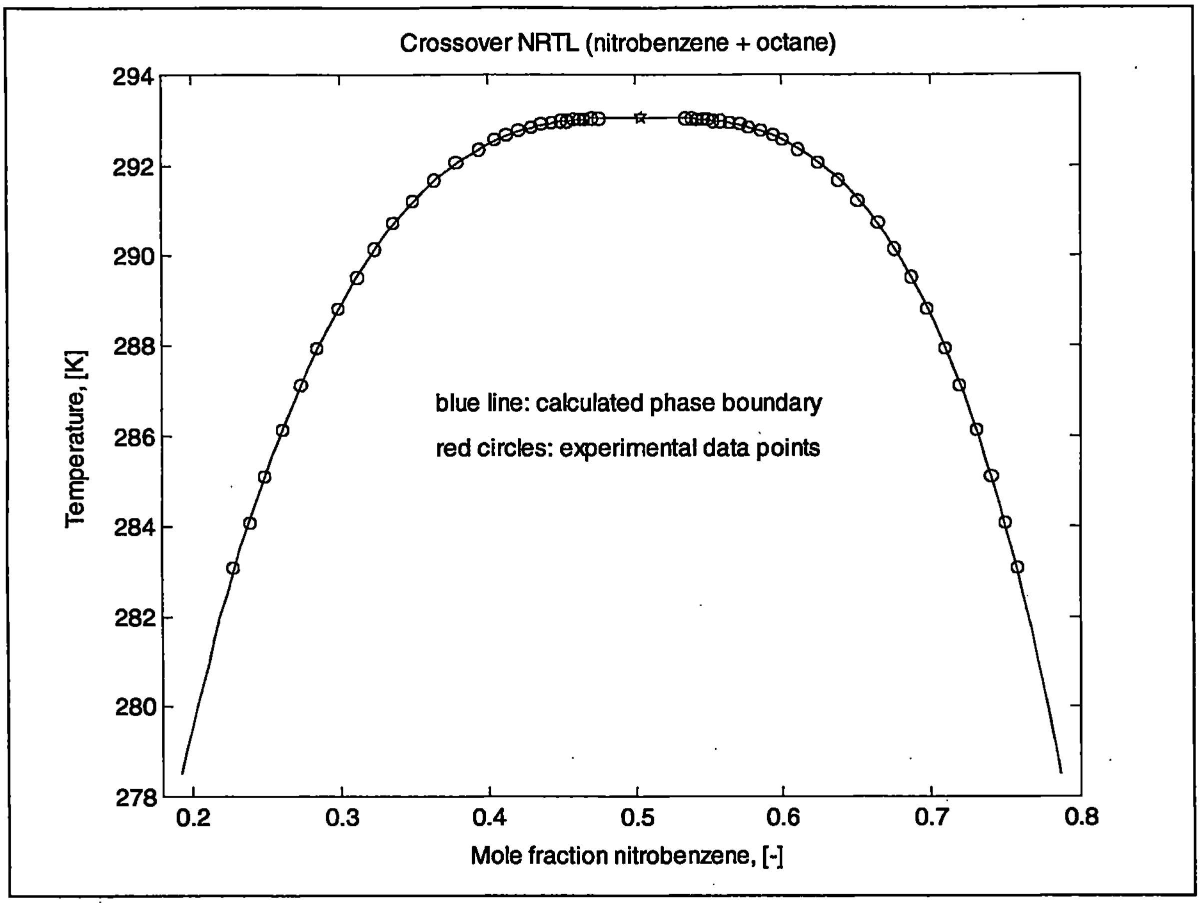
Crossover NRTL (nitrobenzene + octane)
Temperature, [K]
294
292
290
288
286
284
282
280
278
0.2
0.3
0.4
0.5
0.6
0.7
0.8
Mole fraction nitrobenzene, [-]
blue line: calculated phase boundary
red circles: experimental data points

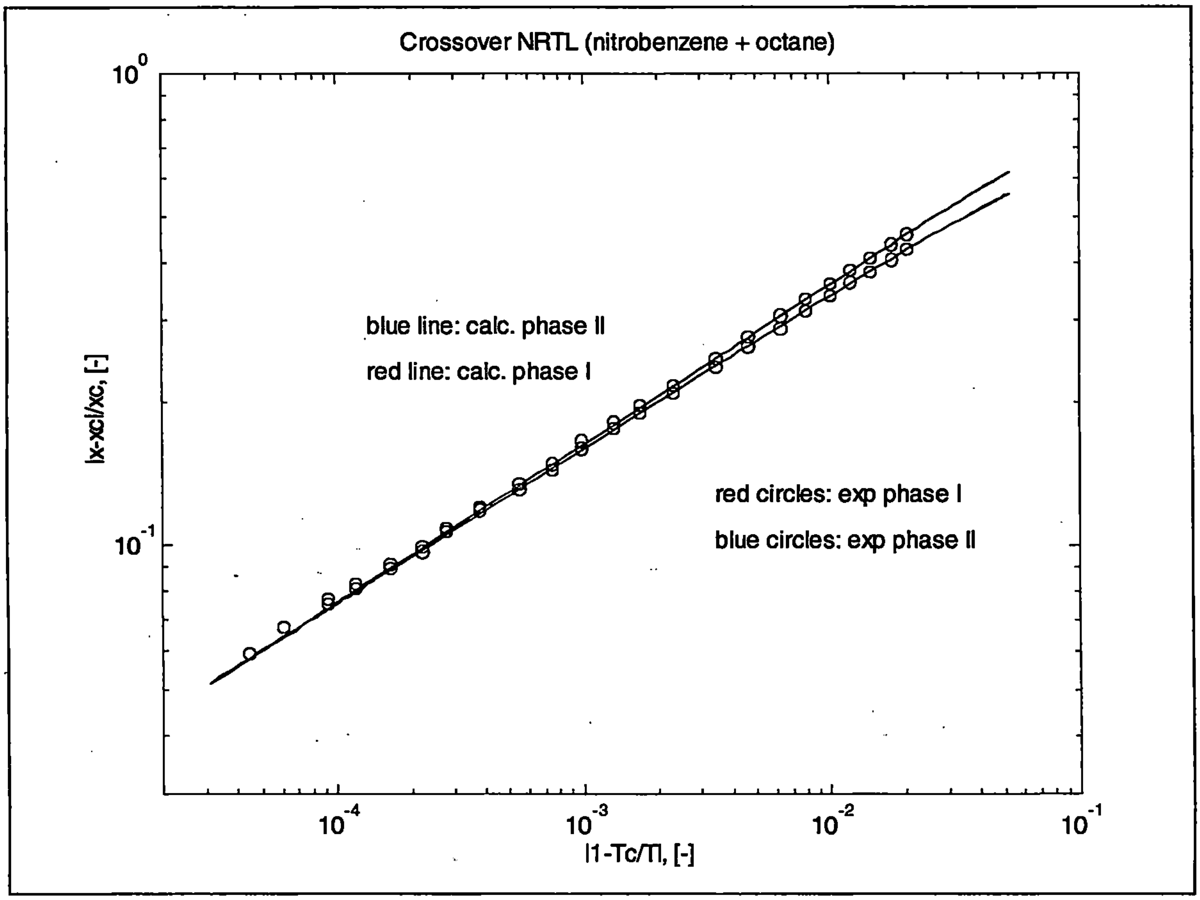
Crossover NRTL (nitrobenzene + octane)
|x-xc|/xc, [-]
10^0
10^{-1}
10^{-4}
10^{-3}
10^{-2}
10^{-1}
|1-Tc/T|, [-]
blue line: calc. phase II
red line: calc. phase I
red circles: exp phase I
blue circles: exp phase II

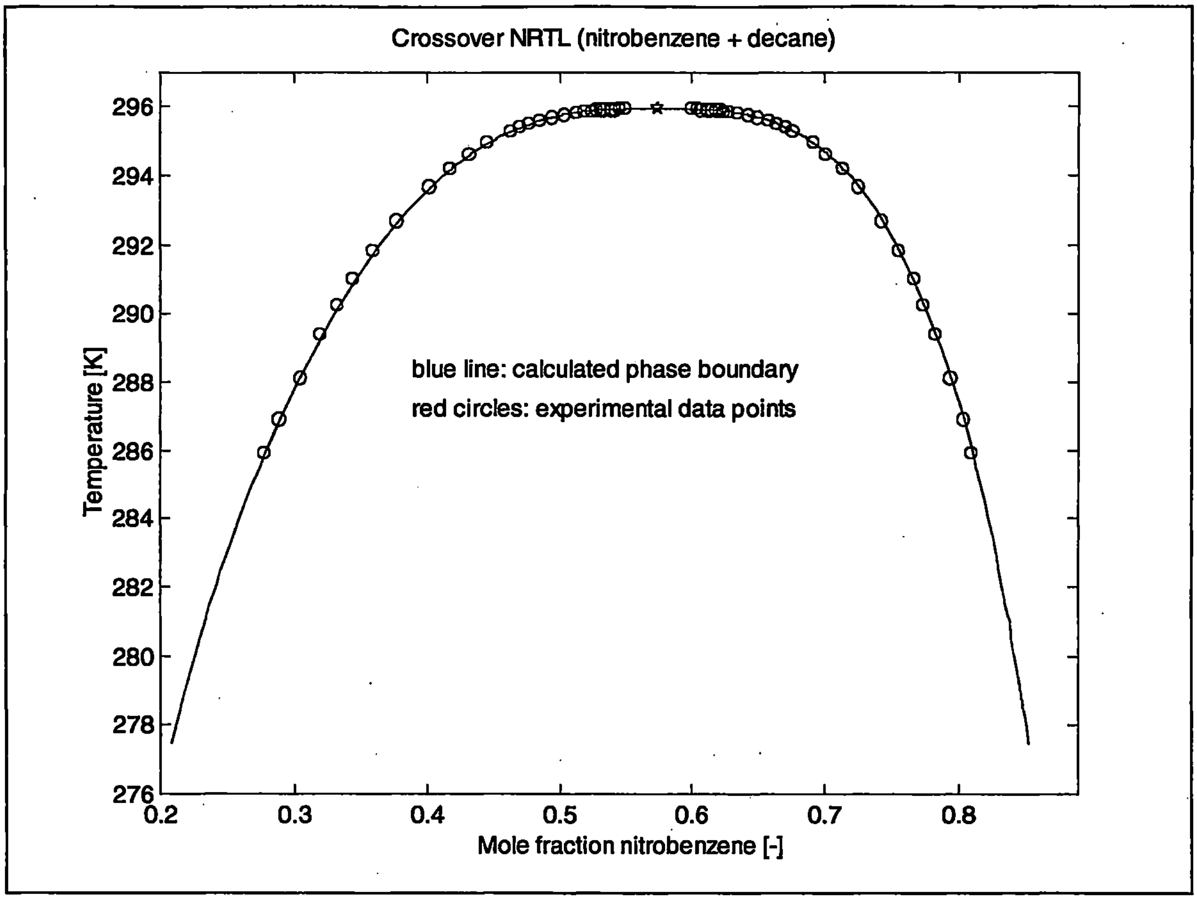
Crossover NRTL (nitrobenzene + decane)
blue line: calculated phase boundary
red circles: experimental data points
Temperature [K]
296
294
292
290
288
286
284
282
280
278
276
0.2
0.3
0.4
0.5
0.6
0.7
0.8
Mole fraction nitrobenzene [-]

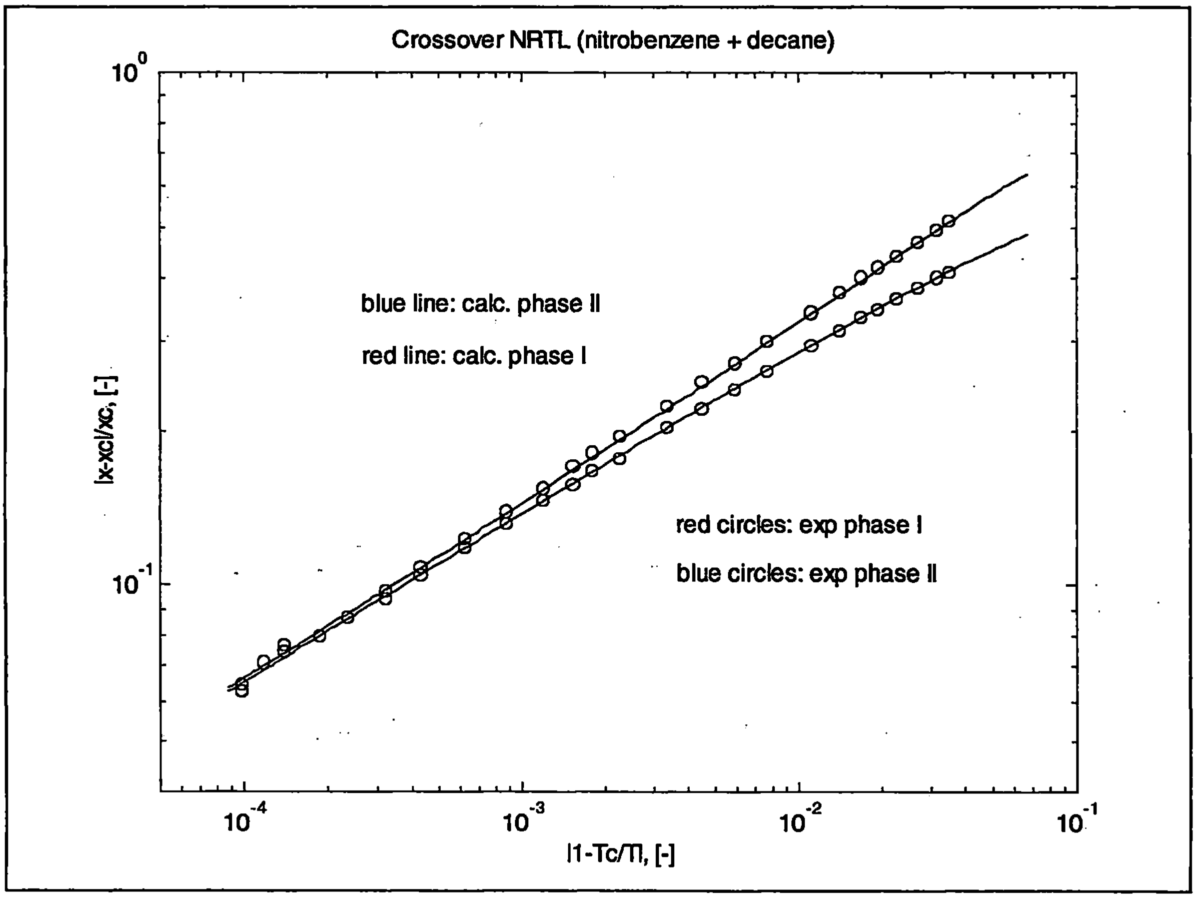
Crossover NRTL (nitrobenzene + decane)
blue line: calc. phase II
red line: calc. phase I
red circles: exp phase I
blue circles: exp phase II
|x-xc|/xc, [-]
10^0
10^{-1}
10^{-4}
10^{-3}
10^{-2}
10^{-1}
|1-Tc/T|, [-]

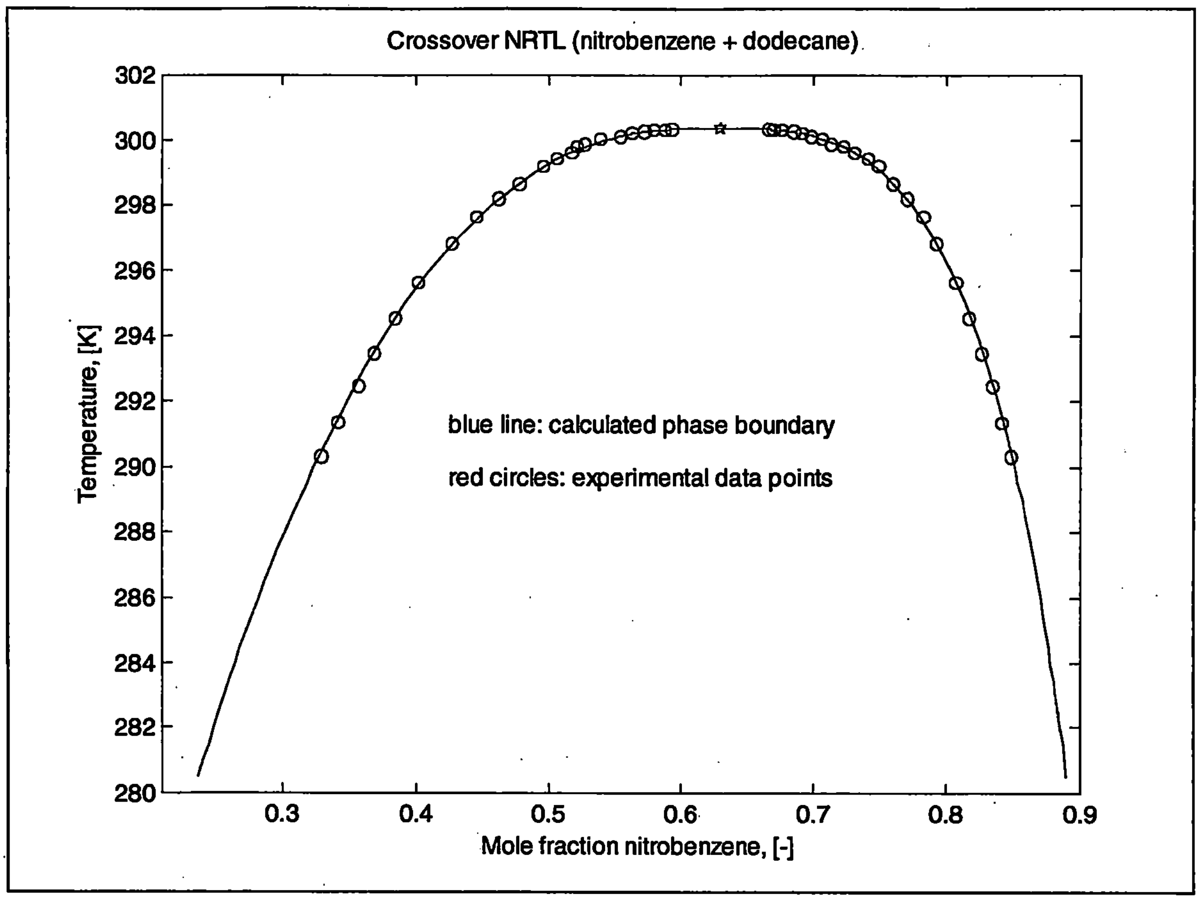
Crossover NRTL (nitrobenzene + dodecane)
Temperature, [K]
302
300
298
296
294
292
290
288
286
284
282
280
0.3
0.4
0.5
0.6
0.7
0.8
0.9
Mole fraction nitrobenzene, [-]
blue line: calculated phase boundary
red circles: experimental data points

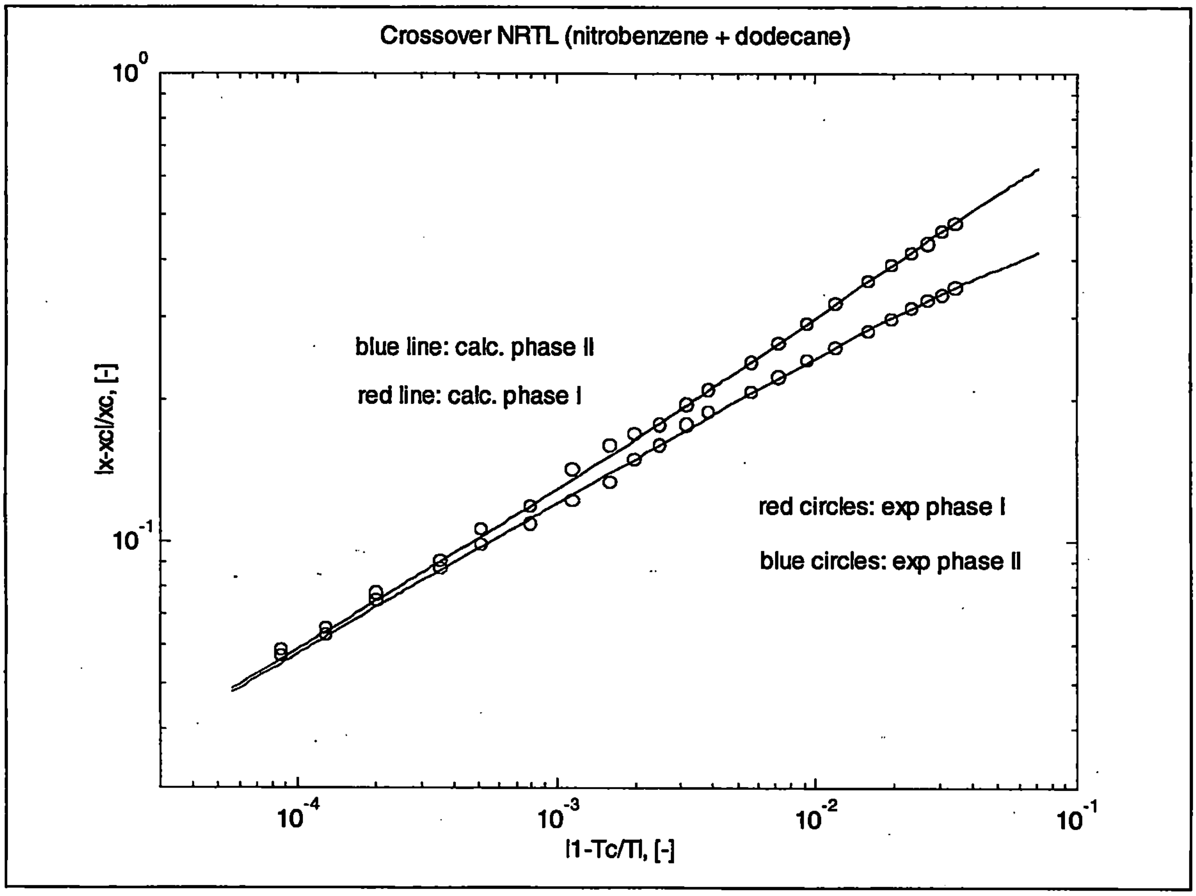
Crossover NRTL (nitrobenzene + dodecane)
|x-xc|/xc, [-]
10^0
10^{-1}
10^{-4}
10^{-3}
10^{-2}
10^{-1}
|1-Tc/T|, [-]
blue line: calc. phase II
red line: calc. phase I
red circles: exp phase I
blue circles: exp phase II

Appendix D

Matlab®-code for Crossover-NRTL model

Program Datdemo

```
%%%%%%%%%%%%%%%%%%%%%%%%%%%%%%%%%%%%%%%%%%%%%%%%%%%%%%%%%%%%%%%%%
% This program optimises the NRTL parameters b-wiggle and, d-wiggle and the the crossover parameter u_bar for
% the crossover-NRTL model. Lambda is fixed at 1 and alpha12 is fixed at 0.2. The NRTL parameters a-wiggle and
% c-wiggle are calculated from the conditions of incipient immiscibility. They depend on the mole fraction in the critical point.
% This optimisation includes the implicit dependence of Y on M (dYdM) and the kernel term.
%%%%%%%%%%%%%%%%%%%%%%%%%%%%%%%%%%%%%%%%%%%%%%%%%%%%%%%%%%%%%%%%%

format compact

% Parameters
alpha12=0.2;
LAMBDA=1;

% Critical Parameters
Tc=293.052;
xc=0.505;

% First estimates for the parameters to be optimised
fitpar(1,1)= 0.35;     % u_bar
fitpar(2,1)= 3.5;      % b_wiggle
fitpar(3,1)= 0.5;      % d_wiggle

% Definition of the OPTIONS used in the optimisation process
%
OPTIONS=[];
OPTIONS = optimset(OPTIONS,'TolX',1e-8,'Display','iter','LevenbergMarquardt','on',...
  'TolCon',1e-8,'TolFun',1e-8,'DiffMaxChange',1e-4,'MaxFunEvals',100000,...
  'Diagnostics','on','DiffMinChange',1e-10,'GradObj','off','GradConstr','off',...
  'DerivativeCheck','off','MaxIter',300);
%
% Explanation of different options:
%
%   - TolX:                 termination tolerance on the parameters
%   - TolCon:               termination tolerance on the constraint violation
%   - TolFun:               termination tolerance on the function value
%   - Display iter:         level of display, iter means: output after every iteration
%   - LevenbergMarquardt:   chooses Levenberg-Marquardt over Gauss-Newton algorithm
%   - DiffMaxChange:        maximum change in variables for finite difference variables
%   - DiffMinChange:        minimum change in variables for finite difference variables
%   - MaxFunEvals:          maximum number of function evaluations allowed
%   - Maxiter:              maximum number of iterations allowed
%   - Diagnostics:          print diagnostic information about the function to be minimised or solved
%   - GradObj:              gradients for the objective function defined by user
%   - GradConstr:           gradients for the (non-)linear constraints defined by user
%   - DerivativeCheck:      compare user-supplied analytic derivatives to finite differencing derivatives
%
%%%%%%%%%%%%%%%%%%%%%%%%%%%%%%%%%%%%%%%%%%%%%%%%%%%%%%%%%%%%%%%%%


% Calculation of a-wiggle and c-wiggle from the conditions of incipient immiscibility
% Estimates for a-wiggle and c-wiggle
Par=[1 1]';

P=FSOLVE('NRTLPar',Par,OPTIONS,xc,alpha12);
a_curl=P(1,1)
c_curl=P(2,1)

% Dataset for nitrobenzene(1) and octane(2)

Data0=...
 [0.444  0.565    292.939
  0.437  0.571    292.892
```

```
    0.430   0.578     292.833
    0.421   0.586     292.761
    0.413   0.594     292.663
    0.405   0.601     292.551
    0.395   0.611     292.371
    0.379   0.625     292.041
    0.365   0.638     291.690
    0.350   0.651     291.216
    0.337   0.664     290.710
    0.324   0.676     290.145
    0.311   0.687     289.516
    0.299   0.698     288.801
    0.284   0.710     287.923
    0.273   0.720     287.098
    0.261   0.731     286.113
    0.249   0.741     285.094
    0.239   0.750     284.089
    0.228   0.758     283.069];


B=size(Data0);

% Number of data points used in data regression
qq=20;%B(1,1);

% Extract T, x1, and x2 from Data set
T=   Data0(1:qq,3);
x1=  Data0(1:qq,1);
x2=  Data0(1:qq,2);

% Plot data
plot(x1,T,'bo')
hold on;
plot(x2,T,'bo')
plot(x1,T,'r')
hold on;
plot(x2,T,'r')
pause
close


% Define reduced properties
T_red=(Tc-T)/Tc;
x1_red=abs(x1-xc)/xc;
x2_red=abs(x2-xc)/xc;

% Plot coexistence-curve data on log-log scale to see if there are any inconsistencies near the critical point
loglog(T_red,x1_red(:,1),'ro')
hold on;
loglog(T_red,x2_red(:,1),'b*')
pause
close

% NRTL- and Crossover-parameters
u_bar=    fitpar(1,1);
b_curl=   fitpar(2,1);
d_curl=   fitpar(3,1);

% Calculate estimates for the crossover-Y (and kappa) based on the parameters given above
%
Bisection
%
%%%%%%%%%%%%%%%%%%%%%%%%%%%%%%%%%%%%%%%%%%%%%%%%%%

% Transformation of variables to vector (+boundary conditions)
%
[Var,LB,UB]=var2vector(T,Y,x1,x2,u_bar,b_curl,d_curl,Data0,qq);
%
%%%%%%%%%%%%%%%%%%%%%%%%%%%%%%%%%%%%%%%%%%%%%%%%%%
```

```
% Start stopwatch
t0=clock;

% Start optimisation routine
%
[Var,fval,exitflag,output,lambda,grad,hessian]=fmincon('fitfun',Var,[],[],[],[],LB,UB,'constraints',OPTIONS,...
  x1,x2,T,Data0,qq,xc,Tc,alpha12,a_curl,c_curl,LAMBDA);
%
%%%%%%%%%%%%%%%%%%%%%%%%%%%%%%%%%%%%%%%%%%%%%%%%%%


% Give execution time and other relevant information
funEvals=sprintf('\n Number of iterations: %g.  Number of function evaluations: %g.', output.iterations, output.funcCount);
disp(funEvals)
disp(sprintf(' Norm of the residual at solution ( norm(FITFUN3(x,Data,h))^2 ): %g ',fval));
execution_time=etime(clock, t0);
disp(sprintf(' Execution time: %g \n',execution_time));

pause

% Show optimised results
[Tcalc,Y,x1calc,x2calc,u_bar,b,d]=vector2var(Var)
a=a_curl;
c=c_curl;

% Plot results
plot(x1calc(:,1),Tcalc,'ro')
hold on
plot(x2calc(:,1),Tcalc,'ro')
plot(x1calc(:,1),Tcalc,'r-')
plot(x2calc(:,1),Tcalc,'r-')
plot(Data0(1:qq,1),Data0(1:qq,3),'b*')
plot(Data0(1:qq,2),Data0(1:qq,3),'b*')
plot(0.505,293.052,'p')
plot((x2calc+x1calc)/2,Tcalc,'ro')
plot((Data0(1:qq,1)+Data0(1:qq,2))/2,Data0(1:qq,3),'b*')
title('Crossover-NRTL (nitrobenzene + octane)');
ylabel('Temperature [K]');
xlabel('Mole fraction nitrobenzene [-]');
text(0.72,292,'red circles: calc')
text(0.72,291,'blue stars: exp')

% Define reduced properties
T_red=(Tc-T)/Tc;
x1_red=abs(x1-xc)/xc;
x2_red=abs(x2-xc)/xc;
[x1_red x2_red];
% Plot coexistence-curve data on log-log scale to see if there are any inconsistencies near the critical point
loglog(T_red,x1_red(:,1),'ro')
hold on;
loglog(T_red,x2_red(:,1),'b*')
title('Crossover NRTL (nitroethane + 3-methylpentane)');
xlabel('Reduced temperature (Tc-T)/T [-]');
ylabel('Reduced mole fraction of nitrobenzene |x-xc|/xc [-]');
text(0.001,0.04,'red circles: exp phase I')
text(0.001,0.03,'blue circles: exp phase II')

T_reduced=(Tc-Tcalc)/Tc;
x1_reduced=abs(x1calc-xc)/xc;
x2_reduced=abs(x2calc-xc)/xc;

loglog(T_reduced,x1_reduced(:,1),'r')
loglog(T_reduced,x2_reduced(:,1),'b')

text(0.00002,0.4,'red line: calc. phase I')
text(0.00002,0.5,'blue line: calc. phase II')

pause
clc
close
```

Subroutine Bisection

```
%%%%%%%%%%%%%%%%%%%%%%%%%%%%%%%%%%%%%%%%%%%%%%%%%%%%%%%%%%%%%%%%%%%%%%
% Calculation of Y in the crossover function with the Bisection method.
% The crossover function of Chen is given by:  1-(1-u)*Y=u*sqrt(1+(LAMBDA/kappaR)^2)*Y^(1/omega)
%%%%%%%%%%%%%%%%%%%%%%%%%%%%%%%%%%%%%%%%%%%%%%%%%%%%%%%%%%%%%%%%%%%%%%

format long

% Rename input
Lambda=LAMBDA;
u_star=0.472;
a=a_curl;
b=b_curl;
c=c_curl;
d=d_curl;
u_roof=u_bar;

% Critical exponents
nu=0.63;
eta=0.0333;
omega=0.85714;
alpha=0.11;
Delta=nu*omega;
gamma=(2-eta)*nu;

% Incoming data
T=Data0(1:qq,3);
x=[x1(1:qq,1) x2(1:qq,1)];

% Absolute tolerance:
Tol=1e-8;


% This part calculates two estimates for Y. When the product of the objective functions is negative, the solution lies between those
% estimates

for s=1:2 % Number of phases
  for t=1:qq % Number of data points
    deltaT=1-Tc./T(t,1);
    deltax=x(t,s)/xc-1;

    [t deltaT]

    Criterium=1;
    Y=zeros(2,1);
    fy=[1 1]';

    if s==1 % Avoid local solutions; give physically realistic start value
      if abs(deltaT)>0.02
        i=35;
      elseif abs(deltaT)>0.003 & abs(deltaT)<0.02
        i=25;
      elseif abs(deltaT)>0.0001 & abs(deltaT)<0.003
        i=11;
      elseif abs(deltaT)>0.00005 & abs(deltaT)<0.0001
        i=7;
      else abs(deltaT)>0.000001 & abs(deltaT)<0.00005
        i=1;
      end;
    else
      if abs(deltaT)>0.02
        i=35;
      elseif abs(deltaT)>0.003 & abs(deltaT)<0.02
        i=20;
      elseif abs(deltaT)>0.0001 & abs(deltaT)<0.003
        i=11;
      elseif abs(deltaT)>0.00005 & abs(deltaT)<0.0001
        i=7;
```

```
  else abs(deltaT)>0.000001 & abs(deltaT)<0.00005
    i=1;
  end;
end;

while Criterium~=0
  Criterium1=1;
  Criterium2=1;

  i=i+1;
  Y=[0.0001+(i-1)/1000; i/100]; % Increase starting values for Y

  if abs(fy(1,1))<1e-4 & fy(2,1)>0  % Corrections for Y-value near or equal to zero
    Y=[Y(1,1)*0.95; Y(2,1)];
  end;
  if abs(fy(2,1))<1e-4 & fy(1,1)>0
    Y=[Y(1,1)*0.95; Y(2,1)];
  end;
  if abs(fy(1,1))<1e-4 & fy(2,1)<0
    Y=[Y(1,1)*0.95; Y(2,1)];
  end;
  if abs(fy(2,1))<1e-4 & fy(1,1)<0
    Y=[Y(1,1)*0.95; Y(2,1)];
  end;


  % Rescaling functions
  TT=Y.^((2*nu-1)/(nu*omega));
  UU=Y.^(1/omega);
  DD=Y.^(-eta/omega);

  % Renormalised dimensionless temperature and mole fraction
  deltaTR=deltaT.*TT.*UU.^(-0.5);
  deltaxR=deltax.*(DD.^(0.5).*UU.^(0.25));
  xR=xc*(deltaxR+1);

  % Renormalised NRTL-parameters
  tau12R= c_curl*(1-d_curl*deltaTR);
  tau21R= a_curl*(1-b_curl*deltaTR);
  G12R=exp(-alpha12*tau12R);
  G21R=exp(-alpha12*tau21R);

  % Calculation of the classical kappa with renormalised variables
  aa=(tau21R.*G21R./(xR+(1-xR).*G21R)+tau12R.*G12R./(1-xR+xR.*G12R));
  bb=(-tau21R.*G21R*xc.*(1-G21R)./(xR+(1-xR).*G21R).^2-tau12R.*G12R*xc.*(G12R-1)./(1-xR+xR.*G12R).^2);
  cc=(2*tau21R.*G21R*xc^2.*(1-G21R).^2./(xR+(1-xR).*G21R).^3+2*tau12R.*G12R*xc^2.*(G12R-1).^2./...
    (1-xR+xR.*G12R).^3);

  ddd=xc^2./(xR.*(1-xR));
  eee=-2*xc^2*aa+2*xc*(1-2*xR).*bb+(xR-xR.^2).*cc;

  kappaCLR2=Y.^(1/(2*omega)).*(ddd+eee);

  % Partial derivative of the Gibbs energy of mixing (NRTL) four times to deltax, evaluated at the critical point
  u0= 2.*xc+8.*xc.^4./((xc-1).^2.*(1-xc))+6.*xc.^4./((xc-1).^3)+24.*(-xc.^2+xc.*(1-xc)).*(-c.*exp(-alpha12.*c).*xc.^2.*...
    (-1+exp(-alpha12.*c)).^2.*(-xc+xc.*exp(-alpha12.*c))./((1-xc+xc.*exp(-alpha12.*c)).^4)+a.*exp(-alpha12.*a).*...
    xc.^2.*(-1+exp(-alpha12.*a)).^2.*(xc-exp(-alpha12.*a).*xc)./((-xc-exp(-alpha12.*a)+exp(-alpha12.*a).*xc).^3.*...
    (xc+(1-xc).*exp(-alpha12.*a))))-24.*xc.^2.*(-a.*exp(-alpha12.*a).*xc.*(-1+exp(-alpha12.*a)).*(xc-...
    exp(-alpha12.*a).*xc)./((-xc-exp(-alpha12.*a)+exp(-alpha12.*a).*xc).^2.*(xc+(1-xc).*exp(-alpha12.*a)))+...
    c.*exp(-alpha12.*c).*xc.*(-1+exp(-alpha12.*c)).*(-xc+xc.*exp(-alpha12.*c))./((1-xc+xc.*exp(-alpha12.*c)).^3))+...
    24.*xc.*(1-xc).*(-a.*exp(-alpha12.*a).*xc.^3.*(-1+exp(-alpha12.*a)).^3.*(xc-exp(-alpha12.*a).*xc)./...
    ((-xc-exp(-alpha12.*a)+exp(-alpha12.*a).*xc).^4.*(xc+(1-xc).*exp(-alpha12.*a)))+c.*exp(-alpha12.*c).*...
    xc.^3.*(-1+exp(-alpha12.*c)).^3.*(-xc+xc.*exp(-alpha12.*c))./((1-xc+xc.*exp(-alpha12.*c)).^5));

  % System-dependent amplitude
  cRho=u0^0.25*(u_bar*u_star*Lambda)^(-0.25);

  kappaCLR2=kappaCLR2/cRho^2;
```

```
   % Objective function to be minimized
   fy=1-(1-u_roof).*Y-u_roof*sqrt(1+LAMBDA^2./kappaCLR2).*Y.^(1/omega);


   % fy(Y)=0 must lie between Y(1,1) and Y(2,1). This means:
   if (fy(1,1)*fy(2,1)>0)
        disp('Args must have different signs!');
   end;
   if ~isreal(fy)==1 | ~isreal(kappaCLR2)
        disp('No complex parts allowed!');
   end;
   if (fy(1,1)*fy(2,1)<0)
     Criterium1=0; % fy(Y)=0 lies between Y(1,1) and Y(2,1)
   end;
   if (~isreal(fy)==0) & (~isreal(kappaCLR2)==0)
     Criterium2=0; % No complex value for kappaCLR2
   end;
   if Criterium1==0 & Criterium2==0 % Good start values for iteration
     Criterium=0;
   end;
 end;

 iter=0;

 % Estimate for the root of fy(Y)=0:
 y=(Y(1,1)+Y(2,1))/2;

 % Rescaling functions
 TT=y^((2*nu-1)/(nu*omega));
 UU=y^(1/omega);
 DD=y^(-eta/omega);

 % Renormalised dimensionless temperature and mole fraction
 deltaTR=deltaT*TT*UU^(-0.5);
 deltaxR=deltax*(DD^(0.5)*UU^(0.25));
 xR=xc*(deltaxR+1);

 % Renormalised NRTL-parameters
 tau12R=    c_curl*(1-d_curl*deltaTR);
 tau21R=    a_curl*(1-b_curl*deltaTR);
 G12R=exp(-alpha12*tau12R);
 G21R=exp(-alpha12*tau21R);

 % Calculation of the classical kappa with renormalised variables
 aa=(tau21R.*G21R./(xR+(1-xR).*G21R)+tau12R.*G12R./(1-xR+xR.*G12R));
 bb=(-tau21R.*G21R*xc.*(1-G21R)./(xR+(1-xR).*G21R).^2-tau12R.*G12R*xc.*(G12R-1)./(1-xR+xR.*G12R).^2);
 cc=(2*tau21R.*G21R*xc^2.*(1-G21R).^2./(xR+(1-xR).*G21R).^3+2*tau12R.*G12R*xc^2.*(G12R-1).^2./...
   (1-xR+xR.*G12R).^3);

 ddd=xc^2./(xR.*(1-xR));
 eee=-2*xc^2*aa+2*xc*(1-2*xR).*bb+(xR-xR.^2).*cc;

 kappaCLR2=y^(1/(2*omega))*(ddd+eee) cRho^2;

 %%%%%%%%%%%%%%%%%%%%%%%%%%%%%%%%%%%%%%%%%%%%%%%%%%%%%%%%%%%%

 % Function evaluation at y
 FY=1-(1-u_roof).*y-u_roof*sqrt(1+LAMBDA^2./kappaCLR2).*y.^(1/omega);

 %%%%%%%%%%%%%%%%%%%%%%%%%%%%%%%%%%%%%%%%%
 %
.% BISECTION METHOD
 %

 while abs(FY)>Tol % Error must be less than Tolerance for convergence
   iter=iter+1;

   if iter>1000
     error('Too many iterations!')
   end;
```

```
      if FY*fy(1,1)>0
        Y(1,1)=y;
      else
        Y(2,1)=y;
      end;

      y=(Y(1,1)+Y(2,1))/2;

      % Rescaling functions
      TT=y^((2*nu-1)/(nu*omega));
      UU=y^(1/omega);
      DD=y^(-eta/omega);

      % Renormalised dimensionless temperature and mole fraction
      deltaTR=deltaT*TT*UU^(-0.5);
      deltaxR=deltax*(DD^(0.5)*UU^(0.25));
      xR=xc*(deltaxR+1);

      % Renormalised NRTL-parameters
      tau12R= c_curl*(1-d_curl*deltaTR);
      tau21R= a_curl*(1-b_curl*deltaTR);
      G12R=exp(-alpha12*tau12R);
      G21R=exp(-alpha12*tau21R);
      %
      % Calculation of the classical kappa with renormalised variables
      aa=(tau21R.*G21R./(xR+(1-xR).*G21R)+tau12R.*G12R./(1-xR+xR.*G12R));
      bb=(-tau21R.*G21R*xc.*(1-G21R)./(xR+(1-xR).*G21R).^2-tau12R.*G12R*xc.*(G12R-1)./(1-xR+xR.*G12R).^2);
      cc=(2*tau21R.*G21R*xc^2.*(1-G21R).^2./(xR+(1-xR).*G21R).^3+2*tau12R.*G12R*xc^2.*(G12R-1).^2./...
        (1-xR+xR.*G12R).^3);

      ddd=xc^2/(xR*(1-xR));
      eee=-2*xc^2*aa+2*xc*(1-2*xR)*bb+(xR-xR.^2)*cc;

      kappaCLR2=y^(1/(2*omega))*(ddd+eee) cRho^2;

      %%%%%%%%%%%%%%%%%%%%%%%%%%%%%%%%%%%%%%%%%%%%%%%%%%%%%%%%%%%%%%%%%%%

      % Function evaluation at y
      FY=1-(1-u_roof)*y-u_roof*sqrt(1+LAMBDA^2/kappaCLR2)*y^(1/omega);
    end;
    YY(t,s)=y;
    kappa(t,s)=kappaCLR2;
  end;

end;

FY=1-(1-u_roof)*YY-u_roof*sqrt(1+LAMBDA^2./kappa).*YY.^(1/omega);

[YY kappa x FY] % Iteration results

% Plot results
hold on
plot(x(1:qq,1),YY(:,1),'kp')
plot(x(1:qq,2),YY(:,2),'bp')
xlabel('x');,ylabel('Y')

pause
close
```

Subroutine FitFun

```
function [f,G]=fitfun(Var,x1in,x2in,Temp,Data0,qq,xc,Tc,alpha12,a_curl,c_curl,LAMBDA,u_bar)

%%%%%%%%%%%%%%%%%%%%%%%%%%%%%%%%%%%%%%%%%%%%%%%%%%%%%%%%%%%%
% CALCULATION OF THE OBJECTIVE FUNCTION
%%%%%%%%%%%%%%%%%%%%%%%%%%%%%%%%%%%%%%%%%%%%%%%%%%%%%%%%%%%%

% Variables
[Tcalc,Y,x1calc,x2calc,u_bar,b_curl,d_curl]=vector2var(Var)

% Calculation of the error
f1=(x1in-x1calc)/0.001;%.*w(:,1)/0.001;
f2=(x2in-x2calc)/0.001;%.*w(:,2)/0.001;
f3=(Temp-Tcalc)/0.003;

% Square of the error
f1N=f1(:)'*f1(:);
f2N=f2(:)'*f2(:);
f3N=f3(:)'*f3(:);

% Objective function
f=(f1N+f2N+f3N)/(qq-3);


% Definition of the partial derivatives of the objective function to the variables
if nargout>1
  G=zeros(length(Var),1);
  G(1:LL,1)=-2*f3/0.003;
  G(LL+1:3*LL,1)=0;
  G(3*LL+1:4*LL,1)=-2*f1(1:LL,1)/0.001;
  G(4*LL+1:5*LL,1)=-2*f2(1:LL,1)/0.001;
end;
```

Subroutine VarToVector

```
function [Var,LB,UB]=var2vector(T,Y,x1,x2,u_bar,b_curl,d_curl,Data0,qq)

%%%%%%%%%%%%%%%%%%%%%%%%%%%%%%%%%%%%%%%%%%%%%%%%%%%%%%%%%%%%
% CONVERSION OF VARIABLES INTO A VECTOR
%%%%%%%%%%%%%%%%%%%%%%%%%%%%%%%%%%%%%%%%%%%%%%%%%%%%%%%%%%%%

Var=[T(:); Y(:); x1(:); x2(:); u_bar; b_curl; d_curl];

% Definition of the boundary conditions: variables must remain between lower and upper bounds
LBY=[Y(:,1)*0.9 Y(:,2)*0.9];
UBY=[Y(:,1)*1.1 Y(:,2)*1.1];

LBx1(:,1)=0.98*Data0(1:qq,1);
LBx2(:,1)=0.98*Data0(1:qq,2);

UBx1(:,1)=1.02*Data0(1:qq,1);
UBx2(:,1)=1.02*Data0(1:qq,2);

for t=1
  for e=1:qq
    if UBY(e,t)>1
      UBY(e,t)=0.9999;
    end;
    if UBx2(t,1)>0.99
      UBx2(t,1)=0.99;
    end;
    if UBx1(t,1)>0.99
      UBx1(t,1)=0.99;
    end;
    if LBx1(e,t)<0
```

```
        LBx1(e,t)=0.001;
      end;
      if LBx2(e,t)<0
        LBx2(e,t)=0.001;
      end;
    end;
end;


LBfitpar= [0.33  3.50   0.54]';
UBfitpar= [0.35  3.54   0.57]';

% Lower bounds
LB=[0.999*Data0(1:qq,3)
      LBY(:);
      LBx1(:);
      LBx2(:);
      LBfitpar];

% Upper bounds
UB=[1.001*Data0(1:qq,3)
      UBY(:);
      UBx1(:);
      UBx2(:);
      UBfitpar];
```

Subroutine VectorToVar

```
function [Tcalc,Y,x1calc,x2calc,u_bar,b_curl,d_curl]=vector2var(Var)

%%%%%%%%%%%%%%%%%%%%%%%%%%%%%%%%%%%%%%%%%%%%%%%%%%%%%%%%%%%%%%%%%%%%%%%%%
% CONVERSION OF A VECTOR INTO VARIABLES
%%%%%%%%%%%%%%%%%%%%%%%%%%%%%%%%%%%%%%%%%%%%%%%%%%%%%%%%%%%%%%%%%%%%%%%%%

L=length(Var)-3;
S=L/5;

% Variables
Tcalc=      Var(1:S,1);
Y=          [Var(S+1:2*S,1)     Var(2*S+1:3*S,1)];
x1calc=     Var(3*S+1:4*S,1);
x2calc=     Var(4*S+1:5*S,1);

% Optimisation parameters
u_bar=   Var(L+1,1);
b_curl=  Var(L+2,1);
d_curl=  Var(L+3,1);
```

Subroutine Constraints

```
function [cc,ceq]=constraints(Var,x1in,x2in,T,Data0,qq,xc,Tc,alpha12,a,c,LAMBDA)

% Output with 16 digits
format long

% Transformation of the vector Var to the original variables
[T,Y,x1,x2,u_bar,b,d]=vector2var(Var);

% Crossover values and universal critical exponents
u_star=0.472;
nu=0.63;
eta=0.0333;
omega=0.85714;
alpha=0.11;
Delta=nu*omega;
gamma=(2-eta)*nu;

% Rescaling functions
TT=Y.^((2*nu-1)/Delta);
DD=Y.^((gamma-2*nu)/Delta);
UU=Y.^(nu/Delta);

% Data input
x=[x1 x2];
dT=1-Tc./T;
dx=x./xc-1;

% Classical NRTL interaction functions
tau21=[a.*(1-b.*dT) a.*(1-b.*dT)];
tau12=[c.*(1-d.*dT) c.*(1-d.*dT)];
G21=exp(-alpha12.*tau21);
G12=exp(-alpha12.*tau12);

% Renormalised mole fraction, temperature, and NRTL interaction functions
dxR=dx.*Y.^((1-2.*eta)./(4.*omega));
xR=xc.*(dxR+1);
dTR=      [dT.*Y(:,1).^((3.*nu-2)./(2.*nu.*omega)) dT.*Y(:,2).^((3.*nu-2)./(2.*nu.*omega))];
tau12R=    [c.*(1-d.*dTR(:,1)) c.*(1-d.*dTR(:,2))];
tau21R=    [a.*(1-b.*dTR(:,1)) a.*(1-b.*dTR(:,2))];
G12R=      exp(-alpha12.*tau12R);
G21R=      exp(-alpha12.*tau21R);


% Help variables
yyy=(xR+(1-xR).*G21R);
zzz=(1-xR+xR.*G12R);
uuuu=(1-xc+xc.*G12R);
tttt=(xc+(1-xc).*G21R);
aaaa=-xc-exp(-alpha12.*a)+exp(-alpha12.*a).*xc;
bbbb=1-xc+xc.*exp(-alpha12.*c);

% Regular part of the Gibbs energy of mixing
deltaGreg=xc.*log(xc)+xc.*(1-xc).*(tau21.*G21./(xc+(1-xc).*G21)+tau12.*G12./(1-xc+xc.*G12))+(1-xc).*log(1-xc)+...
   (log(xc)-log(1-xc)+xc.*(1-xc).*(-tau21.*G21.*(1-G21)./(xc+(1-xc).*G21).^2-tau12.*G12.*(-1+G12)./((1-xc+xc.*G12).^2))+...
   (-2.*xc+1).*(tau21.*G21./(xc+(1-xc).*G21)+tau12.*G12./(1-xc+xc.*G12))).*(x-xc);

DdeltaGregDx= log(xc)-log(1-xc)+xc.*(1-xc).*(-tau21.*G21.*(1-G21)./((xc+(1-xc).*G21).^2)-tau12.*G12.*(-1+G12)./((1-
xc+xc.*G12).^2))+(-2.*xc+1).*(tau21.*G21./(xc+(1-xc).*G21)+tau12.*G12./(1-xc+xc.*G12));


%%%%%%%%%%%%%%%%%%%%%%%%%%%%%%%%%%%%%%%%%%%%%%%%%%%%%%
% The following variables are partial derivatives of the NRTL model, which follow from a Taylor series expansion
% near the critical point (dx=0, dT=0). The variable a0 equals the derivative D3deltaG/(Ddx2DdT) in the critical point.
% The variable u0 equals the derivative D4deltaG/(Ddx4) evaluated at the critical point.
% a0 and u0 are needed to calculated cRho and cT.
%%%%%%%%%%%%%%%%%%%%%%%%%%%%%%%%%%%%%%%%%%%%%%%%%%%%%%
```

```
a0= 2.*xc.*(1-xc).*(-(-a.^2.*exp(-alpha12.*a).^2.*xc.^2.*(-1+exp(-alpha12.*a)).*alpha12.*b./(aaaa.^2)+...
  (-2.*a.*exp(-alpha12.*a).*xc.*(-1+exp(-alpha12.*a)).*(-exp(-alpha12.*a).*alpha12.*a.*b+exp(-alpha12.*a).*...
  alpha12.*a.*b.*xc)./(aaaa.^3)+(a.^2.*exp(-alpha12.*a).^2.*xc.*alpha12.*b+(exp(-alpha12.*a).*alpha12.*a.^2.*b-...
  a.*b.*exp(-alpha12.*a)).*xc.*(-1+exp(-alpha12.*a)))./(aaaa.^2)).*(xc-exp(-alpha12.*a).*xc)-...
  a.^2.*exp(-alpha12.*a).^2.*xc.^2.*(-1+exp(-alpha12.*a)).^2.*(1-xc).*alpha12.*b./(aaaa.^3))./(xc+(1-xc).*...
  exp(-alpha12.*a))+c.^2.*exp(-alpha12.*c).^2.*xc.^2.*(-1+exp(-alpha12.*c)).*alpha12.*d./(bbbb.^3)+...
  (-3.*c.^2.*exp(-alpha12.*c).^2.*xc.^2.*(-1+exp(-alpha12.*c)).*alpha12.*d./(bbbb.^4)+(c.^2.*exp(-alpha12.*c).^2.*...
  xc.*alpha12.*d+(exp(-alpha12.*c).*alpha12.*c.^2.*d-c.*d.*exp(-alpha12.*c)).*xc.*(-1+exp(-alpha12.*c)))./(bbbb.^3)).*...
  (-xc+xc.*exp(-alpha12.*c)))-2.*xc.^2.*((exp(-alpha12.*a).*alpha12.*a.^2.*b-a.*b.*exp(-alpha12.*a)+a.^2.*...
  exp(-alpha12.*a).^2.*(1-xc).*alpha12.*b./aaaa)./(xc+(1-xc).*exp(-alpha12.*a))+(exp(-alpha12.*c).*alpha12.*...
  c.^2.*d-c.*d.*exp(-alpha12.*c)-c.^2.*exp(-alpha12.*c).^2.*xc.*alpha12.*d./bbbb)./bbbb)+2.*(-xc.^2+xc.*(1-xc)).*...
  ((-a.^2.*exp(-alpha12.*a).^2.*alpha12.*b.*xc./aaaa+(exp(-alpha12.*a).*alpha12.*a.^2.*b-a.*b.*exp(-alpha12.*a)-...
  a.*exp(-alpha12.*a).*(-exp(-alpha12.*a).*alpha12.*a.*b+exp(-alpha12.*a).*alpha12.*a.*b.*xc)./aaaa).*...
  (xc-exp(-alpha12.*a).*xc)./aaaa-a.^2.*exp(-alpha12.*a).^2.*xc.*(-1+exp(-alpha12.*a)).*(1-xc).*alpha12.*b./...
  (aaaa.^2))./(xc+(1-xc).*exp(-alpha12.*a))-c.^2.*exp(-alpha12.*c).^2.*xc.*alpha12.*d./(bbbb.^2)-(-2.*c.^2.*...
  exp(-alpha12.*c).^2.*xc.*alpha12.*d./(bbbb.^3)+(exp(-alpha12.*c).*alpha12.*c.^2.*d-c.*d.*exp(-alpha12.*c))./...
  (bbbb.^2)).*(-xc+xc.*exp(-alpha12.*c)));

u0= 2.*xc+8.*xc.^4./((xc-1).^2.*(1-xc))+6.*xc.^4./((xc-1).^3)+24.*(-xc.^2+xc.*(1-xc)).*(-c.*exp(-alpha12.*c).*xc.^2.*...
  (-1+exp(-alpha12.*c)).^2.*(-xc+xc.*exp(-alpha12.*c))./((1-xc+xc.*exp(-alpha12.*c)).^4)+a.*exp(-alpha12.*a).*...
  xc.^2.*(-1+exp(-alpha12.*a)).^2.*(xc-exp(-alpha12.*a).*xc)./((-xc-exp(-alpha12.*a)+exp(-alpha12.*a).*xc).^3.*...
  (xc+(1-xc).*exp(-alpha12.*a))))-24.*xc.^2.*(-a.*exp(-alpha12.*a).*xc.*(-1+exp(-alpha12.*a)).*(xc-...
  exp(-alpha12.*a).*xc)./((-xc-exp(-alpha12.*a)+exp(-alpha12.*a).*xc).^2.*(xc+(1-xc).*exp(-alpha12.*a)))+...
  c.*exp(-alpha12.*c).*xc.*(-1+exp(-alpha12.*c)).*(-xc+xc.*exp(-alpha12.*c))./((1-xc+xc.*exp(-alpha12.*c)).^3))+...
  24.*xc.*(1-xc).*(-a.*exp(-alpha12.*a).*xc.^3.*(-1+exp(-alpha12.*a)).^3.*(xc-exp(-alpha12.*a).*xc)./...
  ((-xc-exp(-alpha12.*a)+exp(-alpha12.*a).*xc).^4.*(xc+(1-xc).*exp(-alpha12.*a)))+c.*exp(-alpha12.*c).*...
  xc.^3.*(-1+exp(-alpha12.*c)).^3.*(-xc+xc.*exp(-alpha12.*c))./((1-xc+xc.*exp(-alpha12.*c)).^5));

% System-dependent amplitudes
cRho=u0^0.25*(u_bar*u_star*LAMBDA)^(-0.25);
cT=a0/sqrt(u0)*sqrt(u_bar*u_star*LAMBDA);

% Singular part of the Gibbs energy of mixing
deltaGsing=xR.*log(xR)+(1-xR).*log(1-xR)+xR.*(1-xR).*(tau21R.*G21R./(xR+(1-xR).*G21R)+tau12R.*G12R./(1-xR+xR.*G12R))-...
  xc.*log(xc)-xc.*(1-xc).*(tau21R.*G21R./(xc+(1-xc).*G21R)+tau12R.*G12R./(1-xc+xc.*G12R))-(1-xc).*log(1-xc)-(log(xc)-...
  log(1-xc)+xc.*(1-xc).*(-tau21R.*G21R.*(1-G21R)./((xc+(1-xc).*G21R).^2)-tau12R.*G12R.*(-1+G12R)./((1-xc+xc.*G12R).^2))+...
  (-2.*xc+1).*(tau21R.*G21R./(xc+(1-xc).*G21R)+tau12R.*G12R./(1-xc+xc.*G12R))).*(xR-xc)-...
  0.5*cT^2*[dT.^2 dT.^2].*nu/(alpha*u_bar*LAMBDA).*(Y.^(-alpha/Delta)-1);

%%%%%%%%%%%%%%%%%%%%%%%%%%%%%%%%%%%%%%%%%%%%%%%%%%%%%%
% The kappa^2 that can be calculated from the classical NRTL equation must be divided by cRho^2.
% This has to be done because kappa^2 in the Landau expansion is calculated by differentiating deltaG two times
% to the product (MD^0.5)=(cRho*dx*D^0.5). The kappa^2 in the classical theory is calculated by differentiating
% deltaG two times to dx!!! Crho and cT relate the Landau variables to the physical variables.
%
% This implies that the (partial) derivatives of kappa^2 to dxR and dTR have also to be divided by Crho^2.
%%%%%%%%%%%%%%%%%%%%%%%%%%%%%%%%%%%%%%%%%%%%%%%%%%%%%%

kappa2=Y.^(1./(2*omega)).*xc.^2.*(1./xR+1./(1-xR)-2.*tau21R.*G21R./yyy-...
  2.*tau12R.*G12R./zzz+2.*(1-xR).*(-tau21R.*G21R.*(1-G21R)./yyy.^2-tau12R.*G12R.*(-1+G12R)./zzz.^2)-...
  2.*xR.*(-tau21R.*G21R.*(1-G21R)./yyy.^2-tau12R.*G12R.*(-1+G12R)./zzz.^2)+xR.*(1-xR).*(2.*tau21R.*G21R.*(1-G21R).^2./...
  yyy.^3+2.*tau12R.*G12R.*(-1+G12R).^2./zzz.^3));

kappa2=kappa2/cRho^2;

Dkappa2DdeltaxR=xc.^3.*Y.^(1./(2.*omega)).*(-1./(xR.^2)+1./((1-xR).^2)+6.*tau21R.*G21R.*(1-G21R)./yyy.^2+...
  6.*tau12R.*G12R.*(-1+G12R)./zzz.^2+3.*(1-xR).*(2.*tau21R.*G21R.*(1-G21R).^2./yyy.^3+2.*tau12R.*
  G12R.*(1+G12R).^2./zzz.^3)-3.*xR.*(2.*tau21R.*G21R.*(1-G21R).^2./yyy.^3+2.*tau12R.*G12R.*(-1+G12R).^2./zzz.^3)+...
  xR.*(1-xR).*(-6.*tau21R.*G21R.*(1-G21R).^3./yyy.^4-6.*tau12R.*G12R.*(-1+G12R).^3./zzz.^4));

Dkappa2DdeltaxR=Dkappa2DdeltaxR/cRho^2;

Dkappa2DdeltaTR=Y.^(1./2.*1./omega).*xc.^2.*(2.*a.*b.*G21R./yyy-2.*a.*tau21R.*alpha12.*b.*G21R./yyy+...
  2.*a.*tau21R.*G21R.^2.*(1-xR).*alpha12.*b./yyy.^2+2.*c.*d.*G12R./zzz-2.*c.*tau12R.*alpha12.*d.*G12R./zzz+...
  2.*c.*tau12R.*G12R.^2.*xR.*alpha12.*d./zzz.^2+2.*(1-xR).*(a.*b.*G21R.*(1-G21R)./yyy.^2-...
  a.*tau21R.*alpha12.*b.*G21R.*(1-G21R)./yyy.^2+2.*a.*tau21R.*G21R.^2.*(1-G21R).*(1-xR).*alpha12.*b./yyy.^3+...
  a.*tau21R.*G21R.^2.*alpha12.*b./yyy.^2+c.*d.*G12R.*(-1+G12R)./zzz.^2-c.*tau12R.*alpha12.*d.*G12R.*(-1+G12R)./zzz.^2+...
  2.*c.*tau12R.*G12R.^2.*(-1+G12R).*xR.*alpha12.*d./zzz.^3-c.*tau12R.*G12R.^2.*alpha12.*d./zzz.^2)-...
  2.*xR.*(a.*b.*G21R.*(1-G21R)./yyy.^2-a.*tau21R.*alpha12.*b.*G21R.*(1-G21R)./yyy.^2+...
  2.*a.*tau21R.*G21R.^2.*(1-G21R).*(1-xR).*alpha12.*b./yyy.^3+a.*tau21R.*G21R.^2.*alpha12.*b./yyy.^2+...
```

```
  c.*d.*G12R.*(-1+G12R)./zzz.^2-c.*tau12R.*alpha12.*d.*G12R.*(-1+G12R)./zzz.^2+...
  2.*c.*tau12R.*G12R.^2.*(-1+G12R).*xR.*alpha12.*d./zzz.^3-c.*tau12R.*G12R.^2.*alpha12.*d./zzz.^2)+...
  xR.*(1-xR).*(-2.*a.*b.*G21R.*(1-G21R).^2./yyy.^3+2.*a.*tau21R.*alpha12.*b.*G21R.*(1-G21R).^2./yyy.^3-...
  6.*a.*tau21R.*G21R.^2.*(1-G21R).^2.*(1-xR).*alpha12.*b./yyy.^4-4.*a.*tau21R.*G21R.^2.*(1-G21R).*alpha12.*b./yyy.^3-...
  2.*c.*d.*G12R.*(-1+G12R).^2./zzz.^3+2.*c.*tau12R.*alpha12.*d.*G12R.*(-1+G12R).^2./zzz.^3-...
  6.*c.*tau12R.*G12R.^2.*(-1+G12R).^2.*xR.*alpha12.*d./zzz.^4+4.*c.*tau12R.*G12R.^2.*(-1+G12R).*alpha12.*d./zzz.^3));

Dkappa2DdeltaTR=Dkappa2DdeltaTR/cRho^2;

DdeltaGsingDdTR=xR.*(1-xR).*(-a.*b.*G21R./yyy+a.*tau21R.*alpha12.*b.*G21R./yyy-a.*tau21R.*G21R.^2.*(1-xR).*alpha12.*
  b./yyy.^2-c.*d.*G12R./zzz+c.*tau12R.*alpha12.*d.*G12R./zzz-c.*tau12R.*G12R.^2.*xR.*alpha12.*d./zzz.^2)-xc.*(1-xc).*
  (-a.*b.*G21R./tttt+a.*tau21R.*alpha12.*b.*G21R./tttt-a.*tau21R.*G21R.^2.*(1-xc).*alpha12.*b./tttt.^2-c.*d.*G12R./uuuu+...
  c.*tau12R.*alpha12.*d.*G12R./uuuu-c.*tau12R.*G12R.^2.*xc.*alpha12.*d./uuuu.^2)-(xc.*(1-xc).*(a.*b.*G21R.*(1-G21R)./tttt.^2-...
  a.*tau21R.*alpha12.*b.*G21R.*(1-G21R)./tttt.^2+a.*tau21R.*G21R.^2.*alpha12.*b./tttt.^2+...
  2.*a.*tau21R.*G21R.^2.*(1-G21R).*(1-xc).*alpha12.*b./(tttt.^3)+c.*d.*G12R.*(-1+G12R)./uuuu.^2-...
  c.*tau12R.*alpha12.*d.*G12R.*(-1+G12R)./uuuu.^2+2.*c.*tau12R.*G12R.^2.*(-1+G12R).*xc.*alpha12.*d./(uuuu.^3)-...
  c.*tau12R.*G12R.^2.*alpha12.*d./uuuu.^2)+(-2.*xc+1).*(-a.*b.*G21R./tttt+a.*tau21R.*alpha12.*b.*G21R./...
  tttt-a.*tau21R.*G21R.^2.*(1-xc).*alpha12.*b./tttt.^2-c.*d.*G12R./uuuu+c.*tau12R.*alpha12.*d.*G12R./uuuu-...
  c.*tau12R.*G12R.^2.*xc.*alpha12.*d./uuuu.^2)).*(xR-xc);

DPdeltaxRDPdeltax= Y.^(1./4.*(1-2.*eta)./omega);
DPdeltaxRDPY= 1./4.*dx.*Y.^(1./4.*(1-2.*eta)./omega).*(1-2.*eta)./(omega.*Y);
DPdeltaTRDPY(:,1)= 1./2.*dT.*Y(:,1).^(1./2.*(3.*nu-2)./(nu.*omega)).*(3.*nu-2)./(nu.*omega.*Y(:,1));
DPdeltaTRDPY(:,2)= 1./2.*dT.*Y(:,2).^(1./2.*(3.*nu-2)./(nu.*omega)).*(3.*nu-2)./(nu.*omega.*Y(:,2));

Dkappa2DY_x=DPdeltaxRDPY.*Dkappa2DdeltaxR;
Dkappa2DY_T=DPdeltaTRDPY.*Dkappa2DdeltaTR;

DPkappa2DPY=kappa2./(2*omega*Y);

% Implicit differentiation: DYDdeltax
DPdxRDPdx=Y.^(1/4*(1-2*eta)/omega);
DPdTRDPdT=Y.^(1/2*(3*nu-2)/(nu*omega));

FY=-u_bar*(1+LAMBDA^2./kappa2).^.5.*Y.^(1/omega)./(omega*Y*(1-u_bar));
FK2=0.5*u_bar*Y.^(1/omega)*LAMBDA^2./((1+LAMBDA^2./kappa2).^.5.*kappa2.^2*(1-u_bar));

Factor1=FK2./(1-FY);

DYDdeltaxTeller=Factor1.*Dkappa2DdeltaxR.*DPdxRDPdx;
DYDdeltaTTeller=Factor1.*Dkappa2DdeltaTR.*DPdTRDPdT;
DYDdeltaxNoemer=(1-Factor1.*(Dkappa2DY_T+Dkappa2DY_x+DPkappa2DPY));

DYDdeltax=DYDdeltaxTeller./DYDdeltaxNoemer;

DPdxRDY=.5.*dx.*(Y.^((gamma-2.*nu)./Delta)).^.5.*(Y.^(nu./Delta)).^.25.*(gamma-2.*nu)./(Delta.*Y)+.25.*dx.*...
  (Y.^((gamma-2.*nu)./Delta)).^.5.*(Y.^(nu./Delta)).^.25.*nu./(Delta.*Y);
DPdTRDY=[dT dT].*Y.^((2.*nu-1)./Delta).*(2.*nu-1)./(Delta.*Y.*(Y.^(nu./Delta)).^.5)-.5.*[dT dT].*Y.^((2.*nu-1)./Delta).*...
  nu./((Y.^(nu./Delta)).^.5.*Delta.*Y);

DPkernelDPY=.5.*cT.^2.*[dT dT].^2.*nu.*Y.^(-alpha./Delta)./(u_bar.*LAMBDA.*Delta.*Y);

DPdeltaGsingDdTR= xc.*(dxR+1).*(1-xR).*(-a.*b.*G21R./(xR+(1-xR).*G21R)+a.*tau21R.*alpha12.*b.*G21R./(xR+(1-xR).*G21R)-...
  a.*tau21R.*G21R.^2.*(1-xR).*alpha12.*b./((xR+(1-xR).*G21R).^2)-c.*d.*G12R./(1-xR+xc.*(dxR+1).*G12R)+c.*tau12R.*...
  alpha12.*d.*G12R./(1-xR+xc.*(dxR+1).*G12R)-c.*tau12R.*G12R.^2.*xc.*(dxR+1).*alpha12.*d./((1-xR+xc.*(dxR+1).*...
  G12R).^2))-xc.*(1-xc).*(-a.*b.*G21R./(xc+(1-xc).*G21R)+a.*tau21R.*alpha12.*b.*G21R./(xc+(1-xc).*G21R)-a.*...
  tau21R.*G21R.^2.*(1-xc).*alpha12.*b./((xc+(1-xc).*G21R).^2)-c.*d.*G12R./(1-xc+xc.*G12R)+c.*tau12R.*alpha12.*d.*...
  G12R./(1-xc+xc.*G12R)-c.*tau12R.*G12R.^2.*xc.*alpha12.*d./((1-xc+xc.*G12R).^2))-(xc.*(1-xc).*(a.*b.*G21R.*...
  (1-G21R)./((xc+(1-xc).*G21R).^2)-a.*tau21R.*alpha12.*b.*G21R.*(1-G21R)./((xc+(1-xc).*G21R).^2)+a.*tau21R.*...
  G21R.^2.*alpha12.*b./((xc+(1-xc).*G21R).^2)+2.*a.*tau21R.*G21R.^2.*(1-G21R).*(1-xc).*alpha12.*b./...
  ((xc+(1-xc).*G21R).^3)+c.*d.*G12R.*(-1+G12R)./((1-xc+xc.*G12R).^2)-c.*tau12R.*alpha12.*d.*G12R.*(-1+G12R)./...
  ((1-xc+xc.*G12R).^2)-c.*tau12R.*G12R.^2.*alpha12.*d./((1-xc+xc.*G12R).^2)+2.*c.*tau12R.*G12R.^2.*(-1+G12R).*...
  xc.*alpha12.*d./((1-xc+xc.*G12R).^3))+(-2.*xc+1).*(-a.*b.*G21R./(xc+(1-xc).*G21R)+a.*tau21R.*alpha12.*b.*...
  G21R./(xc+(1-xc).*G21R)-a.*tau21R.*G21R.^2.*(1-xc).*alpha12.*b./((xc+(1-xc).*G21R).^2)-c.*d.*G12R./(1-xc+xc.*G12R)+...
  c.*tau12R.*alpha12.*d.*G12R./(1-xc+xc.*G12R)-c.*tau12R.*G12R.^2.*xc.*alpha12.*d./((1-xc+xc.*G12R).^2))).*(xR-xc);

DPdeltaGsingDdxR= xc.*log(xc.*(dxR+1))-xc.*log(1-xc.*(dxR+1))+xc.*(1-xc.*(dxR+1)).*(tau21R.*G21R./(xc.*(dxR+1)+(1-xc.*...
  (dxR+1)).*G21R)+tau12R.*G12R./(1-xc.*(dxR+1)+xc.*(dxR+1).*G12R))-xc.^2.*(dxR+1).*(tau21R.*G21R./(xc.*(dxR+1)+...
  (1-xc.*(dxR+1)).*G21R)+tau12R.*G12R./(1-xc.*(dxR+1)+xc.*(dxR+1).*G12R))+xc.*(dxR+1).*(1-xc.*(dxR+1)).*(-tau21R.*...
  G21R.*(xc-xc.*G21R)./((xc.*(dxR+1)+(1-xc.*(dxR+1)).*G21R).^2)-tau12R.*G12R.*(-xc+xc.*G12R)./((1-xc.*(dxR+1)+...
```

```
  xc.*(dxR+1).*G12R).^2))-(log(xc)-log(1-xc)+xc.*(1-xc).*(-tau21R.*G21R.*(1-G21R)./((xc+(1-xc).*G21R).^2)-...
  tau12R.*G12R.*(-1+G12R)./((1-xc+xc.*G12R).^2))+(-2.*xc+1).*(tau21R.*G21R./(xc+(1-xc).*G21R)+tau12R.*G12R./...
  (1-xc+xc.*G12R))).*xc;

DPdeltaGsingDPY=DPdeltaGsingDdTR.*DPdTRDY+DPdeltaGsingDdxR.*DPdxRDY+DPkernelDPY;

DPdeltaGsingDPdx= xc.*DD.^.5.*UU.^.25.*log(xc.*(dx.*DD.^.5.*UU.^.25+1))-xc.*DD.^.5.*UU.^.25.*log(1-xc.*...
  (dx.*DD.^.5.*UU.^.25+1))+xc.*DD.^.5.*UU.^.25.*(1-xc.*(dx.*DD.^.5.*UU.^.25+1)).*(a.*(1-b.*dTR).*...
  exp(-alpha12.*a.*(1-b.*dTR))./(xc.*(dx.*DD.^.5.*UU.^.25+1)+(1-xc.*(dx.*DD.^.5.*UU.^.25+1)).*...
  exp(-alpha12.*a.*(1-b.*dTR)))+c.*(1-d.*dTR).*exp(-alpha12.*c.*(1-d.*dTR))./(1-xc.*(dx.*DD.^.5.*UU.^.25+...
  1)+xc.*(dx.*DD.^.5.*UU.^.25+1).*exp(-alpha12.*c.*(1-d.*dTR))))-xc.^2.*(dx.*DD.^.5.*UU.^.25+1).*DD.^.5.*...
  UU.^.25.*(a.*(1-b.*dTR).*exp(-alpha12.*a.*(1-b.*dTR))./(xc.*(dx.*DD.^.5.*UU.^.25+1)+(1-xc.*(dx.*DD.^.5.*...
  UU.^.25+1)).*exp(-alpha12.*a.*(1-b.*dTR)))+c.*(1-d.*dTR).*exp(-alpha12.*c.*(1-d.*dTR))./(1-xc.*...
  (dx.*DD.^.5.*UU.^.25+1)+xc.*(dx.*DD.^.5.*UU.^.25+1).*exp(-alpha12.*c.*(1-d.*dTR))))+xc.*...
  (dx.*DD.^.5.*UU.^.25+1).*(1-xc.*(dx.*DD.^.5.*UU.^.25+1)).*(-a.*(1-b.*dTR).*exp(-alpha12.*a.*...
  (1-b.*dTR)).*(xc.*DD.^.5.*UU.^.25-xc.*DD.^.5.*UU.^.25.*exp(-alpha12.*a.*(1-b.*dTR)))./((xc.*...
  (dx.*DD.^.5.*UU.^.25+1)+(1-xc.*(dx.*DD.^.5.*UU.^.25+1)).*exp(-alpha12.*a.*(1-b.*dTR))).^2)-c.*...
  (1-d.*dTR).*exp(-alpha12.*c.*(1-d.*dTR)).*(-xc.*DD.^.5.*UU.^.25+xc.*DD.^.5.*UU.^.25.*exp(-alpha12.*...
  c.*(1-d.*dTR)))./((1-xc.*(dx.*DD.^.5.*UU.^.25+1)+xc.*(dx.*DD.^.5.*UU.^.25+1).*exp(-alpha12.*c.*...
  (1-d.*dTR))).^2))-(log(xc)-log(1-xc)+xc.*(1-xc).*(-a.*(1-b.*dTR).*exp(-alpha12.*a.*(1-b.*dTR)).*...
  (1-exp(-alpha12.*a.*(1-b.*dTR)))./((xc+(1-xc).*exp(-alpha12.*a.*(1-b.*dTR))).^2)-c.*(1-d.*dTR).*...
  exp(-alpha12.*c.*(1-d.*dTR)).*(-1+exp(-alpha12.*c.*(1-d.*dTR)))./((1-xc+xc.*exp(-alpha12.*c.*...
  (1-d.*dTR))).^2))+(-2.*xc+1).*(a.*(1-b.*dTR).*exp(-alpha12.*a.*(1-b.*dTR))./(xc+(1-xc).*exp(-alpha12.*...
  a.*(1-b.*dTR)))+c.*(1-d.*dTR).*exp(-alpha12.*c.*(1-d.*dTR))./(1-xc+xc.*exp(-alpha12.*c.*(1-d.*dTR))))).*...
  xc.*DD.^.5.*UU.^.25;

DDELTAGSINGDDELTAX=DPdeltaGsingDPdx+DPdeltaGsingDPY.*DYDdeltax;

%%%%%%%%%%%%%%%%%%%%%%%%%%%%%%%%%%%%%%%%%%%%%%%%%%%%%%%%%%%%%%
% Inequality constraints can be: -kappa^2(:,1)<0 and -kappa^2(:,2)<0.
%%%%%%%%%%%%%%%%%%%%%%%%%%%%%%%%%%%%%%%%%%%%%%%%%%%%%%%%%%%%%%

cc=  [-kappa2(:,1);
      -kappa2(:,2)];

%%%%%%%%%%%%%%%%%%%%%%%%%%%%%%%%%%%%%%%%%%%%%%%%%%%%%%%%%%%%%%
% The following equality constraints imply phase equilibrium and the crossover function. Of course, they equal zero
% when they are satisfied.
%%%%%%%%%%%%%%%%%%%%%%%%%%%%%%%%%%%%%%%%%%%%%%%%%%%%%%%%%%%%%%

ceq=...
  [DDELTAGSINGDDELTAX(:,2)-DDELTAGSINGDDELTAX(:,1);
  deltaGsing(:,1)-deltaGsing(:,2)+(x(:,2)-x(:,1)).*DDELTAGSINGDDELTAX(:,1)/xc;
  1-(1-u_bar)*Y(:,1)-u_bar*(1+LAMBDA^2./kappa2(:,1)).^0.5.*Y(:,1).^(1/omega);
  1-(1-u_bar)*Y(:,2)-u_bar*(1+LAMBDA^2./kappa2(:,2)).^0.5.*Y(:,2).^(1/omega)];
```

Subroutine NRTLPar

```
% This subroutine calculates the NRTL parameters a-wiggle and c-wiggle from the conditions of incipient immiscibility

function f=NRTLPar(Par,xc,alpha12)

a_curl=Par(1,1);
c_curl=Par(2,1);

tau21=a_curl;
tau12=c_curl;
G12=exp(-alpha12*tau12);
G21=exp(-alpha12*tau21);

hai=(tau21*G21/(xc+(1-xc)*G21)+tau12*G12/(1-xc+xc*G12));
hoi=(-tau21*G21*(1-G21)/(xc+(1-xc)*G21)^2-tau12*G12*(G12-1)/(1-xc+xc*G12)^2);
hei=(2*tau21*G21*(1-G21)^2/(xc+(1-xc)*G21)^3+2*tau12*G12*(G12-1)^2/(1-xc+xc*G12)^3);
hui=(-6*tau21*G21*(1-G21)^3/(xc+(1-xc)*G21)^4-6*tau12*G12*(G12-1)^3/(1-xc+xc*G12)^4);

d2deltaGdx12=      1/xc + 1/(1-xc) - 2*hai + 2*(1-2*xc)*hoi + (xc-xc^2)*hei;
d3deltaGdx13=      -1/xc^2 + 1/(1-xc)^2 - 6*hoi + (3-6*xc)*hei + (xc-xc^2)*hui;

f=[d2deltaGdx12 d3deltaGdx13]';
```

Appendix E

Matlab®-code for 2T-Landau expansion

Program Datdemo

```
%%%%%%%%%%%%%%%%%%%%%%%%%%%%%%%%%%%%%%%%%%%%%%%%%%%%%%%%%%%%%%%%%%%%%%%%%%%%%%%%%%%%%%%%%%%%%%%%
% This program optimises the NRTL parameters b-wiggle and, d-wiggle and the the crossover parameter u_bar for
% the 2T-Landau model. The parameters ct and crho are translated to the NRTL model. Lambda is fixed at 1 and alpha12 is
% fixed at 0.2. The NRTL parameters a-wiggle and c-wiggle are calculated from the conditions of incipient immiscibility. They
% depend on the mole fraction in the critical point. This optimisation includes the implicit dependence of Y on M (dYdM) and the
% kernel term.
%%%%%%%%%%%%%%%%%%%%%%%%%%%%%%%%%%%%%%%%%%%%%%%%%%%%%%%%%%%%%%%%%%%%%%%%%%%%%%%%%%%%%%%%%%%%%%%%

% Crossover exponents and properties
omega=0.85714;
nu=0.63;
eta=0.0333;
gamma=(2-eta)*nu;
Delta=nu*omega;
alpha=0.11;
alpha12=0.2;
u_star=0.472;
Lambda=1;

% Standard deviations
sigma_x=0.001;
sigma_T=0.003;

% Critical parameters
Tc=293.052;
xc=0.505;

% Data set for nitrobenzene(1) – octane(2)
Data=...
 [
  0.475  0.535    293.039
  0.471  0.539    293.034
  0.466  0.543    293.025
  0.463  0.546    293.017
  0.459  0.550    293.004
  0.455  0.554    292.987
  0.450  0.559    292.970
  0.444  0.565    292.939
  0.437  0.571    292.892
  0.430  0.578    292.833
  0.421  0.586    292.761
  0.413  0.594    292.663
  0.405  0.601    292.551
  0.395  0.611    292.371
  0.379  0.625    292.041
  0.365  0.638    291.690
  0.350  0.651    291.216
  0.337  0.664    290.710
  0.324  0.676    290.145
  0.311  0.687    289.516
  0.299  0.698    288.801
  0.284  0.710    287.923
  0.273  0.720    287.098
  0.261  0.731    286.113
  0.249  0.741    285.094
  0.239  0.750    284.089
  0.228  0.758    283.069];

B=size(Data);

% Number of points used for data regression
Points=B(1,1);

% Estimates for the parameters
u_bar=0.45;
b=2;
```

```
d=1;


% Plot data
hold on
plot(Data(1:Points,1),Data(1:Points,3))
plot(Data(1:Points,2),Data(1:Points,3))
plot(Data(1:Points,1),Data(1:Points,3),'r*')
plot(Data(1:Points,2),Data(1:Points,3),'r*')

pause
close

% Definition of the OPTIONS used in the optimisation process
OPTIONS=[];
OPTIONS = optimset(OPTIONS,'TolX',1e-10,'Display','iter','LevenbergMarquardt','on',...
  'TolCon',1e-10,'TolFun',1e-10,'DiffMaxChange',1e-3,'MaxFunEvals',50000,'LargeScale','off',...
  'Diagnostics','on','DiffMinChange',1e-12,'GradConstr','off','DerivativeCheck','off','MaxIter',200,'GradObj','off');
%
% Explanation of different options:
%
%    - TolX:                  termination tolerance on the parameters
%    - TolCon:                termination tolerance on the constraint violation
%    - TolFun:                termination tolerance on the function value
%    - Display iter:          level of display, iter means: output after every iteration
%    - LevenbergMarquardt:    chooses Levenberg-Marquardt over Gauss-Newton algorithm
%    - DiffMaxChange:         maximum change in variables for finite difference variables
%    - DiffMinChange:         minimum change in variables for finite difference variables
%    - MaxFunEvals:           maximum number of function evaluations allowed
%    - Maxiter:               maximum number of iterations allowed
%    - Diagnostics:           print diagnostic information about the function to be minimised or solved
%    - GradObj:               gradients for the objective function defined by user
%    - GradConstr:            gradients for the (non-)linear constraints defined by user
%    - DerivativeCheck:       compare user-supplied analytic derivatives to finite differencing derivatives
%
%%%%%%%%%%%%%%%%%%%%%%%%%%%%%%%%%%%%%%%%%%%%%%%%%%%%%%%%%%%%%%%%%%%%%%%%%%%%%%%%%%%%%%%%


% Calculation of a-wiggle and c-wiggle from the conditions of incipient immiscibility
% Estimates for a-wiggle and c-wiggle
Par=[1 1]';
P=FSOLVE('NRTLPar',Par,OPTIONS,xc,alpha12);
a=P(1,1);
c=P(2,1);

% Extract T, x1, and x2 from Data set
x1_exp=       Data(1:Points,1);
x2_exp=       Data(1:Points,2);
T_exp=        Data(1:Points,3);

x1=x1_exp;
x2=x2_exp;
T=T_exp;

% Calculate estimates for the crossover-Y (and kappa) based on the parameters given above
%
Y=Bisection(x1, T, nu, omega, gamma, Delta, alpha, eta, xc, Tc,Lambda,Points,a,c,b,d,u_bar,alpha12,u_star);
%
%%%%%%%%%%%%%%%%%%%%%%%%%%%%%%%%%%%%%%%%%%%%%%%%%%%%%%%%%%%%%%%%%%%%%%%%%%%%%%%%%%%%%%%%

% Transformation of variables to vector (+boundary conditions)
%
[Var,LB,UB]=var2vector(Y,x1,T,b,d,u_bar,Data,Points);
%
%%%%%%%%%%%%%%%%%%%%%%%%%%%%%%%%%%%%%%%%%%%%%%%%%%%%%%%%%%%%%%%%%%%%%%%%%%%%%%%%%%%%%%%%

% Start stopwatch
t0=clock;

% Optimisation routine
[Var,fval,exitflag,output,lambda,grad,hessian]=fmincon('fitfun',Var,[],[],[],[],LB,UB,'constraints', OPTIONS, x1_exp, x2_exp,...
  T_exp, nu, omega, gamma, Delta, alpha, eta, xc, Tc, Lambda, sigma_x, sigma_T,alpha12,a,c,Data);

% Give execution time and other relevant information
funEvals=sprintf('\n Number of iterations: %g.  Number of function evaluations: %g.', output.iterations, output.funcCount);
disp(funEvals)
```

```
disp(sprintf(' Norm of the residual at solution ( norm(FITFUN2(x,Data,h))^2 ): %g ',fval));
execution_time=etime(clock, t0);
disp(sprintf(' Execution time: %g \n',execution_time));

% Show optimised results
[Y,x1_calc,T_calc,b,d,u_bar]=vector2var(Var)

% Reduced properties
dx=(x1_calc/xc-1);
dT=(1-Tc./T_calc);

% Help variables
aaaa=-xc-exp(-alpha12.*a)+exp(-alpha12.*a).*xc;
bbbb=1-xc+xc.*exp(-alpha12.*c);

% Landau amplitudes
u0=( 2.*xc+8.*xc.^4./((xc-1).^2.*(1-xc))+6.*xc.^4./((xc-1).^3)+24.*(-xc.^2+xc.*(1-xc)).*(-c.*exp(-alpha12.*c).*...
  xc.^2.*(-1+exp(-alpha12.*c)).^2.*(-xc+xc.*exp(-alpha12.*c))./((1-xc+xc.*exp(-alpha12.*c)).^4)+a.*exp(-alpha12.*a).*...
  xc.^2.*(-1+exp(-alpha12.*a)).^2.*(xc-exp(-alpha12.*a).*xc)./((-xc-exp(-alpha12.*a)+exp(-alpha12.*a).*xc).^3.*...
  (xc+(1-xc).*exp(-alpha12.*a))))-24.*xc.^2.*(-a.*exp(-alpha12.*a).*xc.*(-1+exp(-alpha12.*a)).*(xc-...
  exp(-alpha12.*a).*xc)./((-xc-exp(-alpha12.*a)+exp(-alpha12.*a).*xc).^2.*(xc+(1-xc).*exp(-alpha12.*a)))+...
  c.*exp(-alpha12.*c).*xc.*(-1+exp(-alpha12.*c)).*(-xc+xc.*exp(-alpha12.*c))./((1-xc+xc.*exp(-alpha12.*c)).^3))+...
  24.*xc.*(1-xc).*(-a.*exp(-alpha12.*a).*xc.^3.*(-1+exp(-alpha12.*a)).^3.*(xc-exp(-alpha12.*a).*xc)./...
  ((-xc-exp(-alpha12.*a)+exp(-alpha12.*a).*xc).^4.*(xc+(1-xc).*exp(-alpha12.*a)))+c.*exp(-alpha12.*c).*xc.^3.*...
  (-1+exp(-alpha12.*c)).^3.*(-xc+xc.*exp(-alpha12.*c))./((1-xc+xc.*exp(-alpha12.*c)).^5)))

G_13=6*( ((-xc.^2+xc.*(1-xc)).*(-(-a.^2.*exp(-alpha12.*a).^2.*xc.^2.*(-1+exp(-alpha12.*a)).*alpha12.*b./...
  (aaaa.^2)+(-2.*a.*exp(-alpha12.*a).*xc.*(-1+exp(-alpha12.*a)).*(-exp(-alpha12.*a).*alpha12.*a.*b+...
  exp(-alpha12.*a).*alpha12.*a.*b.*xc)./(aaaa.^3)+(a.^2.*exp(-alpha12.*a).^2.*xc.*alpha12.*b+...
  (exp(-alpha12.*a).*alpha12.*a.^2.*b-a.*b.*exp(-alpha12.*a)).*xc.*(-1+exp(-alpha12.*a)))./(aaaa.^2)).*...
  (xc-exp(-alpha12.*a).*xc)-a.^2.*exp(-alpha12.*a).^2.*xc.^2.*(-1+exp(-alpha12.*a)).^2.*(1-xc).*alpha12.*...
  b./(aaaa.^3))./(xc+(1-xc).*exp(-alpha12.*a))+c.^2.*exp(-alpha12.*c).^2.*xc.^2.*(-1+exp(-alpha12.*c)).*...
  alpha12.*d./(bbbb.^3)+(-3.*c.^2.*exp(-alpha12.*c).^2.*xc.^2.*(-1+exp(-alpha12.*c)).*alpha12.*d./(bbbb.^4)+...
  (c.^2.*exp(-alpha12.*c).^2.*xc.*alpha12.*d+(exp(-alpha12.*c).*alpha12.*c.^2.*d-c.*d.*exp(-alpha12.*c)).*...
  xc.*(-1+exp(-alpha12.*c)))./(bbbb.^3)).*(-xc+xc.*exp(-alpha12.*c)))+xc.*(1-xc).*(-c.^2.*exp(-alpha12.*c).^2.*...
  xc.^3.*(-1+exp(-alpha12.*c)).^2.*alpha12.*d./(bbbb.^4)-(-4.*c.^2.*exp(-alpha12.*c).^2.*xc.^3.*...
  (-1+exp(-alpha12.*c)).^2.*alpha12.*d./(bbbb.^5)+(2.*c.^2.*exp(-alpha12.*c).^2.*xc.^2.*(-1+exp(-alpha12.*c)).*...
  alpha12.*d+(exp(-alpha12.*c).*alpha12.*c.^2.*d-c.*d.*exp(-alpha12.*c)).*xc.^2.*(-1+exp(-alpha12.*c)).^2)./...
  (bbbb.^4)).*(-xc+xc.*exp(-alpha12.*c))+(-a.^2.*exp(-alpha12.*a).^2.*xc.^3.*(-1+exp(-alpha12.*a)).^2.*...
  alpha12.*b./(aaaa.^3)+(-3.*a.*exp(-alpha12.*a).*xc.^2.*(-1+exp(-alpha12.*a)).^2.*(-exp(-alpha12.*a).*...
  alpha12.*a.*b+exp(-alpha12.*a).*alpha12.*a.*b.*xc)./(aaaa.^4)+(2.*a.^2.*exp(-alpha12.*a).^2.*xc.^2.*...
  (-1+exp(-alpha12.*a)).*alpha12.*b+(exp(-alpha12.*a).*alpha12.*a.^2.*b-a.*b.*exp(-alpha12.*a)).*xc.^2.*...
  (-1+exp(-alpha12.*a)).^2)./(aaaa.^3)).*(xc-exp(-alpha12.*a).*xc)-a.^2.*exp(-alpha12.*a).^2.*xc.^3.*...
  (-1+exp(-alpha12.*a)).^3.*(1-xc).*alpha12.*b./(aaaa.^4))./(xc+(1-xc).*exp(-alpha12.*a)))-xc.^2.*...
  ((-a.^2.*exp(-alpha12.*a).^2.*alpha12.*b.*xc./aaaa+(exp(-alpha12.*a).*alpha12.*a.^2.*b-a.*b.*...
  exp(-alpha12.*a)-a.*exp(-alpha12.*a).*(-exp(-alpha12.*a).*alpha12.*a.*b+exp(-alpha12.*a).*alpha12.*a.*b.*xc)./...
  aaaa).*(xc-exp(-alpha12.*a).*xc)./aaaa-a.^2.*exp(-alpha12.*a).^2.*xc.*(-1+exp(-alpha12.*a)).*(1-xc).*...
  alpha12.*b./(aaaa.^2))./(xc+(1-xc).*exp(-alpha12.*a))-c.^2.*exp(-alpha12.*c).^2.*xc.*alpha12.*d./(bbbb.^2)-...
  (-2.*c.^2.*exp(-alpha12.*c).^2.*xc.*alpha12.*d./(bbbb.^3)+(exp(-alpha12.*c).*alpha12.*c.^2.*d-c.*d.*...
  exp(-alpha12.*c))./(bbbb.^2)).*(-xc+xc.*exp(-alpha12.*c)))))

d1=-G_13/u0

% Calculate x2 from x1
x2_calc=2*xc-x1_calc+2*xc*d1*dT;

% Plot results
x1_calc=[ xc
          x1_calc];
x2_calc=[ xc
          x2_calc];
T_calc=[  Tc
          T_calc];
plot(x1_calc,T_calc,'r')
hold on;
plot(x1_exp,T,'bo')
plot(x2_calc,T_calc,'r')
plot(x2_exp,T,'bo')
xlabel('x1,x2 [-]')
ylabel('T [K]')
title('2T-Landau with kernel term in terms of NRTL-model with symmetry correction for nitrobenzene + octane')
text(0.72,292,'red stars: calc')
text(0.72,291,'blue circles: exp')
plot((x2_calc+x1_calc)/2,T_calc,'r.')
plot((x2+x1)/2,T,'bo')
```

Subroutine Constraints

```
function [cineq,ceq,G,Geq]=constraints(Var, x1_exp, x2_exp, T_exp, nu, omega, gamma, Delta, alpha, eta, xc, Tc,...
  Lambda, sigma_x, sigma_T,alpha12,a,c,Data0);

G=[];
Geq=[];
u_star=0.472;

[Y,x,T,b,d,u_bar]=vector2var(Var);

% Reduced variables
dx=(x/xc-1);
dT=(1-Tc./T);

% Help variables
aaaa=-xc-exp(-alpha12.*a)+exp(-alpha12.*a).*xc;
bbbb=1-xc+xc.*exp(-alpha12.*c);

% 2T-Landau amplitudes calculated for NRTL
a0= (2.*xc.*(1-xc).*(-(-a.^2.*exp(-alpha12.*a).^2.*xc.^2.*(-1+exp(-alpha12.*a)).*alpha12.*b./(aaaa.^2)+...
  (-2.*a.*exp(-alpha12.*a).*xc.*(-1+exp(-alpha12.*a)).*(-exp(-alpha12.*a).*alpha12.*a.*b+exp(-alpha12.*a).*...
  alpha12.*a.*b.*xc)./(aaaa.^3)+(a.^2.*exp(-alpha12.*a).^2.*xc.*alpha12.*b+(exp(-alpha12.*a).*alpha12.*a.^2.*...
  b-a.*b.*exp(-alpha12.*a)).*xc.*(-1+exp(-alpha12.*a)))./(aaaa.^2)).*(xc-exp(-alpha12.*a).*xc)-a.^2.*...
  exp(-alpha12.*a).^2.*xc.^2.*(-1+exp(-alpha12.*a)).^2.*(1-xc).*alpha12.*b./(aaaa.^3))./(xc+(1-xc).*...
  exp(-alpha12.*a))+c.^2.*exp(-alpha12.*c).^2.*xc.^2.*(-1+exp(-alpha12.*c)).*alpha12.*d./(bbbb.^3)+...
  (-3.*c.^2.*exp(-alpha12.*c).^2.*xc.^2.*(-1+exp(-alpha12.*c)).*alpha12.*d./(bbbb.^4)+(c.^2.*...
  exp(-alpha12.*c).^2.*xc.*alpha12.*d+(exp(-alpha12.*c).*alpha12.*c.^2.*d-c.*d.*exp(-alpha12.*c)).*xc.*...
  (-1+exp(-alpha12.*c)))./(bbbb.^3)).*(-xc+xc.*exp(-alpha12.*c)))-2.*xc.^2.*((exp(-alpha12.*a).*alpha12.*...
  a.^2.*b-a.*b.*exp(-alpha12.*a)+a.^2.*exp(-alpha12.*a).^2.*(1-xc).*alpha12.*b./aaaa)./(xc+(1-xc).*...
  exp(-alpha12.*a))+(exp(-alpha12.*c).*alpha12.*c.^2.*d-c.*d.*exp(-alpha12.*c)-c.^2.*exp(-alpha12.*c).^2.*...
  xc.*alpha12.*d./bbbb)./bbbb)+2.*(-xc.^2+xc.*(1-xc)).*((-a.^2.*exp(-alpha12.*a).^2.*alpha12.*b.*xc./aaaa+...
  (exp(-alpha12.*a).*alpha12.*a.^2.*b-a.*b.*exp(-alpha12.*a)-a.*exp(-alpha12.*a).*(-exp(-alpha12.*a).*...
  alpha12.*a.*b+exp(-alpha12.*a).*alpha12.*a.*b.*xc)./aaaa).*(xc-exp(-alpha12.*a).*xc)./aaaa-a.^2.*...
  exp(-alpha12.*a).^2.*xc.*(-1+exp(-alpha12.*a)).*(1-xc).*alpha12.*b./(aaaa.^2))./(xc+(1-xc).*exp(-alpha12.*a))-...
  c.^2.*exp(-alpha12.*c).^2.*xc.*alpha12.*d./(bbbb.^2)-(-2.*c.^2.*exp(-alpha12.*c).^2.*xc.*alpha12.*d./...
  (bbbb.^3)+(exp(-alpha12.*c).*alpha12.*c.^2.*d-c.*d.*exp(-alpha12.*c))./(bbbb.^2)).*(-xc+xc.*exp(-alpha12.*c))));

u0= (2.*xc+8.*xc.^4./((xc-1).^2.*(1-xc))+6.*xc.^4./((xc-1).^3)+24.*(-xc.^2+xc.*(1-xc)).*(-c.*exp(-alpha12.*c).*...
  xc.^2.*(-1+exp(-alpha12.*c)).^2.*(-xc+xc.*exp(-alpha12.*c))./((1-xc+xc.*exp(-alpha12.*c)).^4)+a.*...
  exp(-alpha12.*a).*xc.^2.*(-1+exp(-alpha12.*a)).^2.*(xc-exp(-alpha12.*a).*xc)./((-xc-exp(-alpha12.*a)+...
  exp(-alpha12.*a).*xc).^3.*(xc+(1-xc).*exp(-alpha12.*a))))-24.*xc.^2.*(-a.*exp(-alpha12.*a).*xc.*...
  (-1+exp(-alpha12.*a)).*(xc-exp(-alpha12.*a).*xc)./((-xc-exp(-alpha12.*a)+exp(-alpha12.*a).*xc).^2.*...
  (xc+(1-xc).*exp(-alpha12.*a)))+c.*exp(-alpha12.*c).*xc.*(-1+exp(-alpha12.*c)).*(-xc+xc.*exp(-alpha12.*c))./...
  ((1-xc+xc.*exp(-alpha12.*c)).^3))+24.*xc.*(1-xc).*(-a.*exp(-alpha12.*a).*xc.^3.*(-1+exp(-alpha12.*a)).^3.*...
  (xc-exp(-alpha12.*a).*xc)./((-xc-exp(-alpha12.*a)+exp(-alpha12.*a).*xc).^4.*(xc+(1-xc).*exp(-alpha12.*a)))+...
  c.*exp(-alpha12.*c).*xc.^3.*(-1+exp(-alpha12.*c)).^3.*(-xc+xc.*exp(-alpha12.*c))./((1-xc+xc.*exp(-alpha12.*c)).^5)));

G_13=6*( ((-xc.^2+xc.*(1-xc)).*(-(-a.^2.*exp(-alpha12.*a).^2.*xc.^2.*(-1+exp(-alpha12.*a)).*alpha12.*b./...
  (aaaa.^2)+(-2.*a.*exp(-alpha12.*a).*xc.*(-1+exp(-alpha12.*a)).*(-exp(-alpha12.*a).*alpha12.*a.*b+...
  exp(-alpha12.*a).*alpha12.*a.*b.*xc)./(aaaa.^3)+(a.^2.*exp(-alpha12.*a).^2.*xc.*alpha12.*b+...
  (exp(-alpha12.*a).*alpha12.*a.^2.*b-a.*b.*exp(-alpha12.*a)).*xc.*(-1+exp(-alpha12.*a)))./(aaaa.^2)).*...
  (xc-exp(-alpha12.*a).*xc)-a.^2.*exp(-alpha12.*a).^2.*xc.^2.*(-1+exp(-alpha12.*a)).^2.*(1-xc).*alpha12.*...
  b./(aaaa.^3))./(xc+(1-xc).*exp(-alpha12.*a))+c.^2.*exp(-alpha12.*c).^2.*xc.^2.*(-1+exp(-alpha12.*c)).*...
  alpha12.*d./(bbbb.^3)+(-3.*c.^2.*exp(-alpha12.*c).^2.*xc.^2.*(-1+exp(-alpha12.*c)).*alpha12.*d./(bbbb.^4)+...
  (c.^2.*exp(-alpha12.*c).^2.*xc.*alpha12.*d+(exp(-alpha12.*c).*alpha12.*c.^2.*d-c.*d.*exp(-alpha12.*c)).*...
  xc.*(-1+exp(-alpha12.*c)))./(bbbb.^3)).*(-xc+xc.*exp(-alpha12.*c)))+xc.*(1-xc).*(-c.^2.*exp(-alpha12.*c).^2.*...
  xc.^3.*(-1+exp(-alpha12.*c)).^2.*alpha12.*d./(bbbb.^4)-(-4.*c.^2.*exp(-alpha12.*c).^2.*xc.^3.*...
  (-1+exp(-alpha12.*c)).^2.*alpha12.*d./(bbbb.^5)+(2.*c.^2.*exp(-alpha12.*c).^2.*xc.^2.*(-1+exp(-alpha12.*c)).*...
  alpha12.*d+(exp(-alpha12.*c).*alpha12.*c.^2.*d-c.*d.*exp(-alpha12.*c)).*xc.^2.*(-1+exp(-alpha12.*c)).^2)./...
  (bbbb.^4)).*(-xc+xc.*exp(-alpha12.*c))+(-a.^2.*exp(-alpha12.*a).^2.*xc.^3.*(-1+exp(-alpha12.*a)).^2.*...
  alpha12.*b./(aaaa.^3)+(-3.*a.*exp(-alpha12.*a).*xc.^2.*(-1+exp(-alpha12.*a)).^2.*(-exp(-alpha12.*a).*...
  alpha12.*a.*b+exp(-alpha12.*a).*alpha12.*a.*b.*xc)./(aaaa.^4)+(2.*a.^2.*exp(-alpha12.*a).^2.*xc.^2.*...
  (-1+exp(-alpha12.*a)).*alpha12.*b+(exp(-alpha12.*a).*alpha12.*a.^2.*b-a.*b.*exp(-alpha12.*a)).*xc.^2.*...
  (-1+exp(-alpha12.*a)).^2)./(aaaa.^3)).*(xc-exp(-alpha12.*a).*xc)-a.^2.*exp(-alpha12.*a).^2.*xc.^3.*...
  (-1+exp(-alpha12.*a)).^3.*(1-xc).*alpha12.*b./(aaaa.^4))./(xc+(1-xc).*exp(-alpha12.*a)))-xc.^2.*...
  ((-a.^2.*exp(-alpha12.*a).^2.*alpha12.*b.*xc./aaaa+(exp(-alpha12.*a).*alpha12.*a.^2.*b-a.*b.*...
  exp(-alpha12.*a)-a.*exp(-alpha12.*a).*(-exp(-alpha12.*a).*alpha12.*a.*b+exp(-alpha12.*a).*alpha12.*a.*b.*xc)./...
  aaaa).*(xc-exp(-alpha12.*a).*xc)./aaaa-a.^2.*exp(-alpha12.*a).^2.*xc.*(-1+exp(-alpha12.*a)).*(1-xc).*...
  alpha12.*b./(aaaa.^2))./(xc+(1-xc).*exp(-alpha12.*a))-c.^2.*exp(-alpha12.*c).^2.*xc.*alpha12.*d./(bbbb.^2)-...
  (-2.*c.^2.*exp(-alpha12.*c).^2.*xc.*alpha12.*d./(bbbb.^3)+(exp(-alpha12.*c).*alpha12.*c.^2.*d-c.*d.*...
  exp(-alpha12.*c))./(bbbb.^2)).*(-xc+xc.*exp(-alpha12.*c)))));

% System-dependent amplitudes
cT=a0/sqrt(u0)*sqrt(u_bar*u_star*Lambda);
```

```
cRho=u0^0.25*(u_bar*u_star*Lambda)^(-0.25);
d1=-G_13/u0;

% Landau variables
t=cT*dT;
M=cRho*(dx-d1*dT);

% Help variables
term1=(u_star*u_bar*Lambda*M.^2.*Y.^(-(-gamma+nu)/Delta))./M.^2;
term2=t.*Y.^((2.*nu-1)./Delta);

DDeltaA_RDM= t.*M.*Y.^((gamma-1)./Delta)+1./6.*u_star.*u_bar.*Lambda.*M.^3.*Y.^((2.*gamma-3.*nu)./Delta)+.5.*...
  (1./2.*t.*M.^2.*Y.^((gamma-1)./Delta).*(gamma-1)./(Delta.*Y)+1./24.*u_star.*u_bar.*Lambda.*M.^4.*...
  Y.^((2.*gamma-3.*nu)./Delta).*(2.*gamma-3.*nu)./(Delta.*Y)+.5.*t.^2.*nu.*Y.^(-alpha./Delta)./(u_bar.*Lambda.*Delta.*Y)).*...
  u_bar.^2.*Y.^(1./omega).*Lambda.^3.*u_star.*M.*Y.^(-(-amma+nu)./Delta)./((1+Lambda.^2./(term2+1./2.*M.^2.*term1)).^.5.*...
  (term2+1./2.*M.^2.*term1).^2.*(1u_bar).*(1+u_bar.*(1+Lambda.^2./(term2+1./2.*M.^2.*term1)).^.5.*Y.^(1./omega)./
  (omega.*Y.*(1-u_bar))).*(1-.5.*u_bar.*Y.^(1./omega).*Lambda.^2.*(t.*Y.^((2.*nu-1)./Delta).*(2.*nu-1)./(Delta.*Y)-
  1./2.*u_star.*u_bar.*Lambda.*M.^2.*Y.^(-(-gamma+nu)./Delta).*(gamma+nu)./(Delta.*Y))./
  ((1+Lambda.^2./(term2+1./2.*M.^2.*term1)).^.5.*(term2+1./2.*M.^2.*term1).^2.*(1-u_bar).*
  (1+u_bar.*(1+Lambda.^2./(term2+1./2.*M.^2.*term1)).^.5.*Y.^(1./omega)./(omega.*Y.*(1-u_bar))))));

kappa2= t.*Y.^((2*nu-1)/Delta)+1/2*u_star*u_bar*Lambda*M.^2.*Y.^(-(-gamma+nu)/Delta);

f=1-(1-u_bar).*Y-u_bar*sqrt(1+Lambda^2./kappa2).*Y.^(1/omega);


% Inequality constraints
cineq=[-kappa2;
      -diff(Y)];

% Equality constraints
ceq=...
  [f;
  DDeltaA_RDM];
```

Appendix F

Matlab®-code for simplified 2T-Landau expansion

Program Datdemo

```
%%%%%%%%%%%%%%%%%%%%%%%%%%%%%%%%%%%%%%%%%%%%%%%%%%%%%%%%%%%%%%%
% This program optimises the crossover parameters cRho and u_bar for the simplified 2T-Landau expansion.
% Lambda is fixed at 1 and alpha12 is fixed at 0.2. The NRTL parameters a-wiggle and
% c-wiggle are calculated from the conditions of incipient immiscibility. They depend on the mole fraction in the critical point.
% This optimisation does not include the implicit dependence of Y on M (dYdM) and the kernel term.
%%%%%%%%%%%%%%%%%%%%%%%%%%%%%%%%%%%%%%%%%%%%%%%%%%%%%%%%%%%%%%%

omega=0.85714;
nu=0.63;
eta=0.0333;
u_star=0.472;
sigma_x0=0.001;
sigma_T0=0.003;

Data=...
[ 0.475  0.535     293.039
  0.471  0.539     293.034
  0.466  0.543     293.025
  0.463  0.546     293.017
  0.459  0.550     293.004
  0.455  0.554     292.987
  0.450  0.559     292.970
  0.444  0.565     292.939
  0.437  0.571     292.892
  0.430  0.578     292.833
  0.421  0.586     292.761
  0.413  0.594     292.663
  0.405  0.601     292.551
  0.395  0.611     292.371
  0.379  0.625     292.041
  0.365  0.638     291.690
  0.350  0.651     291.216];

hold on;
plot(Data(:,1),Data(:,3),'bo')
plot(Data(:,2),Data(:,3),'bo')

pause
close

B=size(Data);

u_bar=0.3;
Lambda=1;
cT=0.5;
cRho=2;

Tc=293.052;
xc=0.505;
B=size(Data);

lam =[u_bar cRho]';
Pars =length(lam);

Points=2*B(1,1);

T=       [Data(1:0.5*Points,3);
          Data(1:0.5*Points,3)];
x_exp=   [Data(1:0.5*Points,1);
          Data(1:0.5*Points,2)];

OPTIONS = optimset(OPTIONS,'TolX',1e-8,'Display','iter','LevenbergMarquardt','on',...
  'TolCon',1e-8,'TolFun',1e-8,'DiffMaxChange',1e-3,'MaxFunEvals',100000,'LargeScale','on',...
  'Diagnostics','on','DiffMinChange',1e-12,'MaxIter',30);
```

```
[lam,resnorm,residual,exitflag,output]= lsqnonlin('fitfun',lam, [], [], OPTIONS, x_exp, Tc, T, nu,...
  omega, eta, u_star, sigma_x0, sigma_T0, Points, Pars, xc,cT,Lambda)

fval = resnorm;

funEvals=sprintf('\n Number of iterations: %g.  Number of function evaluations: %g.', output.iterations, output.funcCount);
disp(funEvals)
disp(sprintf(' Norm of the residual at solution ( norm(FITFUN2(x,Data,h))^2 ): %g ',fval));

kappa2_0                 =abs(1-Tc./T)*cT;
kappa2                   =kappa2_0;
Y_0                      =1./(1+lam(1,1)*((1+Lambda^2./kappa2).^(omega/2)-1));

Err1=10*ones(Points,1);
Err2=10*ones(Points,1);
iter=0;

while abs(Err1)>1e-7 & abs(Err2)>1e-7
  iter=iter+1;
  Y  =(1-(1-(1-lam(1,1))*Y_0).*(1-(lam(1,1)./(1-(1-lam(1,1))*Y_0)).^(1-omega)))./...
      (1+lam(1,1)*((1+Lambda^2./kappa2).^(omega/2)-1));

  TT=Y.^((2*nu-1)/(nu*omega));
  UU=Y.^(1/omega);

  % Renormalised dimensionless temperature and mole fraction
  deltaT=(1-Tc./T);
  deltaTR=cT*deltaT;

  Exp=(2-1/nu)/omega;
  kappa2=-2*deltaTR.*Y.^Exp;

  Err1=sum((kappa2-kappa2_0)./kappa2);
  Err2=sum((Y-Y_0)./Y);

  Y_0=Y;
  kappa2_0=kappa2;
end;

DD=Y.^(-eta/omega);
UU=Y.^(1/omega);
TT=Y.^((2-1/nu)/omega);
deltaTR=cT*(1-Tc./T);

x_calc(1:0.5*Points,1)     =xc*(sqrt( 6*abs(deltaTR(1:0.5*Points,1)).*TT(1:0.5*Points,1)./(u_star*lam(1,1)*Lambda*...
  DD(1:0.5*Points,1).*UU(1:0.5*Points,1)) )/lam(2,1)+1);
x_calc(0.5*Points+1:Points,1) =xc*(-sqrt( 6*abs(deltaTR(0.5*Points+1:Points,1)).*TT(0.5*Points+1:Points,1)./...
  (u_star*lam(1,1)*Lambda*DD(0.5*Points+1:Points,1).*UU(0.5*Points+1:Points,1)) )/lam(2,1)+1);
```

Subroutine FitFun

```
function f = fitfun(lam, x_exp, Tc, T, nu, omega, eta, u_star, sigma_x0, sigma_T0, Points, Pars, xc, cT,Lambda)

u_bar         =lam(1,1);
cRho          =lam(2,1);

sigma_x=SD_x(lam,x_exp,Tc,T,nu,omega,eta,u_star,sigma_x0,sigma_T0,Points,Pars,xc,cT,u_bar,cRho,Lambda);

Free=Points-Pars;

Weight=1./sigma_x.^2;

x_calc=func(Tc, T, nu, omega, eta, cT, cRho, u_bar, Lambda, u_star, Points, xc);

ChiSquare=Weight.*(x_exp-x_calc).^2/Free;

f=ChiSquare;
```

Subroutine SD_x

```
function sigma_x=SD_x(lam,x_exp,Tc,T,nu,omega,eta,u_star,sigma_x0,sigma_T0,Points,Pars,xc,cT,u_bar,cRho,Lambda)

delta=1e-9;
Dummy=0;

T=T+delta;
x_calc_1=func(Tc,T,nu,omega,eta,cT,cRho,u_bar,Lambda,u_star,Points,xc);
T=T-2*delta;
x_calc_2=func(Tc,T,nu,omega,eta,cT,cRho,u_bar,Lambda,u_star,Points,xc);

DxDT=(x_calc_1-x_calc_2)/(2*delta);

sigma_x=sqrt( sigma_x0.^2+ (DxDT.*sigma_T0).^2 );
```

Subroutine Func

```
function x_calc=func(Tc,T,nu,omega,eta,cT,cRho,u_bar,Lambda,u_star,Points,xc)

kappa2_0              =abs(1-Tc./T)*cT;
kappa2=kappa2_0;
Y_0                       =1./(1+u_bar*((1+Lambda^2./kappa2).^(omega/2)-1));

Err1=10*ones(Points,1);
Err2=10*ones(Points,1);
iter=0;

while abs(Err1)>1e-7 & abs(Err2)>1e-7
  iter=iter+1;
  Y                       =real((1-(1-(1-u_bar)*Y_0).*(1-(u_bar./(1-(1-u_bar)*Y_0)).^(1-omega)))./...
    (1+u_bar*((1+Lambda^2./kappa2).^(omega/2)-1)));

  TT=Y.^((2*nu-1)/(nu*omega));
  UU=Y.^(1/omega);

  % Renormalised dimensionless temperature and mole fraction
  deltaT=(1-Tc./T);
  deltaTR=cT*deltaT;

  Exp=(2-1/nu)/omega;
  kappa2=-2*deltaTR.*Y.^Exp;

  Err1=sum((kappa2-kappa2_0)./kappa2);
  Err2=sum((Y-Y_0)./Y);

  Y_0=Y;
  kappa2_0=kappa2;
  if kappa2<0
    ERROR('kappa neg')
  end;
end;

fy=1-(1-u_bar).*Y-u_bar*sqrt(1+Lambda^2./kappa2).*Y.^(1/omega);

DD=Y.^(-eta/omega);
UU=Y.^(1/omega);
TT=Y.^((2-1/nu)/omega);
TR=cT*(1-Tc./T);

x_calc(1:0.5*Points,1)          =xc*(-sqrt( 6*abs(TR(1:0.5*Points,1)).*TT(1:0.5*Points,1)./(u_star*u_bar*Lambda*...
                                 DD(1:0.5*Points,1).*UU(1:0.5*Points,1)) )/cRho+1);
x_calc(0.5*Points+1:Points,1) =xc*(sqrt( 6*abs(TR(0.5*Points+1:Points,1)).*TT(0.5*Points+1:Points,1)./...
                                 (u_star*u_bar*Lambda*DD(0.5*Points+1:Points,1).*UU(0.5*Points+1:Points,1)) )/cRho+1);
```